

Money Creation in Decentralized Finance: A Dynamic Model of Stablecoin and Crypto Shadow Banking*

Ye Li[†] Simon Mayer[‡]

December 22, 2021

Abstract

Stablecoins are at the center of debate surrounding decentralized finance. We develop a dynamic model to analyze the instability mechanism of stablecoins, the complex incentives of stablecoin issuers, and regulatory proposals. The model rationalizes a variety of stablecoin management strategies commonly observed in practice and characterizes an instability trap: Stability can last for a long time, but once debasement happens following negative shocks to the issuer’s reserves, price volatility persists. Capital requirement improves price stability but still fails to eliminate debasement. Restricting the riskiness of reserve assets can surprisingly destabilize price. Finally, we show that data privacy regulation has an unintended benefit of reducing the price volatility of stablecoins issued by data-driven platforms (e.g., Facebook).

Keywords: Stablecoin, instability, regulation, decentralized finance, cash holdings, q-theory

*We are grateful to helpful comments from Pablo Azar (discussant), Ravi Bansal, Bruno Biais, Matthieu Bouvard, Markus Brunnermeier, Jean-Édouard Colliard, Denis Gromb, Sebastian Gryglewicz, Zhiguo He, Shimon Kogan, Roman Kozhan, Konstantin Milbradt, Anil Kashyap, Alexei Ovtchinnikov, Jonathan Payne (discussant), Enrico Perotti, Adriano Rampini, Jean-Charles Rochet (discussant), Fahad Saleh (discussant), Alp Simsek, Spyros Terovitis, Quentin Vandeweyer, Felipe Varas, Ganesh Viswanath-Natraj (discussant), Vish Vishwanathan, Ariel Zetlin-Jones (discussant), and seminar participants at Bank of Finland/BIS 10th Economics of Payments Conference, CESifo Macro Money & International Finance, China International Conference in Finance, Dublin DeFi & Digital Finance Workshop, Duke University (Fuqua), European Central Bank (ECB) Money Market Conference, Econometric Society, Stanford Institute for Theoretical Economics (SITE), Hogege Blockchain Research Institute Conference, University of Amsterdam, UWA Blockchain Conference, and UC Berkeley Decentralized Finance course. Ye acknowledges financial support from Dice Center of Financial Economics. This paper was previously circulated under the title “Managing Stablecoins: Optimal Strategies, Regulation, and Transaction Data as Productive Capital”.

[†]The Ohio State University Fisher College of Business. E-mail: li.8935@osu.edu

[‡]University of Chicago, Booth School of Business. E-mail: simon.mayer@chicagobooth.edu.

1 Introduction

More than a decade ago, Bitcoin heralded a new era of digital payments and decentralized finance (Brunnermeier, James, and Landau, 2019; Duffie, 2019). The substantial volatility of first-generation cryptocurrencies limits their utility as a means of payment.¹ Stablecoins aim to maintain a stable price against fiat currencies and meet the rising demand for blockchain-based safe assets in the fast growing DeFi (Decentralized Finance) sector. The market value of stablecoins more than tripled from January to November 2021, and the boom attracted enormous attention from policy makers. On November 1, 2021, U.S. President’s Working Group on Financial Markets, joined by the Federal Deposit Insurance Corporation (FDIC) and the Office of the Comptroller of the Currency (OCC), released a report on the recent developments of stablecoins (U.S. Department of the Treasury, 2021). U.S. Secretary of the Treasury Janet Yellen emphasized the potential of stablecoins as beneficial payments options and risks due to the lack of legal oversight. In response, U.S. Senate held a hearing on the risks of stablecoins on December 14, 2021.²

In this paper, we aim to provide clarity on the instability mechanism of stablecoins, evaluate regulatory proposals, and analyze the complex incentives of stablecoin issuers with a particular focus on large digital platforms. We formalize the operation of a stablecoin issuer in a dynamic continuous-time model and specify the stablecoin demand following the literature on agents’ transactional demand for low-risk assets (Gorton and Pennacchi, 1990; Moreira and Savov, 2017). The equilibrium features a rich set of dynamic strategies of stablecoin management commonly observed in practice (Bullmann, Klemm, and Pinna, 2019), such as open market operations, requirement of users’ collateral, user fees or subsidies, targeted price band, and the issuances of governance tokens (or “secondary units”) that function as equity shares of the stablecoin issuer.³

A key feature of our model is that the stablecoin issuer’s reserve assets are risky, which is in line the practice. For example, Tether, the issuer of the largest stablecoin by market capitalization (USDT), holds a significant share of reserves in commercial papers of unknown quality.⁴ Shocks to the reserves may trigger debasement in equilibrium that resemble the recent episodes, such as the

¹Flaws in the protocol design of early cryptocurrencies limit payment scalability (Hinzen, John, and Saleh, 2019).

²For the full hearing, “Stablecoins: How Do They Work, How Are They Used, and What Are Their Risks?”, please refer to the website of U.S. Senate Committee on Banking, Housing, and Urban Affairs (www.banking.senate.gov).

³An alternative to collateralization is to use algorithmic supply rules to stabilize price but success has been limited.

⁴According to De and Hochstein (2021), USDT is backed by dollar cash, cash equivalents, and commercial papers (75.85%), secured loans (12.55%), corporate bonds, funds, and precious metals (9.96%), and other investments including cryptocurrencies (1.64%). The default of China Evergrande Group on its commercial papers disrupted cryptocurrency markets precisely due to the concern over Tether’s exposure to the Chinese real estate sector (See Lewitinn (2021)). Stablecoins backed by safe assets are rare and simply a form of narrow banking (Pennacchi, 2012).

8% debasement of USDT in April 2017 and the 3.5% debasement of USDC (USD Coin) in February 2020. The stablecoin issuer can debase its stablecoins to avoid liquidation. In contrast, traditional safe asset issuers, both banks and shadow banks, have to honor their debts or become insolvent.

However, the debasement option induces an amplification mechanism that generates a bimodal distribution of states. In states of high reserves, the issuer maintains a fixed exchange rate, so the stablecoin demand is strong and transaction volume is high. Through open market operations and fees on stablecoin users, the issuer generates revenues that further grow its reserves. In states of low reserves, the issuer off-loads risk to users through debasement, which depresses the stablecoin demand and thus reduces the issuer’s revenues. The issuer can only rebuild its reserves slowly and thus falls into an instability trap. Stability can last for a long time, but once debasement happens following negative shocks to the stablecoin issuer’s reserves, volatility persists. Such ergodic instability resembles that in [Brunnermeier and Sannikov \(2014\)](#).⁵

We show that capital requirement reduces the volatility of stablecoin price and demonstrate how the optimal capital requirement varies with key parameters that drive the stablecoin demand or the issuer’s trade-offs. In particular, we highlight that stablecoin payment systems with stronger network effects, for example, through social interactions and e-commerce activities (e.g., Facebook), should be subject to tougher capital requirements. Notably, regulations restricting the riskiness of the reserve assets have different effects than capital requirement. In particular, our analysis reveals a volatility paradox: Forcing the stablecoin issuer to hold reserves in low-risk assets can make the stablecoin more volatile because the issuer endogenously responds to reduce its reserves.

Moreover, we extend our model by allowing the stablecoin issuer to profit from users’ transaction data. When data becomes a productive capital, its marginal q distorts the stablecoin issuer’s decisions of reserve management. The issuer aggressively draws down its reserves to subsidize users’ data-generating activities rather than preserving reserves for stablecoin management. The data acquisition incentive leads to a more volatile price of the stablecoin. While data privacy and stablecoins have been treated as two separate areas, both under heated debate among regulators, our analysis reveals an unintended consequence of privacy regulation on stablecoins: Limiting platforms’ usage of user-generated data reduces the price volatility of their stablecoins.

The stablecoin issuer’s reserve management is reminiscent of dynamic corporate cash manage-

⁵The banking model of [Klimenko, Pfeil, Rochet, and Nicolo \(2016\)](#) generates ergodic instability under regulations unlike the laissez-faire economy in [Brunnermeier and Sannikov \(2014\)](#) and our paper. The commonality is that the financial-slack variable, which drives the equilibrium dynamics, can be trapped in a certain region by a large probability over the long run. The continuous-time approach allows a complete characterization of equilibrium dynamics. Ergodic instability is often ignored by the traditional approach of log-linearization near the steady state.

ment (Riddick and Whited, 2009; Bolton, Chen, and Wang, 2011; Décamps, Mariotti, Rochet, and Villeneuve, 2011; Hugonnier, Malamud, and Morellec, 2015; He and Kondor, 2016; Gao, Whited, and Zhang, 2020), but different from a traditional firm, the stablecoin issuer can depreciate its liabilities (outstanding stablecoins) through debasement, akin to a country monetizing debts through inflation. Stablecoins share similarities with contingent convertible bonds (CoCos) that share risk between equity investors and debt holders (Pennacchi, 2010; Glasserman and Nouri, 2012, 2016; Chen, Glasserman, Nouri, and Pelger, 2017; Pennacchi and Tchisty, 2018, 2019). But unlike CoCos, risk sharing is done through debasement rather than converting stablecoins into the issuer’s equity, and debasement is under the discretion of the issuer rather than pre-specified trigger events.⁶

Next, we provide more details on the model setup and our main results. In a continuous-time economy, a digital platform issues stablecoins (“tokens”) to a unit mass of representative users. Our setup applies to both centralized stablecoin issuers, such as Tether or Circle, and decentralized autonomous organizations (DAO), such as MakerDAO, that are governed by prescribed internet protocols.⁷ A user’s token holdings deliver a flow utility that captures the transactional benefits. The network effect of tokens as means of payment is modelled by embedding the aggregate holdings in individuals’ flow utility (Cong, Li, and Wang, 2021).⁸ Following Moreira and Savov (2017), we assume that users’ demand for tokens declines in the volatility of token price. Such safety preference is motivated by the link between information sensitivity and asset illiquidity.⁹

Users can trade tokens for numeraire goods (“dollars”) at an endogenous price (the exchange rate) without frictions. The issuer (i.e., the platform) can trade tokens against its reserves, directly influencing the token price. Thus, the token price is at any time optimal from the issuer’s perspective. On the issuer’s balance sheet, the liability side has tokens outstanding and equity. On the asset side, the platform holds reserves that earn an interest rate, grow with token issuance and user fees, and load on Brownian shocks. The shocks capture operational risk and unexpected fluctuations of reserve value. Importantly, our model also allows for double-collateralization that is behind some stablecoin initiatives in practice (e.g., DAI). Under double-collateralization, users are required to post collateral to back their stablecoin holdings subject to margin requirement and

⁶Our model is also related to the continuous-time models of exchange rate determination in small-open economies (e.g., Penati and Pennacchi, 1989) but differs in our endogenous process of money supply.

⁷This is in line with the current focus of policy makers on a technology-neutral approach that emphasizes economic insights over technological aspects of implementation ECB Crypto-Assets Task Force (2019).

⁸This money-in-utility approach follows the macroeconomics literature (Ljungqvist and Sargent, 2004). The modelling of network effect is in the tradition of social interaction (Glaeser, Sacerdote, and Scheinkman, 1996).

⁹To be liquid and circulate as a transaction medium, a security must be designed in a way that deters private information acquisition (e.g., via a safe payoff) and thus avoids asymmetric information between trade counterparties (Gorton and Pennacchi, 1990; DeMarzo and Duffie, 1999; Dang, Gorton, Holmström, and Ordoñez, 2014).

the issuer’s reserves are drawn upon to cover shortfalls in users’ collateral value. Then, the reserve shocks originate from the fluctuation of users’ collateral value, and the size of the shock can be controlled through the margin requirement on the users.

The dollar value of excess reserves (i.e., the platform’s equity on the balance sheet or the difference between reserves and the dollar value of stablecoins outstanding) is the state variable in the issuer’s dynamic optimization program.¹⁰ The value function that solves the Hamilton-Jacobi-Bellman (HJB) equation delivers a state-contingent valuation of the stablecoin issuer’s equity shares (i.e., what practitioners call the governance tokens). The platform pays out dividends to its shareholders when it holds sufficient reserves as risk buffer, which implies an endogenous upper bound on excess reserves. The issuer accumulates reserves through the interests earned on reserves, fees charged to users, and trading profits from open market operations. We specify the lower (liquidation) bound on the equity (excess reserves) to be zero to focus on over-collateralization. Our focus on fully collateralized stablecoins is motivated by the recent regulatory proposals and bank run events that have cast doubts on the viability of under-collateralized stablecoins.¹¹

In spite of over-collateralization, the stablecoin issuer cannot always sustain one-to-one convertibility between tokens and dollars. To avoid costly liquidation, the platform opts for debasement and token price becomes volatile whenever its equity (excess reserves) fall below a threshold. Debasement and volatility trigger a vicious cycle as the depressed token demand leads to a reduction in fee revenues, which causes a slow recovery of equity (excess reserves) and persistent volatility. However, debasement is a valuable option, as it allows the platform to share risk with users. When negative shocks decrease reserves, debasement causes token liabilities to shrink and stabilizes equity. Above the debasement threshold, the platform sustains one-to-one convertibility and token price is stable. Then a strong token demand allows the platform to collect revenues to grow reserves, which further strengthens the peg to dollar. This virtuous cycle implies persistent expansion of platform reserves until it reaches the optimal payout boundary. The stationary distribution of equity (excess reserves) is thus bimodal with two peaks near zero and the payout boundary, respectively.

Importantly, we show that token price debasement occurs even when the platform can replenish

¹⁰A stablecoin issuer has stablecoin liabilities and equity and is different from a money market fund (only equity).

¹¹In December 2020, three U.S. house representatives proposed the [Stablecoin Tethering and Bank Licensing Enforcement \(STABLE\) Act](#) that emphasized full collateralization. On June 16, 2021, a bank run happened to IRON, a partially collateralized token soft pegged to the U.S. dollar. This was the first large-scale bank run in the cryptocurrency market, and major cryptocurrency investors were calling for regulators’ attention ([Tiwari, 2021](#)). Different from [Routledge and Zetlin-Jones \(2021\)](#) who study speculative attacks on under-collateralized stablecoins and coordination failure ([Morris and Shin, 1998](#); [Goldstein and Pauzner, 2005](#)), we characterize a novel mechanism of risk amplification and show that in line with evidence ([Lyons and Viswanath-Natraj, 2020](#); [Kozhan and Viswanath-Natraj, 2021](#)), even over-collateralized stablecoins can debase when the issuer’s reserves fall significantly.

its reserves by issuing new equity subject to issuance costs similar to [Riddick and Whited \(2009\)](#): Following negative shocks, the platform first debases its token and only relies on equity financing as a last resort when the equity (excess reserves) fall to zero.

We evaluate three types of stablecoin regulations. The first is a standard capital requirement that stipulates the minimal degree of excess reserves. It reduces token price volatility and increases welfare but debasement still happens in equilibrium. As long as the threat of liquidation (or costly equity issuance) exists, whether it is due to reserve depletion or the violation of regulation, it is optimal for the stablecoin issuer and users to share risk through debasement. The second type of regulation, which enforces a fixed token price, only hurts welfare by destroying the economic surplus from risk sharing. In practice, it is difficult to commit against debasement, but even if such commitment is possible, our results show that it would not be optimal.¹²

The third type of regulation restricts the riskiness of reserve assets. A volatility paradox emerges: When reserve assets are riskier, the platform hoards more reserves and token price actually becomes more stable. Forcing the platform to hold low-risk reserve assets may destabilize token price as the platform will respond by holding less reserves. As long as the regulation cannot completely eliminate risk, the volatility paradox is a robust equilibrium feature. In terms of welfare, the regulatory outcome depends on the risk-return trade-off (i.e., whether riskier reserves deliver higher expected returns). In sum, capital requirement is the most effective in generating unambiguous welfare gains and stabilizing token price, but still fails to entirely eliminate debasement.

Stablecoins became the subject of heated debate after Facebook and its partners announced their own stablecoin, Libra (now “Diem”), in June 2019.¹³ Leveraging on their existing customer networks, global platforms are able to rapidly scale the reach of their stablecoins.¹⁴ To analyze the advantages of well-established networks in the stablecoin space, we compare platforms with different degrees of network effects. A stronger network effect is associated with a lower frequency of debasement as it allows the platform to extract more fee revenues from users especially when reserves are running low. Stabilizing token price is in the platform’s interest because low volatility stimulates users’ token demand and a stronger network effect implies a greater positive externality

¹²In other words, the system does not feature dynamic inconsistency in the issuer’s choice of debasement. Admittedly, our model may underestimate the value of a perfectly stable token. For example, debasement invites speculation that can in turn amplify price fluctuation and triggers a vicious cycle ([Kondor, 2009](#); [Mayer, 2020](#)).

¹³The announcement triggered a globally-coordinated response under the umbrella of the G7. From then on, the G20, the Financial Stability Board (FSB), and central banks around the world have also embarked on efforts to address the potential risks while harnessing the potential of technological innovation.

¹⁴Another example is JPM Coin, a blockchain-based digital coin for fast payment settlement that is being developed by JP Morgan Chase and was announced in February 2019.

of one user’s adoption on others. However, the platform does not perfectly internalize the network externalities, and token price is still more volatile than the social optimum. Specifically, we show that the optimal capital requirement should be tougher for platforms with stronger network effects.

The enormous amount of transaction data brought by a payment system lures digital platforms to develop their own stablecoins. Following [Parlour, Rajan, and Zhu \(2020\)](#), we extend our model to incorporate data as by-product of transactions.¹⁵ Data helps the platform to improve its productivity in locking in users’ attention and stimulating user activities (for example, through targeted content delivery). When data becomes a productive capital, its marginal q distorts the platform’s stablecoin management. Specifically, the platform faces a new trade-off between data acquisition and reserves preservation. The former requires lower fees to stimulate user activities while the latter calls for higher fees to grow reserves. We show that when data becomes more productive, the platform cuts fees aggressively and, as a result, token price becomes more volatile and debasement becomes more likely. Therefore, a paradox exists: Stablecoins built primarily for data acquisition become increasingly unstable when data becomes more valuable. Our analysis also reveals an unintended benefit of data privacy regulation that limits platforms’ use of user-generated data. By making data less productive, privacy regulation tilts the platforms’ incentive towards reserve preservation rather than data acquisition and therefore stabilizes the platforms’ stablecoins.

2 Background: Crypto Shadow Banking in Decentralized Finance

Blockchain technology supports peer-to-peer transfer of assets on distributed ledgers, potentially eliminating the need to transact through intermediaries ([Raskin and Yermack, 2016](#); [Abadi and Brunnermeier, 2019](#); [Brainard, 2019](#)). Decentralization avoids sizable intermediation costs ([Philippon, 2015](#)). Depending on the blockchain protocols, decentralization can enhance operational resilience by eliminating single point of failure while still achieve scalability ([John, Rivera, and Saleh, 2020](#)).¹⁶ Decentralized finance (“DeFi”) offers blockchain-based alternatives to traditional finan-

¹⁵In the broader literature on the economics of data, [Veldkamp \(2005\)](#), [Ordoñez \(2013\)](#), [Fajgelbaum, Schaal, and Taschereau-Dumouchel \(2017\)](#), and [Jones and Tonetti \(2020\)](#) model data by-product of economic activities.

¹⁶Decentralized ledger technology is nascent and faces many challenges. Settlement finality can be compromised when the nodes of a distributed network disagree ([Biais, Bisiere, Bouvard, and Casamatta, 2019](#); [Ebrahimi, Routledge, and Zetlin-Jones, 2020](#)). Law of one price fails in segmented markets ([Makarov and Schoar, 2020](#)). Proof-of-work protocols face limits on adoption [Hinzen, John, and Saleh \(2019\)](#), system security risks ([Budish, 2018](#); [Pagnotta, 2021](#)), and requires energy consumption that crowds out other users ([Benetton, Compiani, and Morse, 2021](#)). Researchers are active in studying alternative protocols, such as proof-of-stake (e.g., [Saleh, 2020](#); [Fanti, Kogan, and Viswanath, 2019](#); [John, Rivera, and Saleh, 2021](#)). The cost of decentralization also depends on the market structure of decentralized ledger keepers ([Huberman, Leshno, and Moallemi, 2019](#); [Pagnotta and Buraschi, 2018](#); [Easley, O’Hara, and Basu, 2019](#); [Cong, He, and Li, 2020](#); [John, Rivera, and Saleh, 2020](#); [Lehar and Parlour, 2020](#); [Prat and Walter, 2021](#)).

cial services, such as banking, brokerage, and exchanges (Lehar and Parlour, 2021). It also uses smart contracts with coded enforcement via programmable money (Tinn, 2017; Cong and He, 2019; Goldstein, Gupta, and Sverchkov, 2019), a concept independent from blockchain (Halaburda, 2018).

This emerging financial architecture requires blockchain-based currencies. A viable means of payment should maintain a stable value at least within the settlement period (i.e., time needed for generating decentralized consensus on transactions (Chiu and Koepl, 2017)). However, most cryptocurrencies are highly volatile (Hu, Parlour, and Rajan, 2019; Stulz, 2019; Liu and Tsyvinski, 2020). They are platform-specific currencies (Catalini and Gans, 2018; Sockin and Xiong, 2018; Li and Mann, 2020; Bakos and Halaburda, 2019; Gryglewicz, Mayer, and Morellec, 2020; Cong, Li, and Wang, 2021; Danos, Marcassa, Oliva, and Prat, 2021) whose values are unbacked and fluctuate with the supply and demand dynamics native to the hosting platforms (Cong, Li, and Wang, 2019).¹⁷

Stablecoins are advertised as blockchain-based copies of fiat currencies. The total market value is \$130 billion dollars as of November 2021 (up from \$ 28 billion in January). Stablecoins are heavily used in DeFi activities (Saengchote, 2021), and in May 2021 alone, \$766 billion worth of stablecoins were transferred.¹⁸ The issuer can be a corporate entity or a consortium (e.g., a consortium led by Facebook, the developer of Diem).¹⁹ It can also be a decentralized autonomous organization (DAO), an internet protocol whose rules may be updated upon users' consensus on the blockchain (e.g., MakerDAO, the issuer of DAI).²⁰ A stablecoin is backed by the issuer's reserve assets. The price stability is sustained by the issuer conducting open market operations (i.e., trading reserves against stablecoins) and meeting redemption requests (Bullmann, Klemm, and Pinna, 2019). The blockchain-based distributed ledger records the ownership and transfer of stablecoins but verifying reserves still relies on traditional auditing (Calle and Zalles, 2019).

Stablecoins can potentially be the link between DeFi and the real economy. In a statement in November 2021, U.S. Treasury Secretary Janet Yellen commented on stablecoins: "Stablecoins that are well-designed and subject to appropriate oversight have the potential to support beneficial payments options."²¹ The volatility of the first-generation cryptocurrencies, such as Bitcoin and Ether,

¹⁷Unbacked cryptocurrencies are exposed to platform-specific risks (Liu, Sheng, and Wang, 2020; Shams, 2020), issuers' moral hazard (Chod and Lyandres, 2019; Davydiuk, Gupta, and Rosen, 2019; Gan, Tsoukalas, and Netessine, 2021; Garratt and Van Oordt, 2019), and self-fulfilling and speculative beliefs (Garratt and Wallace, 2018; Benetton and Compiani, 2020). Their returns exhibit a factor structure like other risky assets (Liu, Tsyvinski, and Wu, 2019).

¹⁸See Rajpal and Marshall (2021), Op-ed: Stablecoin is the future of virtual payments. How wise regulation can foster its growth, *CNBC* July 13, 2021.

¹⁹Central banks digital currencies are alternatives to privately issued stablecoins (Bech and Garratt, 2017).

²⁰It is technologically feasible to hard-code certain aspects of a protocol. Kim and Zetlin-Jones (2019) propose an ethical framework for developers to determine which aspects should be immutable and which should not.

²¹See Livni and Lipton (2021), Regulators Ask Congress to Create New Rules for Cryptocurrencies, *The New York*

limits their adoption in real-world transactions. Stablecoins, designed to have stable exchange rates with respect to the reference fiat currencies, have the potential to mediate blockchain-based transactions of goods, services, and real assets.

Stablecoins also play important roles in the cryptocurrency community. Traders' activities heavily involve rebalancing between stablecoins and more volatile cryptocurrencies. Cryptocurrency has become an emerging asset class with the total market capitalization around \$1.5 trillion dollars (with roughly \$700 billion in Bitcoin).²² It is estimated that 50 to 60% of Bitcoin trading volume is against USDT, the stablecoin issued by Tether ([J.P. Morgan Global Research, 2021](#)).

In spite of the importance of stablecoins, there does not exist clear legal and regulatory frameworks. Unlike depository institutions, a stablecoin issuer does not have any obligation to guarantee the quality of reserve assets or maintain a fixed token price. Many are concerned that a major stablecoin “breaks the buck” may trigger financial turmoil beyond the cryptocurrency community ([Massad, 2021](#); [Kozhan and Viswanath-Natraj, 2021](#)). The creation of stablecoins is essentially a new form of shadow banking—unregulated safety transformation—with its distinct features.²³

The reserve assets are risky. Major stablecoin issuers hold commercial papers without disclosure on the identities of commercial paper issuers. The default of China Evergrande Group disrupted cryptocurrency markets precisely due to the concern over Tether's exposure to the Chinese real estate sector.²⁴ Tether is the issuer of USDT, the largest stablecoin by market capitalization.²⁵

Panel A of Figure 1 illustrates stablecoin creation with over-collateralization, a common practice among stablecoin issuers ([Bullmann, Klemm, and Pinna, 2019](#)). The issuer's excess reserves buffer the fluctuation of reserve value. The equity shares are called governance tokens (or “secondary units”) that carry the rights to vote on changes of protocols (i.e., control rights) and pay out cash flows generated by fees charged on the stablecoin users. Governance tokens can be issued to replenish reserves, just as traditional corporations can raise cash by issuing equity. A stablecoin issuer essentially takes a leveraged bet on the value of reserve assets. The issuer can increase its leverage by issuing new stablecoins to finance the purchase of reserve assets, just as banks finance

Times November 1, 2021.

²²Nearly half of millennial millionaires have at least 25% of their wealth in cryptocurrencies ([CNBC Survey](#)).

²³A stable value is essential for a transaction medium because it reduces asymmetric information between transaction counterparties ([Gorton and Pennacchi, 1990](#); [DeMarzo and Duffie, 1999](#); [Dang, Gorton, Holmström, and Ordoñez, 2014](#)). Without informational frictions, stability may not be necessary ([Schilling and Uhlig, 2019](#)).

²⁴See [Lewitinn \(2021\)](#), Tether, Bitcoin and Chinese Commercial Paper at Scale: A look at the leading stablecoin's market cap and China's real estate industry., *CoinDesk Insights* November 12, 2021.

²⁵According to [De and Hochstein \(2021\)](#), USDT is backed by dollar cash, cash equivalents, and commercial papers (75.85%), secured loans (12.55%), corporate bonds, funds, and precious metals (9.96%), and other investments including digital tokens (1.64%).

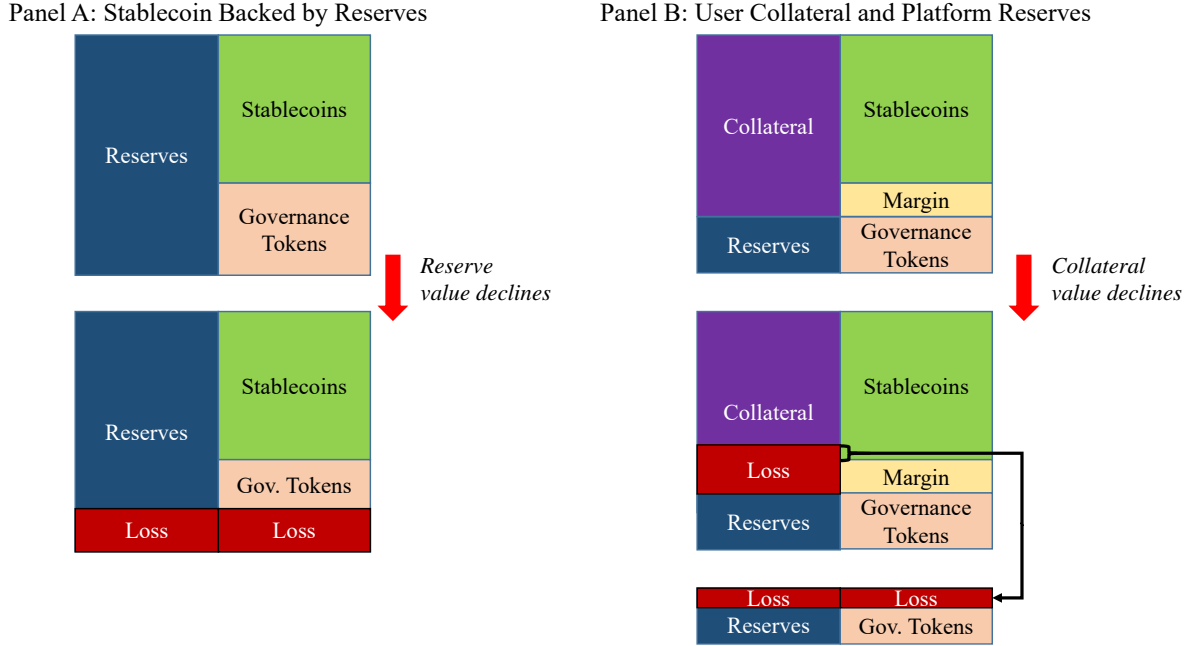


Figure 1: **Crypto Shadow Banking.** This illustrates the two structures of stablecoins. In Panel A, a platform issues stablecoins backed by its reserves. The excess reserves belong to the holders of governance tokens who have the control right (i.e., the control over platform policies). When reserves are invested in risky assets, a potential loss is absorbed by the equity position. As long as the stablecoins are over-collateralized, their value is intact. In Panel B, stablecoins are backed by both the user’s collateral and the platform’s reserves. When the collateral value declines and the user fails to meet the margin requirement, the platform liquidates the collateral and uses the proceeds (and its own reserves) to buy back stablecoins in the secondary market.

their lending and security trading with newly issued deposits (i.e., inside money creation (Tobin, 1963; Bianchi and Bigio, 2014; Piazzesi and Schneider, 2016; Faure and Gersbach, 2017; Donaldson, Piacentino, and Thakor, 2018; Parlour, Rajan, and Walden, 2020)). Unlike banks that commit to redeem deposits at par, the stablecoin issuer can debase the stablecoins.

Panel B of Figure 1 illustrates a more complex structure that is similar to the one adopted by MakerDAO, the issuer of DAI and an early decentralized autonomous organizations.²⁶ A user pledges her holdings of cryptocurrencies and other assets as collateral for newly created stablecoins, subject to a haircut (margin requirement). The user may transfer the stablecoins, which then circulate in the market, but she must maintain the margin requirement. If the collateral value declines and the user cannot maintain the margin, she loses her collateral to the stablecoin issuer, who then liquidates the collateral and uses the proceeds to buy back (and burn) the stablecoins created for this user.²⁷ If the liquidation of collateral does not generate sufficient proceeds, the

²⁶Decentralized autonomous organizations (DAOs) are organizations represented by rules encoded as computer programs and controlled by the organization members through various voting mechanisms on blockchains.

²⁷Burning is to send the stablecoins to an irretrievable digital address

stablecoin issuer’s reserves supplement the expense of stablecoin buy-back.²⁸

The structure in Panel B of Figure 1 resembles shadow banking: A bank sets up a conduit (special purpose vehicle) that tranches risky investments into debt and equity and extends a guarantee to the debt investors (Acharya, Schnabl, and Suarez, 2013). The stablecoin is like the debt (senior) tranche of the conduit. The stablecoin issuer and the user correspond, respectively, to the bank and the conduit. The issuer’s commitment to buy back stablecoins potentially with her own reserves is analogous to the bank’s guarantee. Despite double collateralization, the stablecoin may still break the buck, consistent the findings of Kozhan and Viswanath-Natraj (2021) on a positive relationship between collateral risk and the price volatility of stablecoin DAI.²⁹

We set up our model in the next section following the structure in Panel A of Figure 1 and present the solution in Section 4. Section 5 provides an analysis of several regulatory proposals. In Section 6, we extend our model to incorporate double collateralization in Panel B of Figure 1 and analyze the optimal margin requirement. Section 7 focuses on stablecoins issued by large digital platforms that have strong user network effects and can profit from users’ data.

3 A Model of Stablecoins

Consider a continuous-time economy where a continuum of representative agents (“users”) of unit measure demand stablecoins (“tokens”) that are issued by a platform. The generic consumption goods (“dollars”) are the numeraire in this economy, and we take as exogenous a prevailing interest rate r . Let P_t denote the token price in units of dollars. Users trade tokens with the platform and amongst themselves at the market price P_t per unit without frictions. The platform can influence the token price P_t by trading tokens against its reserves in the market. In equilibrium, the dollar price of token has a law of motion which the atomic users take as given:

$$\frac{dP_t}{P_t} = \mu_t^P dt + \sigma_t^P dZ_t, \tag{1}$$

where the standard Brownian shock, dZ_t , will be introduced below as a shock to the platform’s reserves. We will show how μ_t^P and σ_t^P in equilibrium depend on the platform’s optimal strategies. Next, we first introduce users and then set up the platform’s problem.

²⁸While the repurchase (and burn) of stablecoins is recorded on the blockchain, the liquidation of non-cryptocurrency collateral and reserves happens off-chain and still requires the traditional financial and legal systems.

²⁹The capital structure of a stablecoin issuer (stablecoin liabilities and equity) is different from that of a money market fund (full equity). Money market funds have different fragility mechanisms (Kacperczyk and Schnabl, 2013; Parlato, 2016; Schmidt, Timmermann, and Wermers, 2016; La Spada, 2018; Li, Li, Macchiavelli, and Zhou, 2021).

Users. There is a unit mass of risk-neutral users with time discount rate r . We use $u_{i,t}$ ($i \in [0, 1]$) to denote the dollar value of user i 's holdings of tokens, so user i holds $k_{i,t} = u_{i,t}/P_t$ units of tokens. The aggregate dollar value of token holdings is $N_t \equiv \int_{i \in [0,1]} u_{i,t} dt$. Users hold stablecoins for transactions and as a store of value. We model the transactional benefit of holding stablecoins in a reduced form. Specifically, user i derives a flow utility (convenience yield) from token holdings:

$$\frac{1}{\beta} N_t^\alpha u_{i,t}^\beta A^{(1-\alpha-\beta)} dt - \eta u_{i,t} |\sigma_t^P| dt, \quad (2)$$

where $\alpha, \beta \in (0, 1)$ with $\alpha + \beta < 1$, $A > 0$, and $\eta > 0$. We model the utility from holding means of payment following the classic models of monetary economics (e.g., [Baumol, 1952](#); [Tobin, 1956](#); [Feenstra, 1986](#); [Freeman and Kydland, 2000](#)) and related empirical studies (e.g., [Poterba and Rotemberg, 1986](#); [Lucas and Nicolini, 2015](#); [Nagel, 2016](#)). In this literature, agents derive utility from the real value of holdings, i.e., $u_{i,t}$.³⁰ Following [Rochet and Tirole \(2003\)](#), we introduce network effect via N_t^α . [Cong, Li, and Wang \(2021\)](#) provide a microfoundation of this type of setup where each user's utility is higher when tokens are more widely adopted.³¹ Later we conduct comparative statics analysis on α to show how network effects affect token price stability. The quality of the payment system is captured by parameter A which we will endogenize in Section 7.2. We define transactional utility from an ex ante perspective and the first term in (2) can be viewed as the *expected* transaction benefits in dt . We do not model the ex post circulation of tokens in line with the aforementioned literature on money-in-utility and cash-in-advance constraint.

The user's preference for stability is captured by the parameter $\eta (> 0)$, and is defined on the absolute value of σ_t^P to capture the fact that users are averse to token price fluctuation no matter whether the price moves with ($\sigma_t^P > 0$) or against ($\sigma_t^P < 0$) the platform's reserve shock dZ_t . We motivate such preference for stability following [Moreira and Savov \(2017\)](#): to be liquid and circulate as a transaction medium, a security must be designed in a way that deters private information acquisition and thus avoids asymmetric information between trade counterparties ([Gorton and Pennacchi, 1990](#); [DeMarzo and Duffie, 1999](#); [Dang, Gorton, Holmström, and Ordoñez, 2014](#)).³² One may interpret the flow utility given by (2) as the convenience yield relative to its reference fiat

³⁰We refer readers to the textbook treatments (e.g., [Galí, 2015](#); [Ljungqvist and Sargent, 2004](#); [Walsh, 2003](#)). For the nominal value (i.e., $k_{i,t}$) to affect agents' decisions, additional frictions, such as nominal illusion (e.g., [Shafir, Diamond, and Tversky, 1997](#)) or sticky prices (e.g., [Christiano, Eichenbaum, and Evans, 2005](#)), have to be introduced.

³¹Specifically, when there are more people use tokens, it becomes easier to find a transaction counterparty that accepts tokens, so token holders expect more token usage of means of payment.

³²The disutility from token volatility can also be motivated by risk-averse preference or users' aversion to exchange-rate shocks that cause losses of net worth when assets and liabilities are denominated in different currencies (tokens and dollars) ([Doepke and Schneider, 2017](#); [Gopinath, Boz, Casas, Díez, Gourinchas, and Plagborg-Møller, 2020](#)).

currency due to functionalities such as relaxing collateral constraints in smart contracts.³³

User i pays a proportional fee on her token holdings, $u_{i,t}f_t dt$, where f_t is set by the platform. When f_t is negative, users earn subsidies on their token holdings. Note that as long as the money (token) velocity is constant within the small time interval (dt), transaction volume is proportional to token holdings, N_t . Therefore, an alternative interpretation of f_t is transaction fee. There exists a technical upper bound on the volume of transactions that the platform can handle per unit of time (Hinzen, John, and Saleh, 2019). Without loss of generality, we model the bound as follows:

$$N_t \leq \bar{N}. \quad (3)$$

Let $R_{i,t}$ denote user i 's (undiscounted) *cumulative* payoff from platform activities. The instantaneous payoff depends on user i 's choice of $u_{i,t} \geq 0$ and is given by

$$dR_{it} \equiv \left(\frac{1}{\beta} N_t^\alpha u_{i,t}^\beta A^{(1-\alpha-\beta)} - \eta u_{i,t} |\sigma_t^P| \right) dt + u_{i,t} \left(\frac{dP_t}{P_t} - r dt - f_t dt \right), \quad (4)$$

where the first term is the flow utility (2) and the second term includes the return from token price change net of forgone interests r and fees f_t . A representative user i chooses $u_{i,t} \geq 0$ to maximize

$$\max_{u_{i,t} \geq 0} \mathbb{E}_t [dR_{it}] = \max_{u_{i,t}} \left[\frac{1}{\beta} N_t^\alpha u_{i,t}^\beta A^{(1-\alpha-\beta)} dt + u_{i,t} \left(\mu_t^P - r - f_t - \eta |\sigma_t^P| \right) dt \right]. \quad (5)$$

Note that r is essentially the users' (opportunity) cost of capital as in Jorgenson (1963).³⁴

The Platform. Let S_t denote the total units of tokens outstanding (the token supply). The token market clearing condition is given by

$$S_t = \int_{i \in [0,1]} \frac{u_{i,t}}{P_t} di, \quad (6)$$

or equivalently, in the numeraire (dollar) value:

$$S_t P_t = N_t = \int_{i \in [0,1]} u_{i,t} di. \quad (7)$$

³³Network effects in this interpretation reflect the fact that wider adoption implies more contracting opportunities.

³⁴For agents with infinite intertemporal elasticity of substitution, we do not need to explicitly model the dynamic consumption-savings trade-off and portfolio allocation of savings because the marginal investment in any asset (including tokens) should deliver an expected return r , which is also equal to the marginal return on total savings. Therefore, a user simply maximizes the excess return on token holdings when choosing $u_{i,t}$. As will be shown later, the first order condition of the problem given by (5) equates the marginal benefit of $u_{i,t}$ to r .

The platform chooses the fees and controls the token price, P_t , by adjusting the token supply. This is akin to central banks using open market operations to intervene in the foreign exchange markets (e.g., [Calvo and Reinhart, 2002](#)). When the platform issues more tokens ($dS_t > 0$), it collects dollar revenues as users buy tokens with dollars. When the platform repurchases and burns tokens from users ($dS_t < 0$), it spends dollars to buy tokens from users.³⁵

Let M_t denote the dollar value of the platform's reserve assets. For simplicity, we do not microfound the composition of reserve assets and specify the following law of motion³⁶

$$dM_t = rM_t dt + (P_t + dP_t)dS_t + N_t f_t dt + N_t \sigma dZ_t - dDiv_t. \quad (8)$$

The first term is the interests earned on the reserves balance as r is the prevailing interest rate. The second term is the revenues (losses) from issuing (buying back) tokens the secondary market. From t to $t+dt$, the quantity adjustment dS_t is multiplied by the end-of-period price $P_{t+dt} = P_t + dP_t$. The third term is the fee. In the fourth term, Z_t is a standard Brownian motion, and its increment, dZ_t , captures the shocks to the reserve holdings, which can stem from unexpected operating expenses or risks in the reserve assets. This shock is the only source of uncertainty in the model, and it scales with dollar market capitalization of tokens, $S_t P_t = N_t$.³⁷ Let Div_t denote the *cumulative* dividend process. The platform's reserves decrease when the platform pays its owners dividends, $dDiv_t$. In the baseline, we assume $dDiv_t \geq 0$, reflecting that platform shareholders have limited liability and it is not possible to issue new equity. In [Section 4.2](#), we extend our model to incorporate (costly) equity issuance (i.e., $dDiv_t < 0$ ([Hennessy and Whited, 2005, 2007](#))).

The platform maximizes the expected discounted value of dividend payouts to its owners:

$$V_0 \equiv \max_{\{f_t, dS_t, dDiv_t\}} \mathbb{E} \left[\int_0^\infty e^{-\rho t} dDiv_t \right] \quad \text{subject to (8) and } dDiv_t \geq 0. \quad (9)$$

We assume that the platform's shareholders apply a discount rate ρ which exceeds the interest rate r , that is, $\rho > r$. The assumption that shareholders apply a higher discount rate than the interest rate on reserves is standard in dynamic liquidity management models (e.g., [Riddick and Whited, 2009](#); [Décamps, Mariotti, Rochet, and Villeneuve, 2011](#)) and made to rule out a degenerate solution

³⁵In practice, token burning is to send tokens to irretrievable digital addresses.

³⁶In [Appendix B.3](#), we consider a more general law of motion of M_t . [Section 5.3](#) studies the implications of regulating the riskiness of stablecoin reserve assets.

³⁷The assumption that reserve shocks scale with N_t is inconsequential for our main findings. [Appendix B.3](#) considers an alternative specification for the dynamics dM_t in which reserve shocks scale with the level of reserves M_t rather than with N_t . We show that the results remain qualitatively unchanged under this alternative specification.

in which the firm forever accumulates financial slack and never pays out dividends.³⁸

Liquidation. We assume that the platform is liquidated and its owners’ value falls permanently to zero when its equity (i.e., the excess reserves, $M_t - S_t P_t$) becomes negative. As we show below, the platform optimally maintains $M_t \geq S_t P_t$ to avoid liquidation so that the stablecoin is over-collateralized in equilibrium.³⁹ This distinguishes our analysis from the well-studied mechanism of bank runs that applies to under-collateralized stablecoins with a negative equity of the issuer, i.e., $M_t < S_t P_t$ (Routledge and Zetlin-Jones, 2021).⁴⁰ The case of over-collateralization is likely to be increasingly relevant under recent regulatory proposals and dramatic failure of under-collateralized stablecoins.⁴¹ The conventional wisdom is that debasement will not happen under over-collateralization (Brainard, 2019; G7 Working Group on Stablecoins, 2019; ECB Crypto-Assets Task Force, 2019; Massad, 2021; Gorton and Zhang, 2021). Our analysis below challenges this notion. In Appendix B.6, we present a model that allows under-collateralization (i.e., negative equity) and show that the dynamics are similar in the no-run equilibrium. In fact, as long as there exists a lower (liquidation) bound on equity (i.e., excess reserves), our qualitative results carry through.

4 Equilibrium

In this section, we characterize the analytical properties of the dynamic equilibrium and, to sharpen the economic intuition, we also provide graphical illustrations based on the numerical solutions.

4.1 Managing Stablecoin: Optimal Strategies

User Optimization. A representative user i solves the problem in (5) with the following first-order condition for $u_{i,t}$

$$N_t^\alpha u_{i,t}^{\beta-1} A^{(1-\alpha-\beta)} + \mu_t^P - f_t - \eta |\sigma_t^P| = r, \quad (10)$$

³⁸The wedge, $\rho - r$, can be microfounded with an exogenous Poisson-arriving liquidation with intensity $\rho - r$. The literature on agency cost of cash holdings also provides a rationale for why the return on liquidity holdings is below shareholders’ discount rate (Nikolov and Whited, 2014; Nikolov, Schmid, and Steri, 2019).

³⁹Our model features (small) diffusive shocks, so the platform can maintain $M_t \geq S_t P_t$ via continuous adjustments. If we do not assume liquidation upon $M_t \leq S_t P_t$, there can be under-collateralization and equilibrium multiplicity. On one equilibrium path, users never withdraw en masse and continuously trade tokens at the dynamic price P_t . The other equilibrium paths feature runs (related to the dynamics in Donaldson and Piacentino (2020)). In the no-run equilibrium our analysis carries through as long as there exists a liquidation lower bound on C_t .

⁴⁰Routledge and Zetlin-Jones (2021) study the speculative attacks on under-collateralized stablecoins that are akin to those on currencies (Morris and Shin, 1998; Goldstein, Ozdenoren, and Yuan, 2011).

⁴¹In December 2020, the U.S. house representatives proposed the Stablecoin Tethering and Bank Licensing Enforcement (STABLE) Act that emphasized full collateralization. On June 16, 2021, a bank run happened to IRON, a partially collateralized token. This was the first large-scale run in the cryptocurrency market (Tiwari, 2021).

so total utility from the marginal token holdings is equal to r , the user's discount rate and the prevailing interest rate which is users' (opportunity) cost of capital. The solution is

$$u_{i,t} = \left(\frac{N_t^\alpha A^{(1-\alpha-\beta)}}{r + f_t - \mu_t^P + \eta|\sigma_t^P|} \right)^{\frac{1}{1-\beta}}. \quad (11)$$

Users' choices exhibit strategic complementarity as $u_{i,t}$ increases in the aggregate value N_t .⁴² In equilibrium, $N_t = u_{i,t}$ under user homogeneity, which, through (11), implies

$$N_t = \frac{A}{(r + f_t - \mu_t^P + \eta|\sigma_t^P|)^{\frac{1}{1-\xi}}}. \quad (12)$$

To simplify the notations, we define $\xi \equiv \alpha + \beta$ (< 1). Aggregate token demand decreases in the fees, f_t , and depends on the token price dynamics, which the platform controls. This is the solution within the system throughput (i.e., $N_t < \bar{N}$); otherwise, we have $u_{i,t} = N_t = \bar{N}$. Note that N_t quantifies token usage and can be interpreted as transaction volume.

Platform Optimization. To solve for the platform's optimal strategies, we first note that, given the token price dynamics (i.e., μ_t^P and σ_t^P), the platform can directly set N_t through the fees f_t . Rearranging (12), we can back out the fees implied by the platform's choice of N_t :

$$f_t = \left(\frac{A}{N_t} \right)^{1-\xi} - r + \mu_t^P - \eta|\sigma_t^P|. \quad (13)$$

Using (13), we substitute out f_t in the law of motion of reserves (8) and obtain

$$dM_t - (P_t + dP_t)dS_t = rM_t dt + N_t^\xi A^{1-\xi} dt - rN_t dt + N_t (\mu_t^P - \eta|\sigma_t^P|) dt + N_t \sigma dZ_t - dDiv_t. \quad (14)$$

Next, we show the state variable for the platform's dynamic optimization is the *excess reserves*,

$$C_t \equiv M_t - S_t P_t. \quad (15)$$

⁴²There is a trivial equilibrium where $u_{i,t} = N_t = 0$. We focus on the Pareto-dominant equilibrium where $N_t > 0$.

To derive the law of motion of C_t , we first note that

$$\begin{aligned} dC_t &= dM_t - d(S_t P_t) = dM_t - (P_t + dP_t)dS_t - S_t dP_t \\ &= dM_t - (P_t + dP_t)dS_t - N_t (\mu_t^P dt + \sigma_t^P dZ_t) . \end{aligned} \quad (16)$$

The second equality uses $d(S_t P_t) = dS_t P_t + S_t dP_t + dS_t dP_t$ (by Itô's lemma) and the last equality uses (1) and $N_t = S_t P_t$. From a balance-sheet perspective, the reserves, M_t , are the platform's assets and the outstanding tokens, $S_t P_t$, are the liabilities. The excess reserves constitute the (book) equity. Thus, equation (16) is essentially the differential form of the balance-sheet identity. Using (14) to substitute out $dM_t - (P_t + dP_t)dS_t$ in (16), we obtain the following law of motion:

$$dC_t = \left(rC_t + N_t^\xi A^{1-\xi} - N_t \eta |\sigma_t^P| \right) dt + N_t (\sigma - \sigma_t^P) dZ_t - dDiv_t, \quad (17)$$

with drift $\mu_{C,t} \equiv rC_t + N_t^\xi A^{1-\xi} - N_t \eta |\sigma_t^P|$ and diffusion $\sigma_{C,t} \equiv N_t (\sigma - \sigma_t^P)$. Note that $N_t \mu_t^P$ disappears. As shown in (14), the platform receives more fee revenues (see (13)) when users expect tokens to appreciate ($N_t \mu_t^P$), but such revenues do not increase the platform's excess reserves as they are cancelled out by the appreciation of token liabilities. After netting out the two forces, the drift term, $rC_t + N_t^\xi A^{1-\xi} - N_t \eta |\sigma_t^P|$, is the expected appreciation of the platform's excess reserves.

The platform controls the law of motion of C_t through dividend payouts, $dDiv_t$, aggregate token demand, N_t (or equivalently, fees f_t), and token price volatility σ_t^P . We will show that once we solve for these optimal control variables, the equilibrium processes of token supply, S_t , and token price, P_t , can be obtained. We characterize a Markov equilibrium with the platform's excess reserves, C_t , as the only state variable. We solve for the platform's control variables, $dDiv_t$, σ_t^P , and N_t , as functions of C_t , and thereby, show that (17) is an autonomous law of motion of C_t .

The platform owners' value function at time t is given by

$$V_t = V(C_t) = \max_{\{N, \sigma^P, Div\}} \mathbb{E} \left[\int_{s=t}^{\infty} e^{-\rho(s-t)} dDiv_s \right]. \quad (18)$$

The platform pays dividends when the marginal value of excess reserves is equal to one, i.e., one dollar has the same value either held within the platform or paid out,

$$V'(\bar{C}) = 1. \quad (19)$$

The optimality of payouts at \bar{C} also requires the following super-contact condition (Dumas, 1991),

$$V''(\bar{C}) = 0. \quad (20)$$

The next proposition states that the value function is concave. The declining marginal value of excess reserves implies that \bar{C} in (19) is an endogenous upper bound of the state variable C_t . At any $C_t \in (0, \bar{C})$, the platform does not pay dividends to its owners because the marginal value of excess reserves, $V'(\bar{C})$, is greater than one, i.e., the owners' value of dividend.

Proposition 1 (Value Function and Optimal Payout). *There exists $\bar{C} > 0$ such that $C_t \leq \bar{C}$. For $C_t < \bar{C}$, the value function is strictly concave, and $V'(C_t) > 1$. At $C_t = \bar{C}$, $V'(\bar{C}) = 1$ and the platform pays dividends when $dC_t > 0$ so that dividend payments cause C_t to reflect at \bar{C} .⁴³*

Before characterizing the solution as C_t approaches zero (the lower boundary), we note that

$$\max_{\{N \in [0, \bar{N}]\}} \left\{ N^\xi A^{1-\xi} - \eta N \sigma \right\} > 0, \quad (21)$$

because $N^\xi A^{1-\xi} - \eta N \sigma = 0$ at $N = 0$ and, under $\xi = \alpha + \beta < 1$ as previous stated, the first derivative goes to infinity as N approaches zero, (i.e., $\lim_{N \rightarrow 0} \xi \left(\frac{A}{N}\right)^{1-\xi} - \eta \sigma = +\infty$).

As C_t approaches zero, the platform can only avoid liquidation by reducing the diffusion of C_t (i.e., the shock exposure $\sigma_C(C_t) = N_t(\sigma - \sigma_t^P)$) to zero, which requires

$$\lim_{C \rightarrow 0^+} \sigma^P(C) = \sigma, \quad (22)$$

and by keeping the drift of C_t (i.e., $\mu_C(C_t) = rC_t + N_t^\xi A^{1-\xi} - N_t \eta |\sigma_t^P|$) non-negative, which is already guaranteed by (21) under (22). It is optimal to do so and avoid liquidation because, as we show below, the value of platform as an ongoing concern is positive. In the region $C \in (0, \bar{C})$, we obtain the following Hamilton-Jacobi-Bellman (HJB) equation (with time subscripts suppressed):

$$\rho V(C) = \max_{\{N \in [0, \bar{N}], \sigma^P\}} \left\{ V'(C) \left(rC + N^\xi A^{1-\xi} - \eta N |\sigma^P| \right) + \frac{1}{2} V''(C) N^2 (\sigma - \sigma^P)^2 \right\}. \quad (23)$$

⁴³When $dC_t > 0$ at $C_t = \bar{C}$, the dividend amount is equal to dC_t (i.e., exactly the amount needed to avoid $C_t > \bar{C}$).

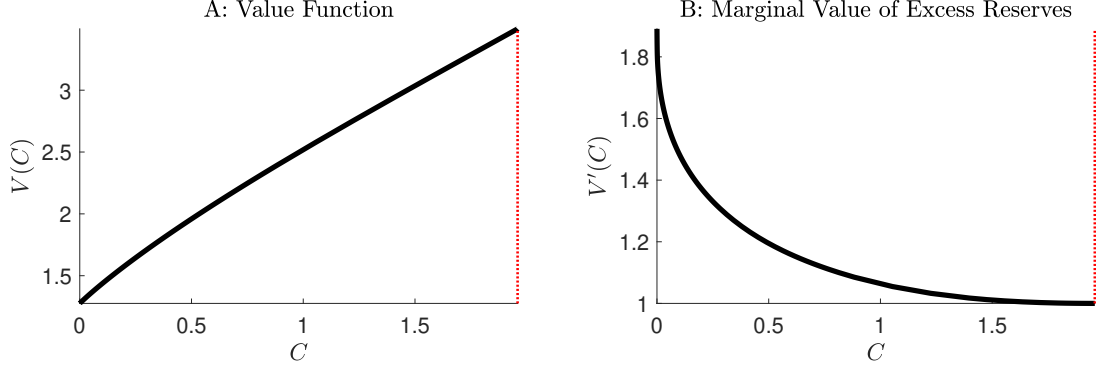


Figure 2: **Value Function.** This illustrates the level and first derivative of the platform's value function. The red dotted lines in both panels mark \bar{C} (defined in Proposition 1). The parameters are $r = 0.05$, $\rho = 0.06$, $\sigma = 0.1$, $\bar{N} = 5$, $\eta = 0.15$, $\alpha = 0.45$, $\beta = 0.05$, and $A = 0.0025$.

Setting $\sigma^P = \sigma$ is always feasible in the HJB equation, which implies:

$$\begin{aligned}
 V(C) &\geq \frac{V'(C)}{\rho} \left(rC + \max_{\{N \in [0, \bar{N}]\}} \{N^\xi A^{1-\xi} - \eta N \sigma\} \right) \\
 &\geq \frac{1}{\rho} \left(\max_{\{N \in [0, \bar{N}]\}} \{N^\xi A^{1-\xi} - \eta N \sigma\} \right) > 0,
 \end{aligned} \tag{24}$$

where the second inequality uses $C \geq 0$ and $V'(C) \geq 1$ and the last inequality follows (21). By the continuity of the value function $V(C)$, a strictly positive lower bound of $V(C)$ on $(0, \bar{C})$ implies that $\lim_{C \rightarrow 0} V(C) > 0$. In sum, we have shown that it is optimal for the platform to implement (22) and thereby avoid liquidation because the value as an ongoing concern is positive as C_t approaches zero. Finally, (22) implies that, when taking the right-limit on both sides of (23), we obtain

$$\lim_{C \rightarrow 0^+} \frac{V(C)}{V'(C)} = \frac{1}{\rho} \max_{\{N \in [0, \bar{N}]\}} \{N^\xi A^{1-\xi} - \eta N \sigma\} = \frac{1}{\rho} \{ \underline{N}^\xi A^{1-\xi} - \eta \underline{N} \sigma \} > 0, \tag{25}$$

where the second equality follows from plugging in the optimal N_t given by

$$\underline{N} \equiv \lim_{C \rightarrow 0^+} N(C) = \arg \max_{N \in [0, \bar{N}]} \{N^\xi A^{1-\xi} - \eta N \sigma\} = A \left(\frac{\xi}{\eta \sigma} \right)^{\frac{1}{1-\xi}} \wedge \bar{N} > 0. \tag{26}$$

The condition (25) serves as another boundary condition for the HJB equation.

As an interim summary, the next proposition summarizes the value function solution as solution to an ordinary differential equation (ODE) problem with an endogenous boundary \bar{C} . Figure 2 plots the numerical solution of value function (Panel A) and the decreasing marginal value of excess

reserves with the red dotted line marking the payout boundary \bar{C} .

Proposition 2 (Value Function). *The value function, $V(C)$, and the boundary \bar{C} solve the ODE (23) on $(0, \bar{C})$ subject to the boundary conditions (19), (20), and (25).*

Next, we fully characterize the platform's optimal choices of σ_t^P and N_t as functions of the state variable, C_t (via the derivatives of $V(C)$). First, we define the platform's *effective risk aversion*:

$$\gamma(C) \equiv -\frac{V''(C)}{V'(C)}. \quad (27)$$

This definition is analogous to the classic measure of absolute risk aversion of consumers (Arrow, 1965; Pratt, 1964). From Proposition 1, $\gamma(C) \geq 0$ and, in $(0, \bar{C})$, $\gamma(C) > 0$. The next proposition states the monotonicity of $\gamma(C)$ in C and summarizes the optimal $\sigma_t^P = \sigma^P(C_t)$ and $N = N(C_t)$.

Proposition 3 (Risk Aversion, Token Volatility, and Token Usage). *The platform's effective risk aversion, $\gamma(C)$, strictly decreases in the level of excess reserve holdings, C . There exists $\tilde{C} \in (0, \bar{C})$ such that, at $C \in (0, \tilde{C})$, $N(C) = \underline{N}$ and $\sigma^P(C)$ strictly decreases in C , given by,*

$$\sigma^P(C) = \sigma - \frac{\eta}{\gamma(C)\underline{N}} \in (0, \sigma), \quad (28)$$

and at $C \in [\tilde{C}, \bar{C}]$, $\sigma^P(C) = 0$ and $N(C)$ increases in C , given by

$$N(C) = \min \left\{ \left(\frac{\xi A^{1-\xi}}{\gamma(C)\sigma^2} \right)^{\frac{1}{2-\xi}}, \bar{N} \right\}. \quad (29)$$

When the platform's reserves are low, i.e., $C \in (0, \tilde{C})$, it is the ratio of users' risk aversion to the platform's risk aversion that determines token volatility. Equation (28) shows that, in this region, when the platform accumulates more reserves and becomes less risk-averse, it absorbs risk from users by tuning down σ_t^P , and when the platform exhausts its reserves, it off-loads the risk in its dollar revenues to users.⁴⁴ The platform and its users engage actively in risk-sharing when $C \in (0, \tilde{C})$. This is illustrated by the numerical solution in Panel A of Figure 3 with \tilde{C} marked by the dashed line. In Panel B, we show that the platform's risk aversion declines in C . In this region of low reserves, transaction volume is pinned to the lowest level given by \underline{N} in (26).

Once the platform's reserves surpass the critical threshold \tilde{C} , its risk aversion becomes sufficiently low and it optimally absorbs all the risk in its dollar revenues, setting $\sigma^P(C)$ to zero which

⁴⁴Equation (28) implies that the condition (25) is equivalent to $\gamma(C)$ (or $-V''(C)$) approaching infinity in the limit.

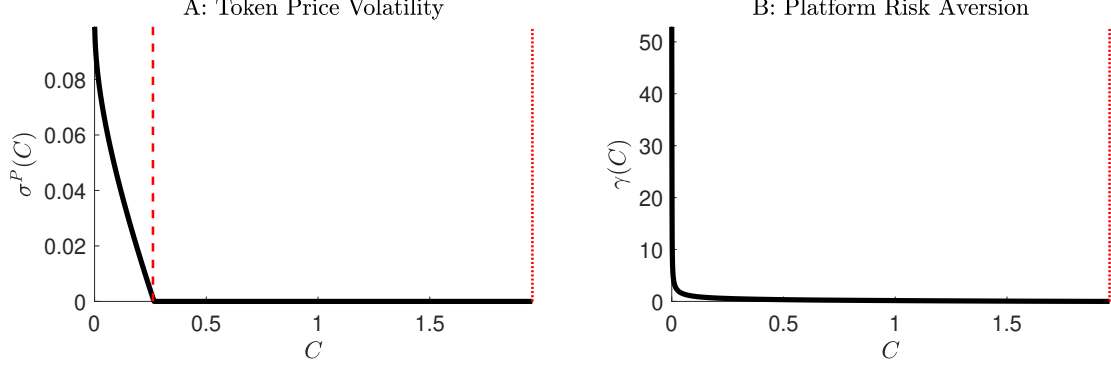


Figure 3: Token Volatility and Platform Risk Aversion. This figure plots token return volatility $\sigma^P(C)$ in Panel A and the effective risk aversion $\gamma(C)$ in Panel B. In Panel A, the red dashed line marks \tilde{C} (in Proposition 3). The red dotted lines in both panels mark \bar{C} (in Proposition 1). The parameterization follows Figure 2.

also implies that in this region $\mu^P(C) = 0$.⁴⁵ As a result, transaction volume starts to rise above the “hibernation level”, \underline{N} , as illustrated by Panel A of Figure 4. Therefore, reserves are absolutely essential for stimulating economic activities on a stablecoin platform.

Interestingly, even though the platform shelters its users from risk at any $C > \tilde{C}$, its risk aversion still shows up in N_t given by (29). As shown in (13), the choice of N_t is implemented through fees. Therefore, the intuition can be more easily explained when we substitute (29), the optimal N_t , and the optimal $\sigma_t^P = 0$ (as well as $\mu_t^P = 0$) into (13) to solve f_t : when $\left(\frac{\xi A^{1-\xi}}{\gamma(C)\sigma^2}\right)^{\frac{1}{2-\xi}} < \bar{N}$,

$$f(C) = \left(\frac{A\gamma(C)\sigma^2}{\xi}\right)^{\frac{1-\xi}{2-\xi}} - r, \quad (30)$$

i.e., the platform charges higher fees to build up its reserves when its precautionary savings motive is strong ($\gamma(C)$ is higher); when $\left(\frac{\xi A^{1-\xi}}{\gamma(C)\sigma^2}\right)^{\frac{1}{2-\xi}} \geq \bar{N}$, i.e., C is sufficiently high such that $\gamma(C)$ falls below $\frac{\xi A^{1-\xi}}{\sigma^2 \bar{N}^{2-\xi}}$, the platform de-links the fees from its risk aversion,

$$f(C) = \left(\frac{A}{\bar{N}}\right)^{1-\xi} - r. \quad (31)$$

The platform faces a risk-return trade-off. The fees serve as a compensation for risk exposure but discourages users from participation. So when the platform’s risk aversion rises, it charges users more per dollar of transaction at the expense of a smaller volume. When the platform’s risk

⁴⁵This result arises because we express the equilibrium token price as a function of C , in that $P_t = P(C_t)$. Thus, token volatility and token returns can be expressed as functions of C too, in that $\sigma_t^P = \sigma^P(C_t)$ and $\mu_t^P = \mu^P(C_t)$. Since $\sigma^P(C) = 0$ for $C > \tilde{C}$, $P'(C)$ must be zero by Itô’s lemma (i.e., $P(C)$ is constant), implying $\mu^P(C) = 0$.

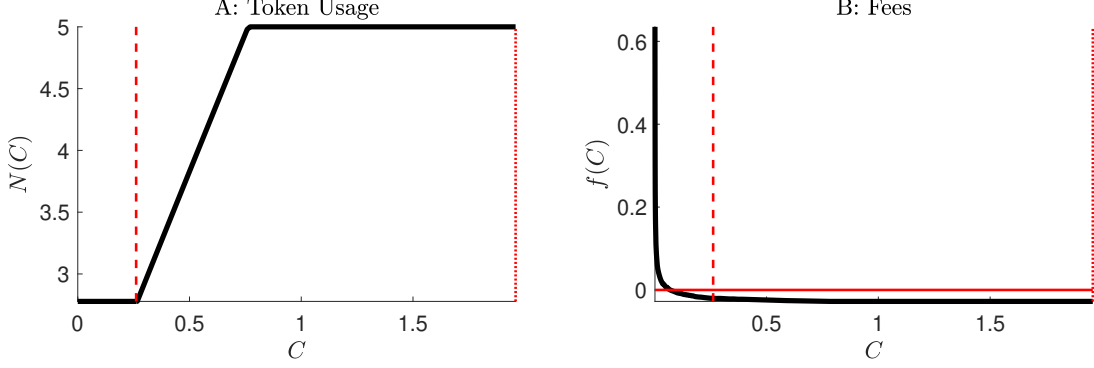


Figure 4: **Token Usage and Fees.** This figure plots token usage $N(C)$ in Panel A and user fees $f(C)$ in Panel B. The red dotted line marks \bar{C} (in Proposition 1). In both panels, the red dashed line marks \tilde{C} (in Proposition 3). In Panel B, the red solid line marks zero. The parameterization follows Figure 2.

aversion declines, the fees decline while the total total usage increases. Once reserves are sufficiently high such that $\gamma(C) \leq \frac{\xi A^{1-\xi}}{\sigma^2 \bar{N}^{2-\xi}}$, the fees no longer decline with the platform's risk aversion, as the platform has maxed out its transaction capacity, i.e., $N_t = \bar{N}$, and it becomes impossible to further stimulate user participation. Likewise, when the platform's reserves are below \tilde{C} and $\sigma^P(C) > 0$, $N_t = \underline{N}$, and the fees are given by

$$f(C) = \left(\frac{A}{\underline{N}}\right)^{1-\xi} + \mu^P(C) - \eta\sigma^P(C) - r. \quad (32)$$

Even though the platform's risk aversion is high, it no longer sacrifices transaction volume for higher fees because user participation has already fallen to a very low level.

Panel B of Figure 4 plots the numerical solution of optimal fees that decrease in excess reserves. Depending on the parameters, fees can actually turn into user subsidies (i.e., fall below zero) when excess reserves are sufficiently high.⁴⁶ The next corollary summarizes the results on fees.

Corollary 1 (Optimal Fees). *Fees, $f(C)$, decrease in excess reserves, C . At $C \in (0, \tilde{C})$, where \tilde{C} is defined in Proposition 3, fees are given by (32). At $C \in [\tilde{C}, \tilde{C}')$, where \tilde{C}' is defined by $\gamma(\tilde{C}') = \frac{\xi A^{1-\xi}}{\sigma^2 \bar{N}^{2-\xi}}$, fees are given by (30). At $C \in [\tilde{C}', \bar{C})$, where \bar{C} is defined in Proposition 1, fees are given by (31).*

When C is below \tilde{C} , an interesting implication of (32) is that the platform charges (compensates) users the expected appreciation (depreciation) of tokens over risk-free rate (i.e., $\mu_t^P - r$ shows up

⁴⁶Specifically, under the particular parameterization, the condition is for fees to turn into subsidies near \bar{C} is that $\frac{A^{1-\xi}}{\bar{N}^{1-\xi}} < r$ where we use (31) and the fact that $\mu^P(C) = 0$ for $C \in (\tilde{C}, \bar{C})$ (to be discussed later in this section).

in f_t). To fully solve the fees, we need to know both $\gamma(C_t)$ and the function $\mu_t^P = \mu^P(C_t)$. In fact, the platform's choice of $\sigma_t^P = \sigma^P(C_t)$ already pins down the function of token price, $P_t = P(C_t)$, so $\mu^P(C_t)$ can be obtained from Itô's lemma. Next, we solve $P_t = P(C_t)$ from the function $\sigma^P(C_t)$. By Itô's lemma,

$$\sigma^P(C) = \frac{P'(C)}{P(C)} N(C) (\sigma - \sigma^P(C)) , \quad (33)$$

where $N(C) (\sigma - \sigma^P(C))$ is the diffusion of state variable C . Using Proposition 2, we solve the value function $V(C)$ and obtain $\gamma(C)$. Using Proposition 3, we obtain the functions $\sigma^P(C)$ and $N(C)$. Plugging $\sigma^P(C)$ and $N(C)$ into (33), we obtain a first-order ODE for the function $P(C)$.

To uniquely solve the function $P(C)$, we need to augment the ODE (33) with a boundary condition. In our model, both the platform and users are not concerned with the level of token price and only care about the expected token return, μ_t^P , and volatility, σ_t^P . Therefore, we have the liberty to impose the following boundary condition:

$$P(\bar{C}) = 1 . \quad (34)$$

i.e., the platform sets an exchange rate of one dollar for one token when C_t reaches \bar{C} . The next corollary states the solution of token price as solution to a first-order ODE problem.

Corollary 2 (Solving Equilibrium Token Price). *Given the solutions of $V(C)$ (and $\gamma(C)$) from Proposition 2 and $\sigma^P(C)$ and $N(C)$ from Proposition 3, the equilibrium dollar price of token, $P(C)$, is a function of C that solves the ODE (33) under the boundary condition (34).*

Proposition 3 states that, once C crosses above the critical threshold \tilde{C} , $\sigma^P(C) = \mu^P(C) = 0$, which, by Itô's lemma, implies that $P'(C) = 0$. Therefore, if the platform's reserves are sufficiently high, it optimally fixes the dollar price (or the redemption value by no arbitrage) of token at $P(C) = 1$. When C falls below \tilde{C} , (33) implies that $P'(C) > 0$ (because $\sigma^P(C) \in (0, \sigma)$ in Proposition 3) so token price comoves with the platform's excess reserves.

The endogenous transition between $P_t = 1$ and $P_t < 1$ happens as the platform accumulates or depletes reserves through various activities laid out in (8) (and then in (17)), including the platform's issuance of new tokens ($dS_t > 0$), users' token redemption ($dS_t < 0$), fee revenues, and shocks to the dollar reserves. The platform's choice of token price is optimally chosen and thus credible in the sense that it the platform does not have any incentives to deviate.

Proposition 4 (Endogenous Token Price Regimes). *At $C \in [\tilde{C}, \bar{C}]$, where \tilde{C} is defined in*

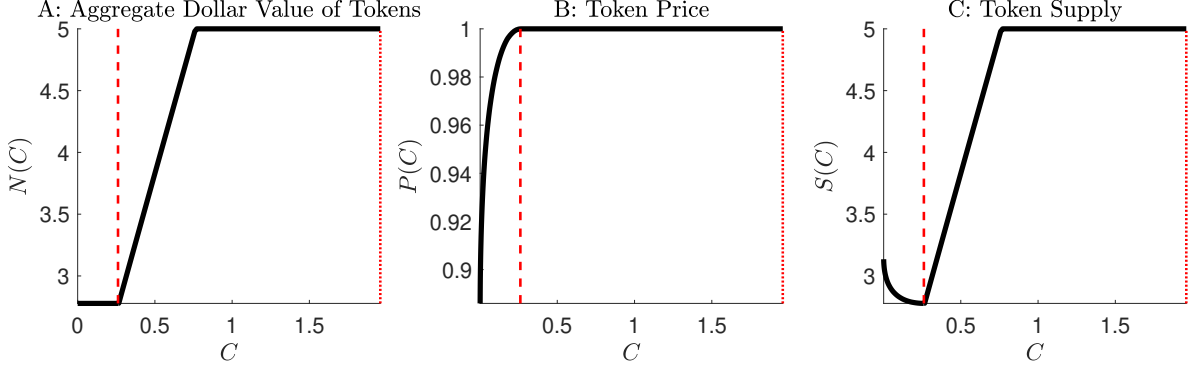


Figure 5: Token Price and Quantity Dynamics. This figure plots the aggregate dollar value of tokens $N(C)$ in Panel A, token price $P(C)$ in Panel B, and token supply $S(C)$ in Panel C. The red dotted lines in all panels mark \bar{C} (defined in Proposition 1). The red dashed lines in all panels mark \tilde{C} (defined in Proposition 3). The parameterization follows Figure 2.

Proposition 3, the platform maintains token price equal to one, i.e., $P(C) = 1$. At $C \in (0, \tilde{C})$, token price comoves with the platform’s excess reserves (i.e., $P'(C) > 0$).

Proposition 4 states that token price stays at one if and only if the platform holds a sufficiently large amount of *excess* reserves ($C > \tilde{C}$). When excess reserves fall below \tilde{C} , the platform optimally debases its tokens. By allowing token price to comove with its excess reserves, the platform off-loads the risk in its dollar reserves to users and thereby prevents liquidation.

Figure 5 plots the numerical solutions of aggregate token value, $N(C) = S(C)P(C)$ (Panel A), token price $P(C)$ (Panel B), and the total quantity of tokens $S(C)$ implied by $N(C)$ and $P(C)$ (Panel C). The dashed line marks \tilde{C} . The platform implements the optimal token price through the manipulation of token supply. When the platform has enough reserves to credibly sustain $P_t = 1$ (i.e., $C > \tilde{C}$), token supply comoves with demand so that $P(C)$ is fixed at one. Below \tilde{C} , a decrease of reserves triggers the platform to supply more tokens in exchange for dollars that replenish reserves. The users respond to token debasement by reducing their token demand to \underline{N} , which in turn reinforces the debasement by reducing the platform’s revenues from open market operations (i.e., $dS_t > 0$) and fees. The system falls into an instability trap.

In practice, stablecoin platforms often claim commitment to maintain a stable token price and substantiate their claims by holding reserves that cover token liabilities. However, such a claim is only credible (incentive-compatible) if the excess reserves are sufficiently high; otherwise, as shown in Proposition 4, it is in the platform’s interest to debase its tokens.

Using parameters in Figure 2 and numerical solutions, we simulate in Figure 6 a path of C_t (Panel A), token price P_t (Panel B), token supply S_t (Panel C), and transaction volume N_t (Panel

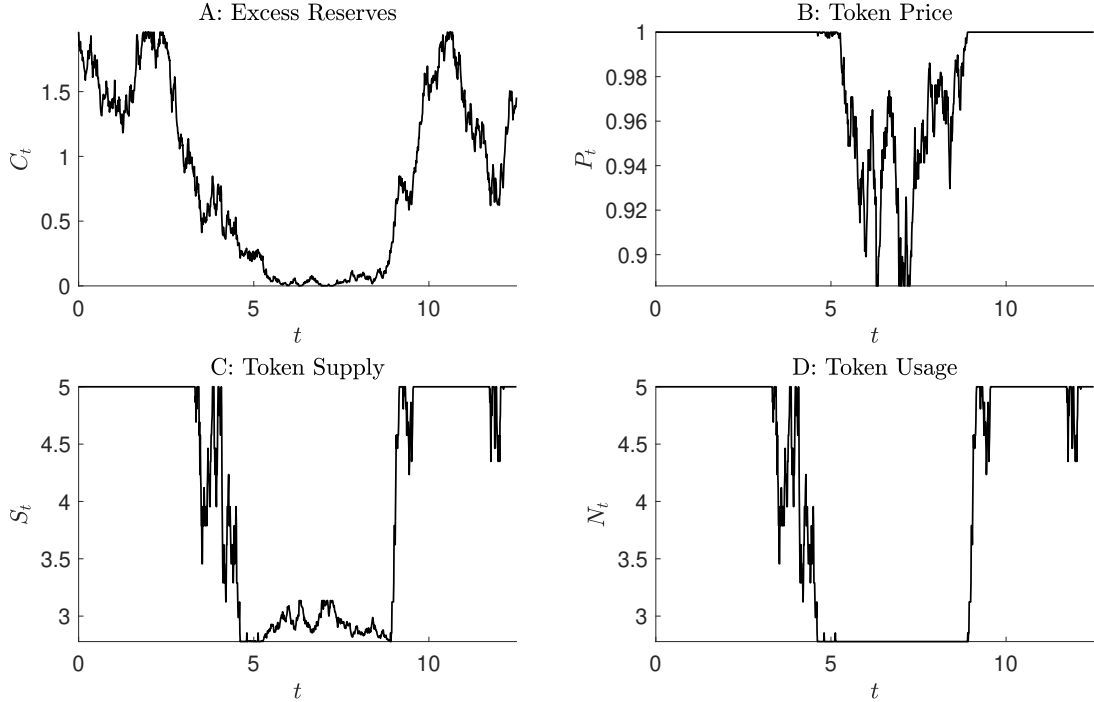


Figure 6: **The Instability Trap in Simulation.** Using the numerical solutions, we simulate a path of excess reserves (Panel A), token price (Panel B), token supply (Panel C), and token usage (Panel D). The horizontal axis records the number of years. The parameterization follows Figure 2.

D). The horizontal axis records the number of years. In the first three years, in spite of the volatility in C_t , the platform manages to sustain a stable token price, and with the transaction volume (or token demand) at the full capacity at \bar{N} , a fixed dollar price of token implies a fixed token supply. Following a sequence of negative shocks between the third and fourth years, the platform raises fees. Users respond by reducing their token demand N_t , so the platform reduces token supply, maintaining $P_t = 1$. The platform optimally trades off replenishing dollars reserves by raising fees and using dollar reserves in token buy-back. As more negative shocks hit between the fourth and ninth years, the platform gives up the peg and off-loads risk to users through the fluctuation of token price. Users' token demand hits \underline{N} , and the platform starts actively expanding token supply in exchange for dollar revenues. Then following a sequence of positive shocks, the recovery started in the ninth year, and by the tenth year, the platform finally restores token price back to one.

We demonstrate the long-run dynamics of the model in Figure 7. Panel A plots the stationary probability density of excess reserves. It shows how much time over the long run the platform spends in different regions of C . The distribution is bimodal. The concentration of probability mass near $C = 0$ is due to the fact that, when the transaction volume (or token demand) gets stuck at the

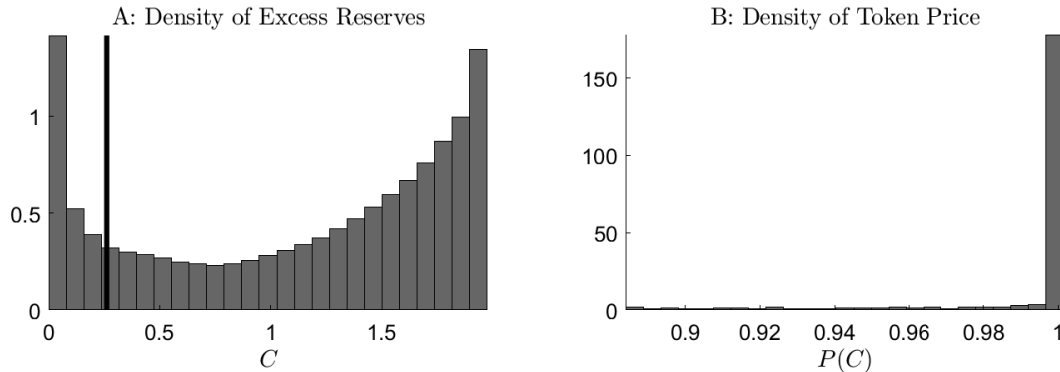


Figure 7: **Long-Run Dynamics and Stationary Density.** We plot stationary probability densities of excess reserves C (Panel A) and token value $P(C)$ (Panel B) in numerical solutions. The solid black line in Panel A depicts $C = \tilde{C}$. The parameterization follows Figure 2.

hibernation level \underline{N} , the platform can only grow out of this region very slowly by accumulating reserves through fee revenues and proceeds from expanding token supply. The platform also spends a lot of time near the payout boundary \bar{C} as this is a stable region where, given a sufficiently high level of reserve buffer, shocks’ impact is limited. In Panel B, we show that, even though $P_t = 1$ seems to be the norm, the system exhibits significant risk of token debasement ($P(C) < 1$), so the stationary probability density of token price has a very long left tail.

4.2 The Optimal Issuance of Equity and Governance Tokens

In this subsection, we take an excursion to analyze the issuance of platform equity (or “governance tokens”). In practice, governance tokens are popular among stablecoin platforms as means of financing. For example, MakerDAO, the issuer of DAI (one of the top five stablecoins by market value), introduced its governance tokens MKR. MKR holders vote on protocol changes and receive payout via buy-backs, just like stock market investors receive payout through share repurchases.

So far, the platform recovers from the low- C region through the accumulation of internal funds. We now allow the platform to raise dollar funds by issuing equity shares subject to a fixed financing cost, χ_0 , and a proportional cost, χ_1 , following [Gao, Whited, and Zhang \(2020\)](#).⁴⁷

⁴⁷Firms face significant financing costs due to asymmetric information and incentive issues. A large literature has sought to measure these costs, in particular, the costs arising from the negative stock price reaction in response to the announcement of a new issue. [Lee, Lochhead, Ritter, and Zhao \(1996\)](#) document that for initial public offerings (IPOs) of equity, the direct costs (underwriting, management, legal, auditing and registration fees) average 11.0% of the proceeds, and for seasoned equity offerings (SEOs), the direct costs average 7.1%. IPOs also incur a substantial indirect cost due to short-run underpricing. An early study by [Asquith and Mullins \(1986\)](#) found that the average stock price reaction to the announcement of a common stock issue was -3% and the loss in equity value as a percentage of the size of the new equity issue was as high as -31% (see [Eckbo, Masulis, and Norli, 2007](#), for a survey).

To characterize the optimal issuance policy, we first note that when issuing equity, the platform raises funds so that C jumps from the (lower) issuance boundary, denoted by \underline{C} , to an interior value \widehat{C} where $V'(\widehat{C}) = 1 + \chi_1$, that is when the issuance amount is $\widehat{C} - \underline{C}$, the marginal contribution of equity issuance to platform value is equal to the marginal cost of issuing new shares. Note that $\widehat{C} \leq \bar{C}$ (the payout boundary) because $V'(\widehat{C}) = 1 + \chi_1 \geq V'(\bar{C}) = 1$ under the concavity of $V(C)$. Next, we show that the platform issues equity only when C falls to zero (i.e., $\underline{C} = 0$).

Consider the *change* of existing shareholders' value after equity issuance: $[V(\widehat{C}) - (\widehat{C} - \underline{C}) - \chi_0 - \chi_1(\widehat{C} - \underline{C})] - V(\underline{C})$. To obtain the post-issuance value of existing shareholders, we deduct the competitive new investors' equity value (equal to the funds they invested), $(\bar{C} - \underline{C})$, and deduct the fixed and proportional issuance costs from the total platform value post-issuance, $V(\widehat{C})$. To calculate the change, we subtract $V(\underline{C})$, the value without issuance. Taking derivative with respect to \underline{C} , we obtain $1 + \chi_1 - V'(\underline{C}) < 0$ for $\underline{C} < \widehat{C}$ because $V'(\underline{C}) > V'(\widehat{C}) = 1 + \chi_1$ under the concavity of $V(C)$.⁴⁸ Therefore, the platform prefers \underline{C} to be as low as possible and optimally sets it to zero.

Finally, as in the baseline model, the platform can avoid liquidation by off-loading risk to users, as shown in (22), and obtain the value given by (25). Therefore, as C approaches zero, the platform only opts for recapitalization at $C = 0$ if recapitalization generates a higher value than liquidation. Accordingly, the lower boundary condition (25) for the value function is modified to

$$\lim_{C \rightarrow 0^+} V(C) = \max \left\{ \lim_{C \rightarrow 0^+} \frac{V'(C)}{\rho} \left\{ \underline{N}^\xi A^{1-\xi} - \eta \underline{N} \sigma \right\}, V(\widehat{C}) - \widehat{C} - \chi_0 - \chi_1 \widehat{C} \right\}, \quad (35)$$

The first term in the max operator is the value obtained from off-loading risk to users, given by (25). The second term is the post-issuance value for existing shareholders. The results in Proposition 1 to 3 and Corollary 1 still hold except that the boundary condition (25) is replaced by (35) with \widehat{C} determined by $V'(\widehat{C}) = 1 + \chi_1$ as previously discussed.

Proposition 5 (Optimal Equity Issuance). *The platform raises external funds through equity issuances only if $C_t = 0$ and when $V(\widehat{C}) - \widehat{C} - \chi_0 - \chi_1 \widehat{C} > \lim_{C \rightarrow 0^+} \frac{V'(C)}{\rho} \{ \underline{N}^\xi A^{1-\xi} - \eta \underline{N} \sigma \}$ (see (35)), where the optimal issuance amount \widehat{C} is given by $V'(\widehat{C}) = 1 + \chi_1$.*

Figure 8 illustrates the solution through a numerical example of costly equity issuance under our baseline parameters and $\chi_0 = 1$ and $\chi_1 = 0.1$. The platform optimally raises new equity when C falls to zero. Notably, there are three lines of defense to avoid liquidation: i) platform

⁴⁸To prove the concavity of value function stated in Proposition 1, we only need the HJB equation (23) and the upper boundary conditions (19) and (20), so recapitalization does not affect value function concavity.

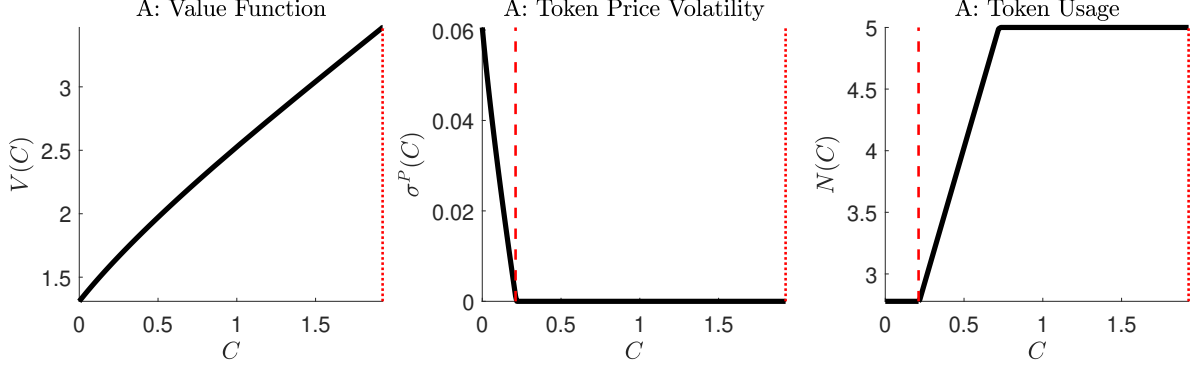


Figure 8: **Solution with Costly Equity Issuance.** In this figure, we plot the valuation function (Panel A), token price volatility (Panel B), and token demand or users' transaction volume (Panel C). The parameterization follows Figure 2, and we set $\chi_0 = 1$ and $\chi_1 = 0.1$. The curves start at $C = 0$, the equity issuance boundary.

(excess) reserves C , ii) debasement $\sigma^P > 0$, and iii) equity issuance. Under these parameter values, our model suggests a pecking order. First, the platform covers negative shocks by drawing on its reserves. Second, the platform debases token price to share risk with users. Third, the platform raises equity and incurs the issuance costs. If the equity issuance costs are sufficiently large, the platform does not raise equity and the solution is the one from the baseline without equity issuance. If, on the other hand, the equity issuance costs are sufficiently small, the platform may not debase the token prior to issuing equity and thus token price remains stable at all times.

Suppose that the equity issuance costs are such that the platform i) recapitalizes once C reaches zero and ii) debases token price prior to equity issuance. Note that when recapitalization happens, C_t jumps from zero to \widehat{C} , which then implies an upward jump in the token demand from $N(0)$ to $N(\widehat{C})$ (for $N(0) < N(\widehat{C})$, see Proposition 3). If the platform does not adjust the token supply, S_t , there will be an upward *predictable* jump in P_t , which implies an arbitrage opportunity. To preclude arbitrage, the platform must expand token supply simultaneously as it issues equity so that the token price stays at the pre-issuance level.⁴⁹ Let us revisit the results on the token price level in Corollary 2 and Proposition 4. Let $P_j(C)$ denote the token price function after the j -th recapitalization. We have

$$P_j(\widehat{C}) = P_{j-1}(0), \quad (36)$$

which replaces (34) as the boundary condition for the price-level ODE (33). Token price level before the first recapitalization, $P_0(C)$ is still solved under the boundary condition (34), i.e., $P_0(\overline{C}) = 1$.

⁴⁹Note that the expansion of token supply brings dollars of equal value into the reserve portfolio. This simultaneous expansion of assets and liabilities does not imply any variation in the excess reserves C_t at \overline{C} .

Corollary 3 (Recapitalization and Token Price Level). *Token price after the j -th recapitalization is solved by the ODE (33) subject to the boundary condition (36).*

In the baseline model without equity issuance, the debasement of token is temporary: token price level falls below 1 when C falls below \tilde{C} due to negative shocks and it recovers back to 1 when the platform accumulates sufficient amount of dollar revenues so that C crosses above \tilde{C} (Proposition 4). When recapitalization happens, the debasement is permanent. After the j -th recapitalization, token price level starts anew at a lower peg, $P_j(\hat{C}) = P_{j-1}(0)$, and if negative shocks deplete the platform’s reserves and triggers another recapitalization, token price level declines along the process and, right after recapitalization, stabilizes at an even lower peg, $P_{j+1}(\hat{C}) = P_j(0)$.

5 Regulating Stablecoins

We analyze three types of regulations. The first type, which is of our focus, stipulates a minimum level of excess reserves (“capital requirement”). The rationale behind is to generate a sufficient risk buffer so that the issuer is unlikely to debase the token. The second type (“stability regulation”) is more direct. It forces the platform to keep the token price fixed. The third type stipulates the riskiness of reserve assets. Our conclusion is that capital requirement, if carefully designed, improves welfare. Stability regulation, in contrast, destroys the economic surplus from risk-sharing, and regulating the riskiness of reserve assets may backfire and destabilizes token price due to the platform endogenous response in its reserve management decisions.

5.1 Capital Requirement

The regulator requires $C \geq C_L$ and forces the platform to liquidate if the requirement is violated. Therefore, C_L replaces zero as the lower (liquidation) bound of excess reserves.⁵⁰ In Figure 9, we plot the payout boundary \bar{C} (Panel A), which is a measure of voluntary over-collateralization, and the welfare measures for different values of C_L . Not so surprisingly, when the capital requirement tightens, the whole region of excess reserves is pushed to the right, resulting in a higher payout boundary \bar{C} in Panel A. Because reserves earn an interest rate r that is below the shareholders’ discount rate ρ , the platform shareholders’ value, V_0 , declines in C_L , as shown in Panel B. Panel C shows that users’ welfare is improved by the capital requirement but there exists a significant

⁵⁰Because the stablecoins are over-collateralized so that coordination failure (or run) does not happen, unlike Carletti, Goldstein, and Leonello (2019), our model does not feature a need to introduce a separate liquidity requirement.

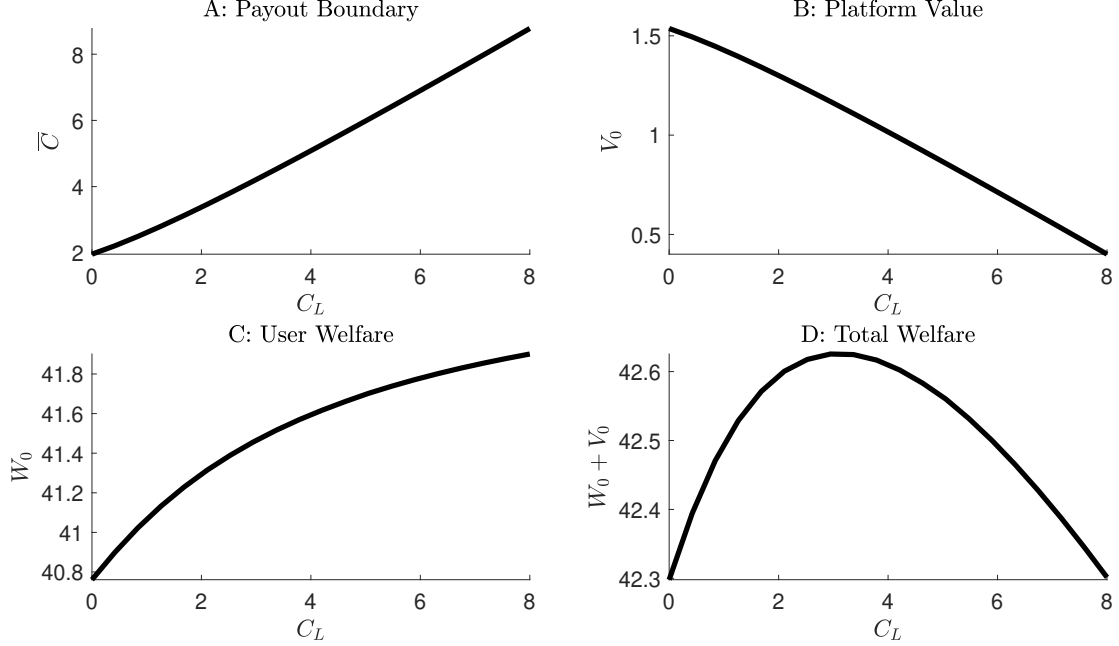


Figure 9: **Capital Requirement and Welfare.** We plot the numerical solutions of payout boundary \bar{C} (Panel A), the platform shareholders' value at $t = 0$, V_0 (Panel B), users' welfare at $t = 0$, W_0 (Panel C), and total welfare $W_0 + V_0$ (Panel D) over the regulatory minimum of excess reserves, C_L . The parameterization follows Figure 2.

degree of decreasing return as the regulator pushes up C_L . Appendix B.4 shows how we calculate user welfare, $W_0 = \mathbb{E} \left[\int_0^\infty e^{-rt} dR_{i,t} \right]$.

What is interesting is that, in Panel D of Figure 9, the total welfare is non-monotonic in C_L . When the regulator increases C_L from zero, the increase of users' welfare overwhelms the decrease of platform value, but as the capital requirement is tightened, the loss of platform value eventually dominates. This suggests the existence of an optimal level of C_L that maximizes the total welfare.

As long as the users' welfare increases faster than the platform value decreases, the regulator can administer a transfer from users to the platform, making the regulation Pareto-improving. For example, the regulator can allow the platform to charge users a membership fees, i.e., a fixed cost of access, and imposes a cap on such fees. This type of access fees is commonly seen in the literature on regulation of utility networks (Laffont and Tirole, 1994; Armstrong, Doyle, and Vickers, 1996).

In Figure 10, we further demonstrate the stabilization effects of capital requirement. In Panel A, we plot the ratio of $\bar{C} - \tilde{C}$ to $\bar{C} - C_L$ that measures the size of the stable subset of C where the platform maintains $P(C) = 1$. As C_L increases, the stable region enlarges. In Panel B, we plot the probability of $C > \tilde{C}$ (i.e., $\sigma^P(C) = 0$) based on the stationary distribution of C , which shows that over the long run the platform spends more time in the stable region when C_L increases. In

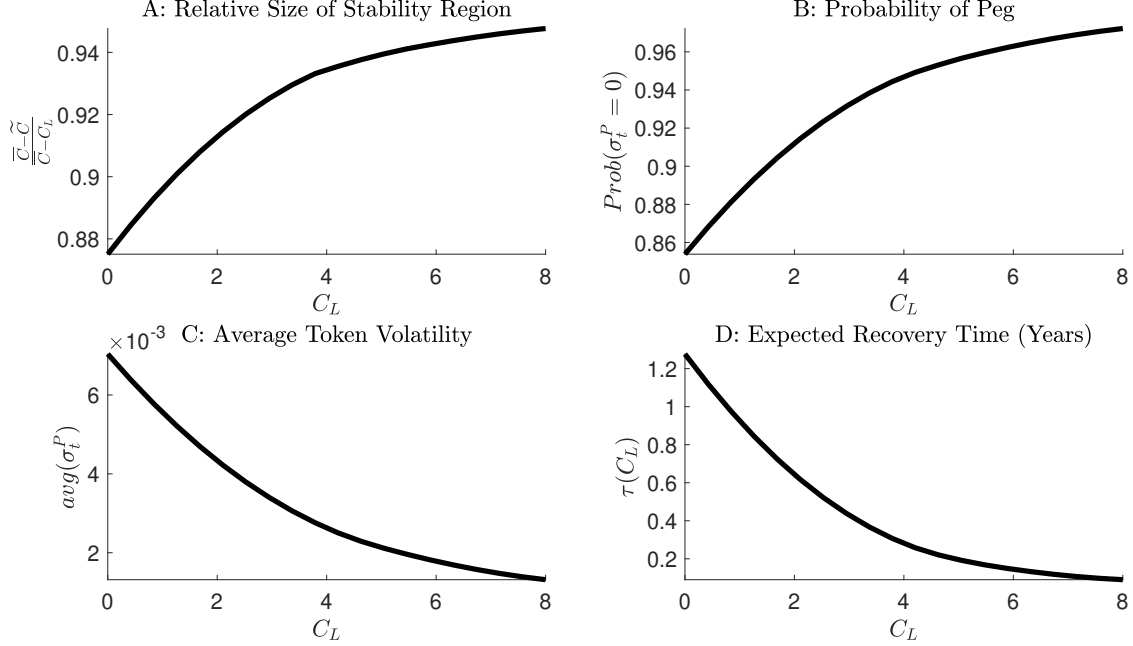


Figure 10: **Capital Requirement and Token Stability.** Using numeric solutions under different values of C_L , we plot the fraction of state space with $P_t = 1$, i.e., $\frac{\tilde{C}-C_L}{\tilde{C}-C_L}$ (Panel A), stationary probability of zero token volatility (Panel B), the long-run average (based on stationary probability density) of token volatility (Panel C), and the expected time to reach \tilde{C} from C_L (Panel D). The parameterization follows Figure 2.

Panel C, we plot the long-run average value of σ_t^P using the stationary probability distribution. A declining pattern emerges, indicating that capital requirement is indeed effective in reducing the token volatility. In Panel D, we plot the expected number of years it takes to reach \tilde{C} from C_L (denoted by $\tau(C_L)$). In Appendix B.1, we show how to calculate $\tau(C_L)$. This recovery time decreases when the capital requirement is tightened. As C_L increases, the platform at C_L still has abundant cash that can self-accumulate by via the interests earned on reserve holdings.

5.2 Stability Regulation

A key difference between stablecoins and bank deposits is that the issuers of stablecoins do not have any obligations to maintain $P_t = 1$ while a large portion of bank deposits offer redemption at par through the deposit insurance mechanism and various regulatory backstops. Should stablecoins be more like regulated deposits and be legally required to maintain a perfectly stable value?

In Panel A of Figure 12, we show that under the zero-volatility requirement (i.e., $\sigma_t^P = 0$), the platform maintains a higher level of excess reserves to reduce the likelihood of liquidation because the option of off-loading risk to users is no longer available. Holding more reserves with an interest

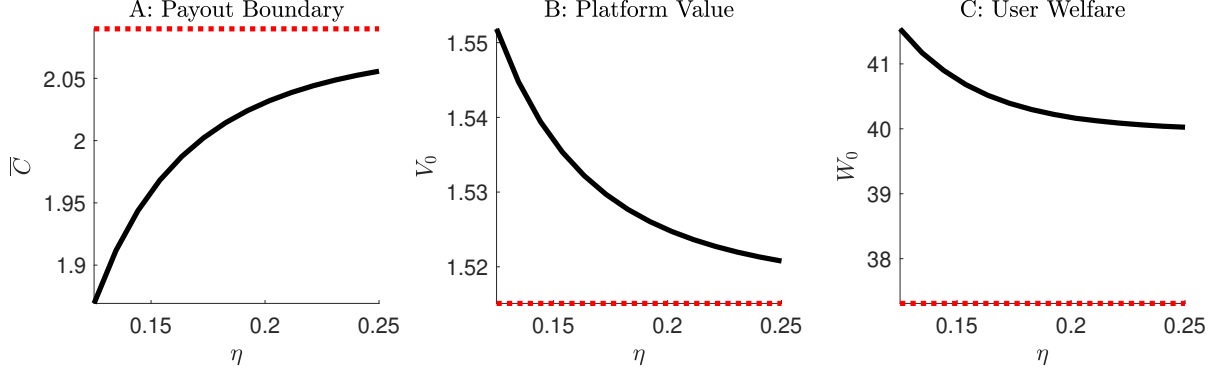


Figure 11: **Risk-Sharing, Stability Regulation, and Welfare.** Using the numerical solutions, we calculate the payout boundary \bar{C} (Panel A), the platform shareholders’ value at $t = 0$, V_0 (Panel B), users’ welfare at $t = 0$, W_0 (Panel C), and the long-run average fees based on stationary probability density (Panel D) over different values of users’ risk aversion η for both the baseline model (solid line) and the model under stability regulation (red dotted line). The parameterization follows Figure 2.

rate below the shareholders’ discount rate reduces the platform value (see Panel B of Figure 12).

An interesting finding is that imposing the stability regulation even decreases users’ welfare (Panel C of Figure 12) across all values of η . This seems to contradict the intuition that, by forcing the platform to maintain a perfectly stable token value, users will benefit, especially when they are more risk-averse. However, the argument ignores that, unable to off-load risk to users, the platform can compensate its risk exposure with higher fees. Stability regulation is counterproductive because it limits the risk-sharing between the platform and its users. When the platform is close to liquidation, its effective risk aversion can be higher than η , so there is economic surplus created from users’ absorbing risk from the platform. Stability regulation shuts down this insurance market. Our results on stability regulation also reveal the fact that a commitment to perfectly stable token does not improve welfare. In practice, stablecoin issuers cannot commit against debasement, but even when such commitment is available, doing so would not be optimal.

5.3 Regulating the Riskiness of Reserve Assets and Volatility Paradox

Another regulatory option is to restrict the riskiness of reserve assets. Many are concerned about the riskiness of reserve assets held by major stablecoin issuers as we discussed in Section 2. To analyze such regulation, we extend our model to incorporate a risk-return trade-off in reserve assets:

$$dM_t = rM_t dt + (P_t + dP_t)dS_t + N_t f_t dt + N_t \sigma dZ_t - dDiv_t + M_t(\hat{\mu} dt + \hat{\sigma} dZ_t), \quad (37)$$

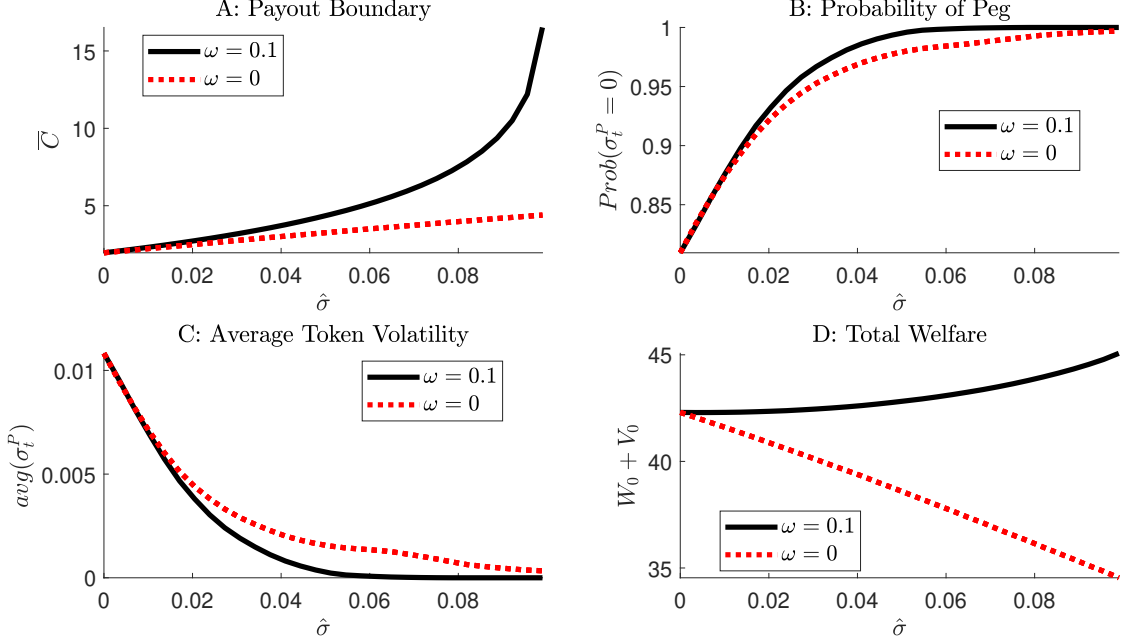


Figure 12: **Reserve Riskiness and Volatility Paradox.** Using the numerical solutions, we calculate the payout boundary \bar{C} (Panel A), the stationary probability of a fixed token price (Panel B), the average volatility σ_t^P (evaluated at the stationary distribution of C), and the total welfare at $t = 0$, $V_0 + W_0$ (Panel D). The parameterization follows Figure 2. We set $\hat{\mu} = \omega\mu$ and present solutions with $\omega = 0.1$ (solid line) and $\omega = 0$ (dotted line). We consider $\hat{\sigma} \in [0, 0.0999]$ so that the regularity condition $r + \hat{\mu} < \rho$ is satisfied.

where $\hat{\mu}, \hat{\sigma} \geq 0$. Relative to (8), the law of motion has an additional term that reflects the expected excess return on reserve holdings and the associated additional risk exposure. In Appendix B.2, we solve this extension. Regulating the riskiness of reserve assets corresponds to stipulating $\hat{\sigma}$. Therefore, to analyze its effects, we conduct comparative statics with respect to $\hat{\sigma}$. As we vary $\hat{\sigma}$, we change $\hat{\mu}$ accordingly while fix the Sharpe ratio at a constant $\omega \equiv \hat{\mu}/\hat{\sigma}$.

In Figure 12, we report the results of two sets of comparative statics with ω equal to 0 and 0.1 respectively.⁵¹ For both cases, more reserve risk (i.e., a higher $\hat{\sigma}$) is associated with a higher payout boundary \bar{C} . This suggests that forcing the platform to hold low-risk assets (i.e., lowering $\hat{\sigma}$ through a regulatory mandate) reduces its incentive to hoard reserves. Moreover, as the platform endogenously responds to reduce reserves, token price becomes more volatile. In Panel B and C, we demonstrate such volatility paradox: Riskier reserves (i.e., a higher $\hat{\sigma}$) is associated with more stable token price, reflected in both a higher probability of $P_t = 1$ and a lower average σ_t^P (evaluated at the stationary distribution of C). Therefore, mandating a decline in $\hat{\sigma}$ destabilizes token price.⁵²

⁵¹Throughout our analysis, the parameters must satisfy the condition $r + \hat{\mu} < \rho$ to preclude a solution in which the platform indefinitely delays dividend payouts because returns on excess reserves exceed the shareholders' discount rate, a standard condition in dynamic liquidity management models (e.g., Riddick and Whited, 2009).

⁵²The key to our mechanism of volatility paradox is the stablecoin issuer's response in liquidity hoarding decisions,

The welfare implications of regulating the riskiness of reserve assets are ambiguous and depend on the Sharpe ratio $\omega = \hat{\mu}/\hat{\sigma}$. In Panel D, we show how the total welfare (the sum of platform value and users' value) varies with $\hat{\sigma}$ under different Sharpe ratios. Under $\omega = 0$, total welfare declines in the riskiness of reserve assets, but the relation flips for $\omega = 0.1$. The intuition is simple. Under $\omega = 0$, an increase in $\hat{\sigma}$ indicates more risk but no more return on reserve holdings. While token price becomes more stable thanks to the platform's build-up of precautionary savings, holding reserves is costly for the platform because the return is below shareholders' discount rate as in [Riddick and Whited \(2009\)](#).⁵³ The platform may charge higher fees on users to compensate the cost of holding more reserves, which offset the benefit of a more stable token price for users. As a result, both the platform's and users' welfare decline. Under $\omega = 0.1$, an increase in $\hat{\sigma}$ brings in a higher expected return on reserve holdings, and with these additional revenues, the platform can reduce fees on stablecoin users and has more cash flows to buffer shocks, relying less on debasement to off-load risk to users. As a result, both parties' welfare can increase.

Our conclusion is two-fold. First, forcing the platform to hold low-risk assets triggers its response to maintain less reserves. Second, the welfare implications depend on the risk-return trade-off.

6 Crypto Shadow Banking with User Collateral

The double-collateralization structure in Panel B of Figure 1 behind many stablecoins (e.g., DAI issued by MakerDAO) fits into our analytical framework. By requiring users to post collateral, the platform gains an additional degree of freedom (margin requirement). When setting the margin requirement, the platform faces the trade-off between reducing risk exposure and user participation.

For each dollar of stablecoins, the platform requires a user to post m_t dollars worth of collateral. In practice, many risky assets are eligible collateral, mainly cryptocurrencies such as Bitcoin and Ether, and thus are highly volatile. Let dZ_t denote a standard Brownian shock. Instead of interpreting it as a shock directly to reserves as in our baseline model, here we interpret the shock in the following way that is tied to the value of the user's collateral portfolio.

For simplicity, we do not model users' choice of collateral portfolio but rather assume that the collateral portfolio has a continuum of assets (indexed by a) and, from t to $t + dt$, a fraction, $2(\delta dt - \sigma dZ_t)$, of these assets incur a percentage loss, denoted by θ_a , which is drawn independently

which is different from the fire sale mechanism of volatility paradox in [Brunnermeier and Sannikov \(2014\)](#).

⁵³As previously discussed, the wedge, $\rho - r$, can be microfounded with an exogenous Poisson-arriving liquidation with intensity $\rho - r$. The literature on agency cost of cash holdings also provides a rationale for why the return on liquidity holdings is below shareholders' discount rate ([Nikolov and Whited, 2014](#); [Nikolov, Schmid, and Steri, 2019](#)).

across assets a from a uniform distribution on $[0, 1]$.⁵⁴ At time t , the expected loss of the collateral portfolio is $\mathbb{E} \left[\frac{1}{2} \times 2(\delta dt - \sigma dZ_t) \right] = \delta dt$, where the expected loss per asset, $\frac{1}{2}$, is multiplied by the fraction of assets in losses. The collateral portfolio also generates an expected value appreciation, denoted by $\tilde{\mu}$. Therefore, for each dollar of stablecoins, a user posts m_t dollars worth of collateral, with an expected net return equal to $\tilde{\mu} - \delta - r$, where the last term represents the cost of giving up the outside option of return r by locking wealth in the collateral portfolio.⁵⁵

Under the collateral requirement, a representative user i 's problem of choosing the optimal dollar value of stablecoin holdings, $u_{i,t}$, given by (5) in the baseline model, is now described below

$$\max_{u_{i,t}} \left\{ \frac{1}{\beta} N_t^\alpha u_{i,t}^\beta A^{(1-\alpha-\beta)} dt + u_{i,t} (\mu_t^P - \eta |\sigma_t^P| - f_t) dt + u_{i,t} m_t (\tilde{\mu} - \delta - r) dt \right\}, \quad (38)$$

where the last term reflects the fact that the user's wealth is being locked in a risky collateral backing the stablecoins worth $u_{i,t}$. As in the baseline model, to solve the platform's optimal strategies, we first note that, given the token price dynamics (i.e., μ_t^P and σ_t^P), the platform can directly set N_t through the fees f_t . Under the collateral requirement, users' optimal choice of $u_{i,t}$ implies the following equation that connects N_t (i.e., the aggregated $u_{i,t}$) and f_t :

$$f_t = \left(\frac{A}{N_t} \right)^{1-\xi} - m_t (r + \delta - \tilde{\mu}) + \mu_t^P - \eta |\sigma_t^P|. \quad (39)$$

Clearly, when $m_t = 1$, $\delta = 0$, and $\tilde{\mu} = 0$ (i.e., the platform does not impose a haircut and the collateral does not have expected losses or gains), equation (39) reduces to (13), the corresponding equation in the baseline model. Given f_t , a higher m_t leads to lower N_t according to (39), which reflects the fact that imposing a stricter collateral requirement leads to lower demand for stablecoins under the parameter restriction, $r + \delta - \tilde{\mu} > 0$ (i.e., it is costly for users to post collateral).

To derive the law of motion of the state variable C_t , the excess reserves, we first derive the

⁵⁴Klimenko, Pfeil, Rochet, and Nicolo (2016) show that $2(\delta dt - \sigma dZ_t)$ is the $\Delta \rightarrow 0$ limit of a random variable whose value is $2(\delta\Delta - \sigma\sqrt{\Delta})$ or $2(\delta\Delta + \sigma\sqrt{\Delta})$ with equal probabilities. Before taking the limit, the parameters, δ and σ , can be chosen so that the random fraction is well-defined within $[0, 1]$. The convergence is akin to that shown by Cox, Ross, and Rubinstein (1979) in their Binomial model of option pricing. In practice, the variation of a collateral asset (i.e., θ_a in our model) can be very large when the collateral is a cryptocurrency. What triggered the dramatic debasement of IRON was the almost 100% drop over two days of the collateral cryptocurrency, TITAN (Tiwari, 2021). The run on IRON in turn exacerbates the sell-off of TITAN.

⁵⁵This expression is analogous to the user's cost of capital (Jorgenson, 1963) with the additional $\tilde{\mu}$.

platform's flow cost per dollar of stablecoins created:

$$\begin{aligned}
& 2(\delta dt - \sigma dZ_t) \times \mathbb{P}(\{m_t(1 - \theta_a) < 1\}) \mathbb{E}[1 - m_t(1 - \theta_a) | m_t(1 - \theta_a) < 1] \\
& = 2(\delta dt - \sigma dZ_t) \times \left(\int_{1 - \frac{1}{m_t}}^1 (1 - m_t(1 - \theta_a)) d\theta_a \right) = \frac{1}{m_t}(\delta dt - \sigma dZ_t). \tag{40}
\end{aligned}$$

In the first line, the fraction of users' collateral assets that incur losses is multiplied by the probability of a sufficiently large loss that leads to the violation of the margin requirement, and the last component is the platform's loss upon receiving and liquidating the collateral (with a remaining value of $m_t(1 - \theta_t)$) and repurchasing the one dollar worth of stablecoins out of circulation. Therefore, given N_t , the dollar value of all stablecoins issued, $-\frac{N_t}{m_t}(\delta dt - \sigma dZ_t)$ enters into the law of motion of reserves (8), replacing $N_t \sigma dZ_t$ (which is essentially the case where $m_t = 1$ and $\delta = 0$). This flow cost is essentially the consequence of the stablecoin issuer extending an guarantee of the stablecoins' value, which is a contingent liability akin to the guarantee that a bank extends to its off-balance-sheet conduits as discussed in Section 2.

Following the derivation in Section 4, we use (39) to substitute out f_t in the law of motion of reserves to obtain the law of motion of excess reserves, C_t :

$$dC_t = \left(rC_t - r(m_t - 1)N_t + m_t(\tilde{\mu} - \delta)N_t + N_t^\xi A^{1-\xi} - N_t \eta |\sigma_t^P| - \frac{N_t \delta}{m_t} \right) dt + N_t \left(\frac{\sigma}{m_t} - \sigma_t^P \right) dZ_t. \tag{41}$$

When $m_t = 1$, $\delta = 0$, and $\tilde{\mu} = 0$, equation (41) reduces to (17) in the baseline model. In Appendix B.5, we provide all omitted solution details and derive the HJB equation of the value function, $V(C_t)$ as well as the platform's optimal choices of fees (or equivalently, $N(C_t)$), token price dynamics (or equivalently, $\sigma^P(C_t)$), and the margin requirement $m(C_t)$. Figure 13 reports the numeric solutions.

In the model with user collateral, the shock to the platform's reserves, dZ_t , originates from the fluctuation of users' collateral value, and the platform's exposure is directly and inversely linked to the margin requirement, m_t , as shown in (41). Therefore, we expect the optimal margin requirement to be higher when the platform's excess reserves run down. This is shown in lower-left Panel of Figure 13. Introducing user collateral does not change the qualitative dynamics of the platform's franchise value, $V(C)$, the transaction volume, $N(C)$, and the token price volatility, $\sigma^P(C)$.

Discussion: immediate liquidation of collateral. When users violate the margin requirement, the platform immediately liquidates users' collateral and repurchase stablecoins out of circu-

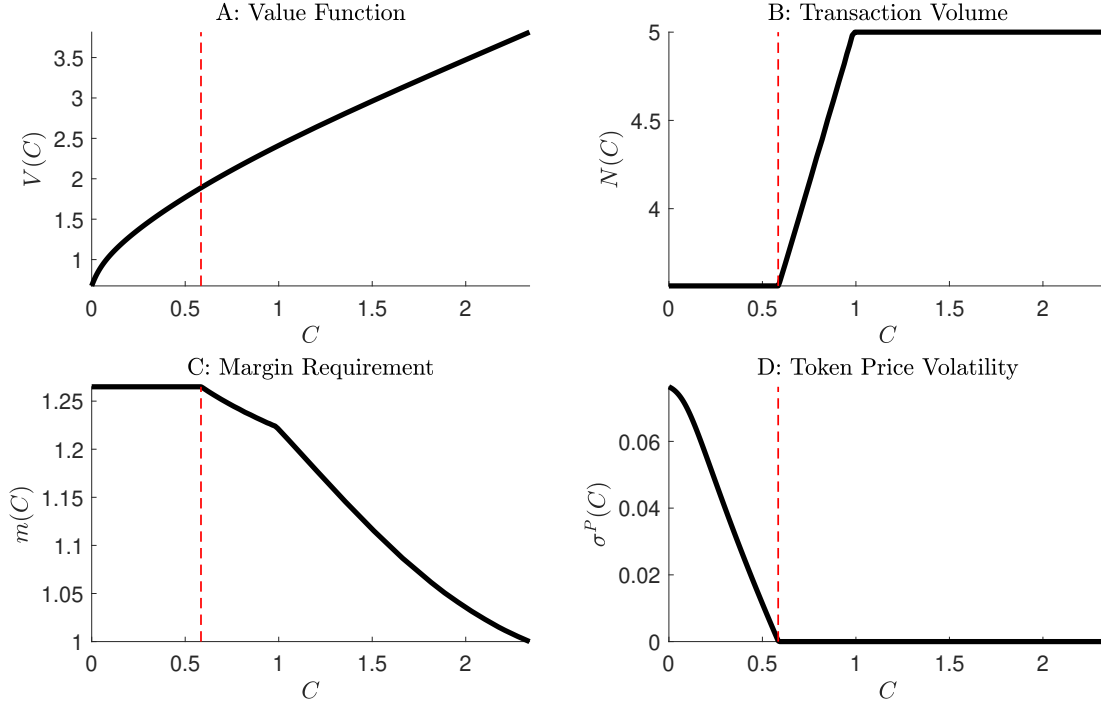


Figure 13: **Margin Requirement.** This figure plots the platform value function (Panel A), token demand or transaction volume (Panel B), optimal marginal requirement (Panel C), and token-price volatility (Panel D) as functions of excess reserves C . The parameterization follows Figure 2 with $\tilde{\mu} = 0.05$ and $\delta = 0.025$.

lation. A question naturally arises: instead of liquidating the collateral and repurchasing stablecoins right away, why not incorporate the collateral assets into the platform’s reserve portfolio? Doing so will create two types of stablecoins, one with the backing of both users’ collateral and reserves (users of these stablecoins have not yet violated the margin requirements) and the other only backed by the platform’s reserves (users of these stablecoins have violated the margin requirement). This is not done in practice, and analytically, it complicates the model by introducing a new stable variable, that is the fraction of stablecoins only backed by the platform’s reserves.

7 Stablecoins, Digital Platforms, and Data Privacy

The interest in stablecoins among practitioners and regulators skyrocketed after Facebook announced its stablecoin project Libra (recently renamed to Diem). Different from other stablecoin issuers, Facebook has the unique advantage of strong network effects. Its comprehensive infrastructure covers social network, social media, and e-commerce (Facebook Shop). For individual users, the benefit of adopting Diem is enormous if other users on Facebook adopts Diem, because a great variety of activities can be enabled by a universal and global means of payment. In this section,

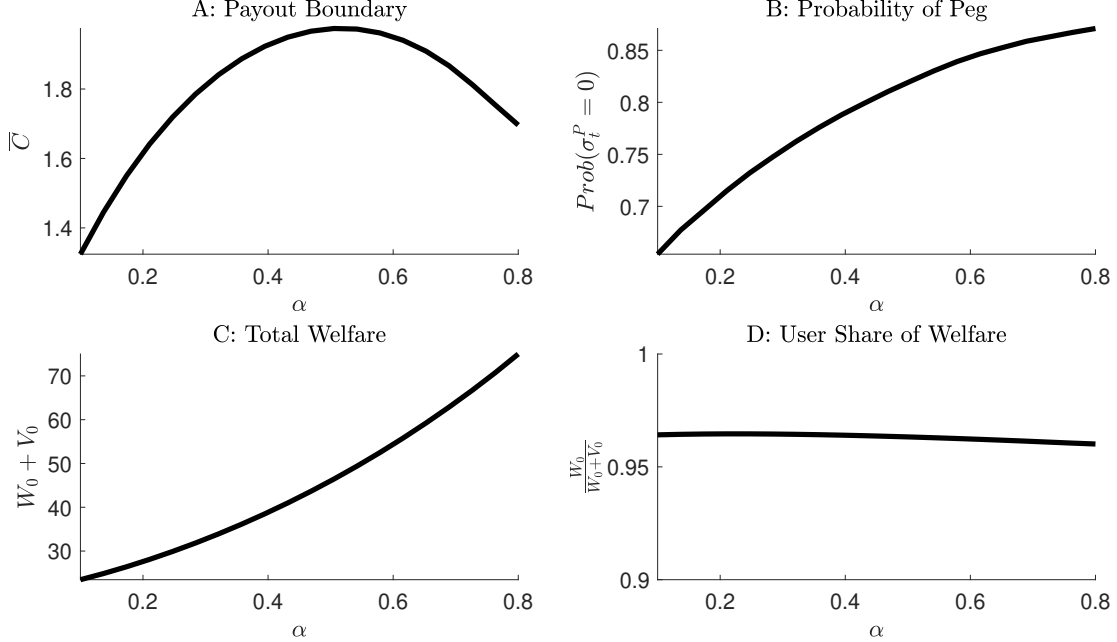


Figure 14: **Network Effects.** We plot the payout boundary (Panel A), the long-run probability of $C > \tilde{C}$ based on stationary distribution (Panel B), the sum of platform value and users' welfare (Panel C), and users' share of total welfare (Panel D) over different values of α (degree of network externality). The parameterization follows Figure 2.

we analyze the role of network effects in stablecoin management and show that regulators should impose more stringent capital requirements on large platforms with strong network effects.

The stablecoin project of Facebook attracted enormous attention also because of the big data ambition of Facebook. Large platforms profit from user-generated data and use targeted content to secure and grow user base. A global payment system enabled by a stablecoin allows the platform to gather transaction data. We extend the model to incorporate transaction data as a productive asset for the platform and explore how data acquisition affects a platform's stablecoin strategies.

7.1 The Role of Network Effects

For simplicity, our analysis is based on the baseline model without users' collateral. In our model, strong network effects are captured by a large value of α (see (2)). In Figure 14, we compare stablecoins with different degrees of network effects. Panel A plots the payout boundary \tilde{C} as a measure of voluntary over-collateralization over different values of α . On the one hand, stronger network effects make the platform more profitable, which encourages precautionary savings to protect the franchise value. On the other hand, stronger network effects imply a higher level of user transactions near $C = 0$ (i.e., \underline{N} in (26)), which then implies a faster recovery out of the low- C

region (through fees and token-issuance revenues) and a weaker incentive to hold reserves. The two counteracting forces lead to a hump-shaped relationship between \bar{C} and α in Panel A of Figure 14.

In Panel B of Figure 14, we show the long-run probability of $C > \tilde{C}$ (based on stationary probability distribution of C) increases in α . Stronger network effects imply that, over the long run, the system spends more time in states with $P(C) = 1$. Under stronger network effects, recovery out of the low- C region is faster due to a higher level of user activities and the resultant faster replenishment of reserves via fees and token-issuance proceeds. Our paper sheds light on why stablecoins issued by Facebook and other technology giants with strong network infrastructure are regarded as more promising than those issued by start-up payment service providers. Stronger network effects lead to stabler tokens and a lower likelihood of token debasement.

Finally, we examine the impact of network effects on welfare. In Panel C of Figure 14, we show that total welfare of the platform and its users increases in the degree of network effects. This explains why it is particularly beneficial for technology giants with strong network infrastructure to introduce stablecoins as common means of payment among their customers. Network infrastructure is not limited to social network and e-commerce. Financial network is another example. JPMorgan Chase introduces JPM Coin to facilitate transactions among institutional clients.

Interestingly, as we gradually increase the degree of network effects in Panel D of Figure 14, the split of total welfare between the platform and its users is rather stable. Under stronger network effects, the monopolistic platform can extract more rents from its users through fees or off-loading risk in distress. However, precisely due to the network effects, individual users do not internalize the positive effect of their adoption on other users, so the platform has incentives to internalize the network externality by stimulating user activities through fee reductions (or subsidies) and token price stability. These two counteracting forces imply that, as network effects become stronger, the platform's share of total surplus does not necessarily increase.

Beyond the implications on stablecoins issued by large digital platforms, our analysis also contributes to the ongoing debate on stablecoin interoperability (Brunnermeier and Payne, 2021). Stablecoins that are interoperable across different DeFi platforms (blockchains) exhibit stronger network effects of user adoption and therefore exhibit less price instability. The increase of welfare in network effects suggests that regulators should encourage interoperability.

Lastly, Figure 15 shows that stablecoins with stronger network effects should be more heavily regulated in terms of capital requirements. In Panel A, we plot the capital requirement C_L^* that maximizes total welfare. In Panel B and C, we plot, respectively, the total welfare with and without

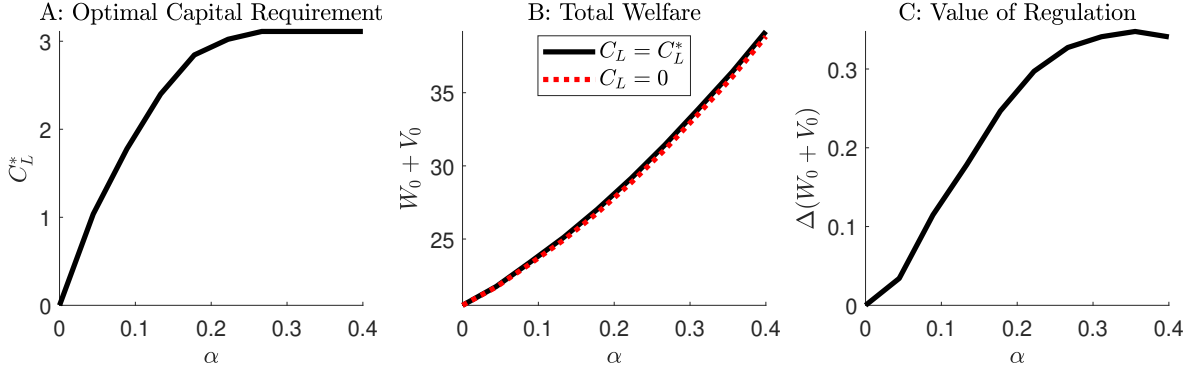


Figure 15: **Capital Requirement and Network Effects.** We calculate the optimal capital requirement C_L^* that maximizes total welfare (Panel A), total welfare both with capital requirement C_L^* (solid black line) and without capital requirement (dotted red line) (Panel B), and the welfare wedge between the optimally regulated equilibrium and the laissez-faire equilibrium (Panel C) over different values of α . Note that Panel C depicts the difference between the solid black line and the dotted red line from Panel B. The rest of parameterization follows Figure 2.

capital requirement and the welfare improvement under optimal capital requirement (relative to the laissez-faire equilibrium). An important insight is that the capital requirement tightens as network effects strengthen. In fact, without network effects ($\alpha = 0$), it is optimal not to impose the capital requirement (i.e., $C_L^* = 0$). The key to this result is the network externality of individual users' token holdings. The platform internalizes the externality in its decisions but the internalization is not perfect. As shown in Figure 14, the platform cannot seize the full surplus as its share of total welfare is rather stable in α and always below 100%. Therefore, as α increases, the total welfare and the component not internalized by the platform both increase. This calls for a tighter capital requirement that raises the overall level of reserves closer to social optimum.

7.2 Payment and Data Privacy

Data is now a major asset of digital platforms. Social networks, such as Facebook and Twitter, utilize user-generated data to target users for content delivery. Payment platforms, such as PayPal and Square, have become data centers (Bank for International Settlements, 2019). They provide services beyond payment, for example, extending loans to consumers and businesses based on data-driven credit analysis. We follow Veldkamp (2005), Ordoñez (2013), Fajgelbaum, Schaal, and Taschereau-Dumouchel (2017), Parlour, Rajan, and Zhu (2020), and Jones and Tonetti (2020) to model data as a by-product of user activities.⁵⁶ We show that data acquisition incentive destabilizes the stablecoin. Our results demonstrate a connection between data privacy and stablecoins, two

⁵⁶Veldkamp and Chung (2019) provide an excellent survey of the literature of data and aggregate economy.

areas that have both attracted enormous attention but have been analyzed separately so far.

We now interpret A in (2) as a measure of effective data units that enhance platform productivity in locking in users' attention and stimulating user activities through user profiling. As previously discussed, we interpret N_t as the transaction volume and specify the following law of motion:

$$dA_t = \kappa A_t^{1-\xi} N_t^\xi dt. \quad (42)$$

Users' transactions generate a flow of raw data, $\kappa N_t^\xi dt$, where the parameter κ captures the technological efficiency of data processing and storage. To what extent the raw data contributes to the effective data units depends on the current amount of effective data via $A_t^{1-\xi}$. The complementarity between the old and new data captures the fact that the value of new data increases in the quality of statistical algorithms, which in turn depends on the amount of existing data that are needed to train the algorithms.⁵⁷ The Cobb-Douglas form is chosen for analytical convenience. To guarantee the convergence of the objective function, we impose the parametric restriction $\rho > \kappa \bar{n}^\xi$.

As platform productivity improves, we assume transaction capacity to increase accordingly, i.e., $\bar{N}_t = \bar{n}A_t$, where $\bar{n} > 0$ is constant. User optimization is static and follows the baseline model. As shown in (12), the transaction volume (or token demand) $N_t \equiv n_t A_t$ where

$$n_t = \frac{1}{(r + f_t - \mu_t^P + \eta|\sigma_t^P|)^{\frac{1}{1-\xi}}} \wedge \bar{n}. \quad (43)$$

As in the baseline model, the platform sets n_t through the fees, f_t , and sets the dynamics of token price through its choice of σ_t^P . The model now has three natural state variables, reserves M_t , token supply S_t , and data stock A_t . Similar to the baseline model, $C_t = M_t - S_t P_t$ and A_t summarize payoff-relevant information, driving the platform value, $V_t = V(C_t, A_t)$, and the dollar value of token, $P_t = P(C_t, A_t)$. To simplify the notations, we will suppress the time subscripts.

We conjecture that the system is homogeneous in A , and in particular, the platform's value function and dollar value of token are given by $V(C, A) = v(c)A$ and $P(C, A) = P(c)$, respectively, where the excess reserves-to-data ratio is the key state variable for the platform's optimal strategies:

$$c \equiv \frac{C}{A}. \quad (44)$$

We will confirm the conjecture as we solve the platform's optimization problem in the following.

⁵⁷Related, in Farboodi, Mihet, Philippon, and Veldkamp (2019), data have increasing return to scale.

First, to derive the law of motion of c_t , we follow the derivation of the baseline model to obtain

$$dC_t = \left(rC_t + A_t n_t^\xi - \eta A_t n_t |\sigma_t^P| \right) dt + A_t n_t (\sigma - \sigma_t^P) dZ_t - dDiv_t. \quad (45)$$

Given (42) and (45), the law of motion of c_t reads

$$dc_t = \left(rc_t + n_t^\xi - \eta n_t |\sigma_t^P| - \kappa n_t^\xi c_t \right) dt + n_t (\sigma - \sigma_t^P) dZ_t - \frac{dDiv_t}{A_t}. \quad (46)$$

Under the value function conjecture, $V(C, A) = v(c)A$, and the laws of motion of A (42) and c (46), the HJB equation for $v(c)$ in the interior region (where $dDiv_t = 0$) is given by

$$\rho v(c) = \max_{n \in [0, \bar{n}], \sigma^P} \left\{ [v(c) - v'(c)c] \kappa n^\xi + v'(c) \left(rc + n^\xi - \eta n |\sigma^P| \right) + \frac{1}{2} v''(c) n^2 (\sigma - \sigma^P)^2 \right\}. \quad (47)$$

The first term on the right side contains the marginal value of user-generated data (“data q”)

$$q(c) = \frac{\partial V(C, A)}{\partial A} = v(c) - v'(c)c. \quad (48)$$

When the marginal value of reserves, $V_A(C, A) = v'(c)$, falls to one, the platform pays out dividends. We define the payout boundary as \bar{c} through $v'(\bar{c}) = 1$. The optimality of \bar{c} also implies $v''(\bar{c}) = 0$. Note that as in the baseline model, when C (or c) approaches zero, the platform can avoid liquidation by setting $\sigma^P(c) = \sigma$ to off-load risk to its users and gradually replenish reserves.⁵⁸ For simplicity, we do not consider recapitalization (equity issuance). In sum, the platform’s excess reserves, C_t , move in $[0, \bar{c}A]$. As data grows, the platform accumulates more excess reserves.

Proposition 6 (Platform Optimization under Data-Driven Productivity). *The value function takes the form $v(c_t)A_t$, where $v(c_t)$ solves the HJB equation (47) subject to the conditions $v'(\bar{c}) = 1$, $v''(\bar{c}) = 0$, and $\lim_{c \rightarrow 0} \sigma^P(c) = \sigma$. The amount of excess reserves, C_t , stays below $\bar{c}A_t$ where the upper bound increases with A_t , the effective data units. At $C_t = \bar{c}A_t$, the platform pays dividends when $dC_t > 0$ so that dividend payments cause c_t to reflect at \bar{c} .⁵⁹*

Next, we characterize the optimal transaction volume and volatility. Following our analysis of

⁵⁸The boundary condition for $v(c)$ is that as c approaches zero, $-v''(c)$ approaches infinity (see footnote 44).

⁵⁹When $dC_t > 0$ at $C_t = \bar{c}A_t$, the dividend amount is equal to dC_t (i.e., exactly the amount needed to avoid $C_t > \bar{c}A_t$).

the baseline model, we define the effective risk aversion based on $v(c)$:

$$\Gamma(c) = -\frac{v''(c)}{v'(c)}. \quad (49)$$

The following proposition summarizes the optimal choices of $n(c)$ and $\sigma^P(c)$.

Proposition 7 (Data q , Token Volatility, and Transaction Volume). *At c where the platform maintains $P(c) = 1$ (and $\sigma^P(c) = 0$), the optimal transaction volume (token usage) is*

$$N = n(c)A = \left[\frac{\xi}{\Gamma(c)\sigma^2} \left(1 + \frac{\kappa q(c)}{v'(c)} \right) \right]^{\frac{1}{2-\xi}} A \wedge \bar{n}A; \quad (50)$$

otherwise, the optimal token volatility is

$$\sigma^P(c) = \sigma - \frac{\eta}{\Gamma(c)n(c)} \in (0, \sigma), \quad (51)$$

and the optimal transaction volume (token usage) is

$$N = n(c)A = \left[\frac{\xi}{\eta\sigma} \left(1 + \frac{\kappa q(c)}{v'(c)} \right) \right]^{\frac{1}{1-\xi}} A \wedge \bar{n}A. \quad (52)$$

The optimal transaction volume is proportional to A , the effective data units. Therefore, as the platform gathers more user-generated data following (42), it induces more transactions. With data as a productive asset, the platform faces a new trade-off. It can accumulate more reserves through higher fees or, by reducing fees, boost the transaction volume to accumulate more data. Therefore, the ratio of marginal value of data (the data q) and marginal value of reserves, $q(c)/v'(c)$, emerges in both (50) and (52). When the data q is high relative to the marginal value of reserves, the platform implements a high transaction volume through low fees. As a reminder, given the token price dynamics, the monotonic relationship between transaction volume and fees is given by (43).

The optimal choice of token volatility resembles that of the baseline model. In the region where $\sigma^P(c) > 0$, it is the ratio of users' risk aversion to the platform's risk aversion that drives $\sigma^P(c)$. And in this region, the optimal transaction volume in (52), even scaled by A , is no longer the constant as in the baseline model but depends on $q(c)/v'(c)$ instead, showing the trade-off between investing in data and accumulating reserves. Moreover, the optimal transaction volume depends on users' risk aversion η as η determines the cost of obtaining insurance from users (losing transaction volume after off-loading risk to users). When the platform absorbs all risk (i.e., $\sigma^P(c) = 0$), the

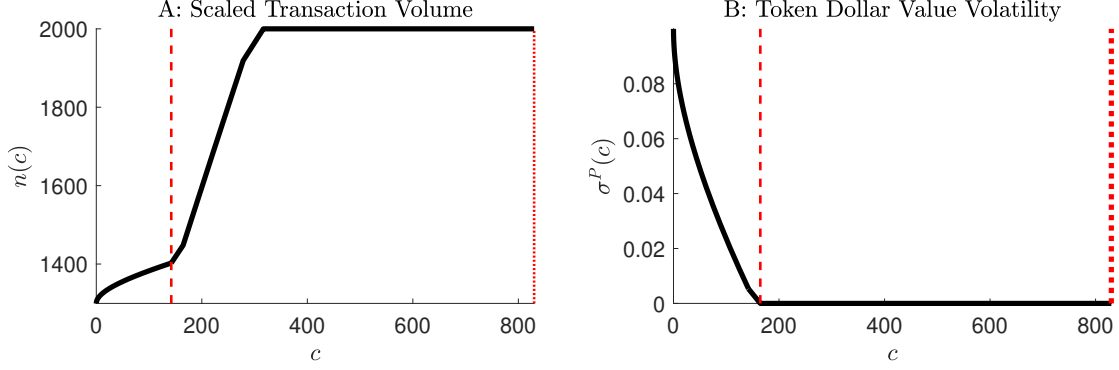


Figure 16: Transaction Volume and Token Volatility. This figure plots the A_t -scaled transaction volume $n(c)$ in Panel A and token return volatility $\sigma^P(c)$ in Panel B. In both panels, the red dotted lines mark the payout boundary \bar{c} , and the red dashed line marks \tilde{c} , the threshold that separates the regions of volatile and constant token prices. The parameterization follows Figure 2 with the additional parameters $\bar{n} = 2000$ and $\kappa = 0.00025$. Note that $\bar{n} = 2000$ implies that for $A_0 = 0.0025$, $\bar{N}_t = \bar{n}A_t = 5$ as under the parameterization in the baseline (see Figure 2).

optimal transaction volume varies with its own risk aversion $\Gamma(c)$ (50) because $\Gamma(c)$ drives the required risk compensation through higher fees that causes the transaction volume to decline.

Panel A of Figure 16 reports the optimal transaction volume. In contrast to Panel A of Figure 4 where the transaction volume is constant in the region where $\sigma^P(c) > 0$, the A -scaled volume now increases in c . The intuition is that as reserves become more abundant relative to data, the platform lowers fees to acquire more data through users' transactions at the expense of less dollar revenues for reserve accumulation. Panel B of Figure 16 shows a similar token volatility dynamics as Panel A of Figure 3 from the baseline model but in the space of $c = C/A$ (instead of C).

In our model, the technological advance in data acquisition and analysis can be captured by an increase of the parameter κ . In Figure 17, we examine the impact of data technology improvement on the operation of stablecoin platforms. In Panel A, we show that in response to an increase in κ , the platform optimally raises the (A -scaled) payout boundary, \bar{c} , which suggests a greater degree of over-collateralization. However, this does not translate into a more stable token price. As shown in Panel B, the long-run (stationary) probability of sustaining the peg decreases as the platform becomes more efficient in acquiring and utilizing user-generated data.

Therefore, our analysis reveals a paradox—if a digital platform introduces stablecoin to enhance its payment system and acquisition of transaction data, its stablecoin becomes more volatile precisely when data becomes more important. Conversely, stablecoins issued by platforms that respect user privacy and refrain from data usage are more stable in value according to our model.

To understand the mechanism, we plot the average fees and average transaction volume (both

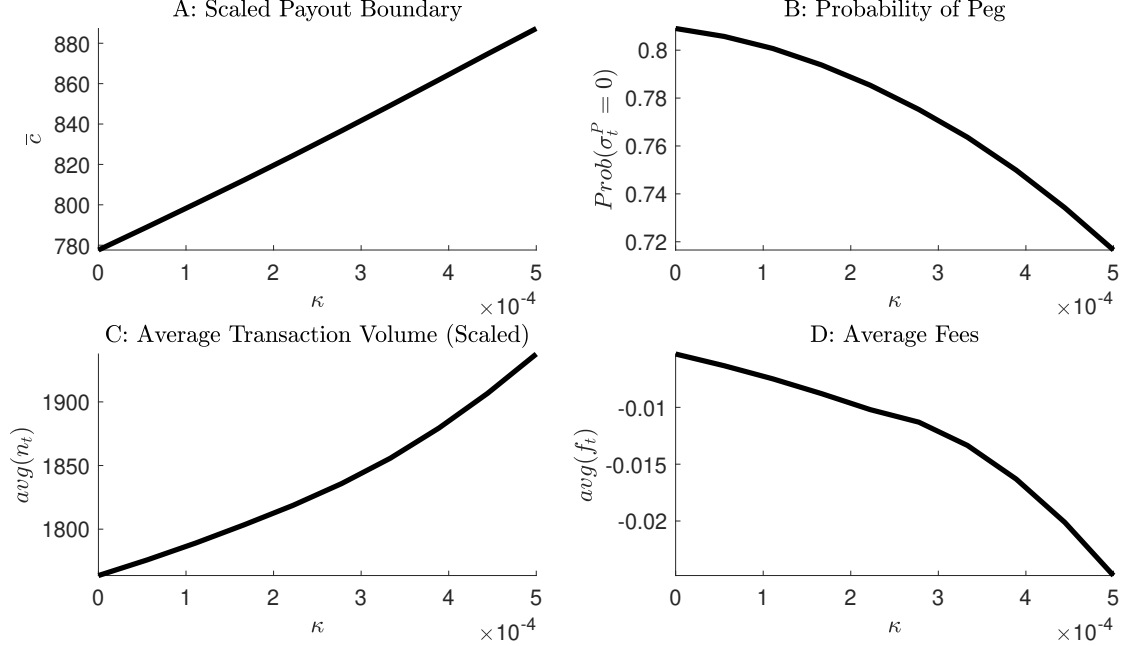


Figure 17: **Data Technology Progress and Platform Operation.** We plot the A -scaled payout boundary (Panel A), the probability of $P(c) = 1$ (Panel B), the average transaction volume (Panel C), and the average fees per dollar of transactions (Panel D) over κ (the efficiency of data technology). The moments in Panel B, C, and D are based on the stationary distribution of c . The parameterization follows Figure 2 with $\bar{n} = 2000$.

calculated from the stationary distribution of c) against κ in Panel C and D of Figure 17. To accumulate transaction data, the platform would like to increase the transaction volume. This is achieved through lower fees. In fact, the average fees per dollar of transaction even dips increasingly into the negative territory (i.e., becoming subsidies to users), a prediction in line with the practice that large digital platforms offer subsidies to grow user activities (Rochet and Tirole, 2006; Rysman, 2009). However, lowering fees reduce cash flows to the reserve buffer so that even though the platform hold more reserves at the payout boundary (see Panel A of Figure 17), it accumulates reserves at a slower pace on average over the state (c) space, which destabilizes the token. In sum, data acquisition incentive makes the stablecoin issuer more aggressive in subsidizing users at the expense of its own precautionary savings that are key to the stabilization of token price.

Our model highlights an unintended benefit of privacy regulation. Regulations that restrict the stablecoin issuer’s ability to collect and utilize user-generated data can be interpreted as a decrease in κ . $Prob(\sigma_t^P = 0)$ decreases in κ as shown in Panel B of Figure 17, so privacy regulations improve the stability of token value (i.e., reducing the probability of the stablecoin breaking the buck).

8 Conclusion

As decentralized finance develops rapidly, stablecoin initiatives arise to meet the demand for stable means of payment in the blockchain space. Stablecoins are issued by private entities or decentralized autonomous organizations (DAOs) that promise to maintain price stability by holding reserves for open market operations and users' redemption. However, as issuers maximize their own payoffs rather than total welfare, conflicts of interests naturally arise between the issuers and stablecoin users, making room for welfare-enhancing regulations. Digital networks (e.g., Facebook) plan to introduce their own stablecoins. Behind such initiatives, the incentives are complex especially when a payment system allows the platform to gather and profit from users' transaction data.

In spite of the enormous attention from both regulators and practitioners, to this date, there has not been a unified framework to address these issues. In this paper, we fill this gap and develop a dynamic model of stablecoin management. The equilibrium rationalizes a rich set of strategies and features two endogenous regimes. When the issuer's reserves are sufficiently high, the stablecoin price is fixed. When the reserves fall below a critical threshold, the stablecoin price comoves with the issuer's reserves, allowing risk sharing between the issuer and stablecoin users.

The system is bimodal and exhibits a unique instability mechanism. Above the reserve threshold, the issuer credibly sustains a fixed price, which induces a strong token demand that allows the issuer to profit from open market operations and further grow reserve holdings. This virtuous cycle turns into a vicious cycle when reserves fall below the threshold after negative shocks. As the stablecoin price becomes volatile, the users' token demand declines, so the issuer has to either drain its reserves further to stabilize price through open market operations or let debasement continue. The vicious cycle can be broken by issuing equity (governance tokens) to replenish reserves.

We evaluate several regulatory proposals and find that capital requirement improves welfare and should strengthen for payment platforms with strong network effects. In contrast, a legally binding commitment to price stability destroys welfare. We also demonstrate a volatility paradox: Forcing a stablecoin issuer to hold low-risk assets may destabilize the stablecoin. Its welfare implications depend on how the expected return on reserve assets comove with riskiness. Finally, our model can be easily extended to incorporate a q-theory of data acquisition. Investing in data crowds out reserve hoarding and thus destabilizes the stablecoin price. Therefore, data privacy regulation has an unintended benefit of improving the price stability of stablecoins issued by data-rich platforms.

References

- Abadi, J. and M. K. Brunnermeier (2019). Blockchain economics. Working paper, Princeton University.
- Acharya, V. V., P. Schnabl, and G. Suarez (2013). Securitization without risk transfer. *Journal of Financial Economics* 107(3), 515–536.
- Armstrong, M., C. Doyle, and J. Vickers (1996). The access pricing problem: A synthesis. *The Journal of Industrial Economics* 44(2), 131–150.
- Arrow, K. J. (1965). *Aspects of the Theory of Risk Bearing*. Helsinki: Yrjo Jahnssonin Saatio.
- Asquith, P. and D. W. Mullins (1986). Signalling with dividends, stock repurchases, and equity issues. *Financial Management* 15(3), 27–44.
- Bakos, Y. and H. Halaburda (2019). The role of cryptographic tokens and icos in fostering platform adoption. *Working Paper*.
- Bank for International Settlements (2019). Chapter 3. Big tech in finance: opportunities and risks. Technical report, Bank for International Settlements.
- Baumol, W. J. (1952). The transactions demand for cash: An inventory theoretic approach. *The Quarterly Journal of Economics* 66(4), 545–556.
- Bech, M. L. and R. Garratt (2017). Central bank cryptocurrencies. Bis quarterly review, Bank for International Settlements.
- Benetton, M. and G. Compiani (2020). Investors’ beliefs and asset prices: A structural model of cryptocurrency demand. working paper, University of Chicago and University of California at Berkeley.
- Benetton, M., G. Compiani, and A. Morse (2021). When cryptomining comes to town: High electricity-use spillovers to the local economy. working paper, University of Chicago and University of California at Berkeley.
- Biais, B., C. Bisiere, M. Bouvard, and C. Casamatta (2019). The blockchain folk theorem. *The Review of Financial Studies* 32(5), 1662–1715.

- Bianchi, J. and S. Bigio (2014). Banks, liquidity management and monetary policy. Working Paper Series 20490, National Bureau of Economic Research.
- Bolton, P., H. Chen, and N. Wang (2011). A unified theory of tobin's q, corporate investment, financing, and risk management. *The Journal of Finance* 66(5), 1545–1578.
- Brainard, L. (2019, October). Digital currencies, stablecoins, and the evolving payments landscape. Speech by Governor Lael Brainard at The Future of Money in the Digital Age, Sponsored by the Peterson Institute for International Economics and Princeton University's Bendheim Center for Finance, Washington, D.C.
- Brunnermeier, M. K., H. James, and J.-P. Landau (2019, September). The digitalization of money. Working Paper 26300, National Bureau of Economic Research.
- Brunnermeier, M. K. and J. Payne (2021). Platforms, tokens, and interoperability. working paper, Princeton University.
- Brunnermeier, M. K. and Y. Sannikov (2014). A macroeconomic model with a financial sector. *American Economic Review* 104(2), 379–421.
- Budish, E. (2018, June). The economic limits of bitcoin and the blockchain. Working Paper 24717, National Bureau of Economic Research.
- Bullmann, D., J. Klemm, and A. Pinna (2019). In search for stability in crypto-assets: are stablecoins the solution? Occasional Paper Series 230, European Central Bank.
- Calle, G. and D. B. Zalles (2019). Will businesses ever use stablecoins? white paper, R3 Reports.
- Calvo, G. A. and C. M. Reinhart (2002). Fear of floating. *The Quarterly Journal of Economics* 117(2), 379–408.
- Carletti, E., I. Goldstein, and A. Leonello (2019). The interdependence of bank capital and liquidity. BAFFI CAREFIN Working Papers 19128, BAFFI CAREFIN, Centre for Applied Research on International Markets Banking Finance and Regulation, Università Bocconi, Milano, Italy.
- Catalini, C. and J. S. Gans (2018). Initial coin offerings and the value of crypto tokens. *Working Paper*.

- Chen, N., P. Glasserman, B. Nouri, and M. Pelger (2017). Contingent capital, tail risk, and debt-induced collapse. *The Review of Financial Studies* 30(11), 3921–3969.
- Chiu, J. and T. V. Koepl (2017). The economics of cryptocurrencies—Bitcoin and beyond.
- Chod, J. and E. Lyandres (2019). A theory of ICOs: Diversification, agency, and information asymmetry. *Management Science* (forthcoming).
- Christiano, L. J., M. Eichenbaum, and C. L. Evans (2005). Nominal rigidities and the dynamic effects of a shock to monetary policy. *Journal of Political Economy* 113(1), 1–45.
- Cong, L. W. and Z. He (2019). Blockchain disruption and smart contracts. *The Review of Financial Studies* 32(5), 1754–1797.
- Cong, L. W., Z. He, and J. Li (2020). Decentralized Mining in Centralized Pools. *The Review of Financial Studies* 34(3), 1191–1235.
- Cong, L. W., Y. Li, and N. Wang (2019). Token-based platform finance. Charles A. Dice Center Working Paper 2019-28, The Ohio State University Fisher College of Business.
- Cong, L. W., Y. Li, and N. Wang (2021). Tokenomics: Dynamic adoption and valuation. *The Review of Financial Studies* 34(3), 1105–1155.
- Cox, J. C., S. A. Ross, and M. Rubinstein (1979). Option pricing: A simplified approach. *Journal of Financial Economics* 7(3), 229–263.
- Dang, T. V., G. Gorton, B. Holmström, and G. Ordoñez (2014). Banks as secret keepers. Working Paper 20255, National Bureau of Economic Research.
- Danos, V., S. Marcassa, M. Oliva, and J. Prat (2021). Fundamental pricing of utility tokens. *Working Paper*.
- Davydiuk, T., D. Gupta, and S. Rosen (2019). De-crypto-ing signals in initial coin offerings: Evidence of rational token retention. Working paper, Carnegie Mellon University and Temple University.
- Décamps, J.-P., T. Mariotti, J.-C. Rochet, and S. Villeneuve (2011). Free cash flow, issuance costs, and stock prices. *The Journal of Finance* 66(5), 1501–1544.

- DeMarzo, P. M. and D. Duffie (1999). A liquidity-based model of security design. *Econometrica* 67(1), 65–99.
- Doepke, M. and M. Schneider (2017). Money as a unit of account. *Econometrica* 85(5), 1537–1574.
- Donaldson, J. R. and G. Piacentino (2020). Money runs. *Journal of Monetary Economics* forthcoming.
- Donaldson, J. R., G. Piacentino, and A. Thakor (2018). Warehouse banking. *Journal of Financial Economics* 129(2), 250 – 267.
- Duffie, D. (2019). Digital currencies and fast payment systems: Disruption is coming. working paper, Stanford University Graduate School of Business.
- Dumas, B. (1991). Super contact and related optimality conditions. *Journal of Economic Dynamics and Control* 15(4), 675 – 685.
- Easley, D., M. O’Hara, and S. Basu (2019). From mining to markets: The evolution of bitcoin transaction fees. *Journal of Financial Economics*.
- Ebrahimi, Z., B. Routledge, and A. Zetlin-Jones (2020). Getting blockchain incentives right. Working paper, Carnegie Mellon University Tepper School of Business.
- ECB Crypto-Assets Task Force (2019). Stablecoins: Implications for monetary policy, financial stability, market infrastructure and payments, and banking supervision in the euro area. Occasional Paper Series 247, European Central Bank.
- Eckbo, B. E., R. W. Masulis, and O. Norli (2007). Chapter 6 – security offerings. In B. E. Eckbo (Ed.), *Handbook of Corporate Finance: Empirical Corporate Finance*, Volume 1 of *Handbook of Finance Series*, pp. 233–373. Elsevier/North-Holland.
- Fajgelbaum, P. D., E. Schaal, and M. Taschereau-Dumouchel (2017). Uncertainty Traps. *The Quarterly Journal of Economics* 132(4), 1641–1692.
- Fanti, G., L. Kogan, and P. Viswanath (2019). Economics of proof-of-stake payment systems. Working paper.
- Farboodi, M., R. Mihet, T. Philippon, and L. Veldkamp (2019, January). Big data and firm dynamics. Working Paper 25515, National Bureau of Economic Research.

- Faure, S. and H. Gersbach (2017). Money creation and destruction. Working Paper 6565, CESifo.
- Feenstra, R. C. (1986). Functional equivalence between liquidity costs and the utility of money. *Journal of Monetary Economics* 17(2), 271 – 291.
- Freeman, S. and F. E. Kydland (2000). Monetary aggregates and output. *American Economic Review* 90(5), 1125–1135.
- G7 Working Group on Stablecoins (2019). Investigating the impact of global stablecoins. Technical report, Committee on Payments and Market Infrastructures, Bank for International Settlements.
- Galí, J. (2015). *Monetary Policy, Inflation, and the Business Cycle: An Introduction to the New Keynesian Framework and Its Applications Second edition*. Number 10495 in Economics Books. Princeton University Press.
- Gan, J. R., G. Tsoukalas, and S. Netessine (2021). Initial coin offerings, speculation, and asset tokenization. *Management Science* 67(2), 914–931.
- Gao, X., T. M. Whited, and N. Zhang (2020). Corporate Money Demand. *The Review of Financial Studies* 34(4), 1834–1866.
- Garratt, R. and M. R. Van Oordt (2019). Entrepreneurial incentives and the role of initial coin offerings. working paper, University of California at Santa Barbara and Bank of Canada.
- Garratt, R. and N. Wallace (2018). Bitcoin 1, bitcoin 2,: An experiment in privately issued outside monies. *Economic Inquiry* 56(3), 1887–1897.
- Glaeser, E. L., B. Sacerdote, and J. A. Scheinkman (1996). Crime and Social Interactions. *The Quarterly Journal of Economics* 111(2), 507–548.
- Glasserman, P. and B. Nouri (2012). Contingent capital with a capital-ratio trigger. *Management Science* 58(10), 1816–1833.
- Glasserman, P. and B. Nouri (2016). Market-triggered changes in capital structure: Equilibrium price dynamics. *Econometrica* 84(6), 2113–2153.
- Goldstein, I., D. Gupta, and R. Sverchkov (2019). Initial coin offerings as a commitment to competition. Technical report, Carnegie Mellon University and University of Pennsylvania The Wharton School.

- Goldstein, I., E. Ozdenoren, and K. Yuan (2011). Learning and Complementarities in Speculative Attacks. *The Review of Economic Studies* 78(1), 263–292.
- Goldstein, I. and A. Pauzner (2005). Demand–deposit contracts and the probability of bank runs. *The Journal of Finance* 60(3), 1293–1327.
- Gopinath, G., E. Boz, C. Casas, F. J. Díez, P.-O. Gourinchas, and M. Plagborg-Møller (2020, March). Dominant currency paradigm. *American Economic Review* 110(3), 677–719.
- Gorton, G. and G. Pennacchi (1990). Financial intermediaries and liquidity creation. *The Journal of Finance* 45(1), 49–71.
- Gorton, G. B. and J. Zhang (2021). Taming wildcat stablecoins. working paper, Federal Reserve Board and Yale University.
- Gryglewicz, S., S. Mayer, and E. Morellec (2020). Optimal financing with tokens. *Working Paper*.
- Halaburda, H. (2018). Blockchain revolution without the blockchain? *Commun. ACM* 61(7), 27–29.
- He, Z. and P. Kondor (2016). Inefficient investment waves. *Econometrica* 84(2), 735–780.
- Hennessy, C. A. and T. M. Whited (2005). Debt dynamics. *The Journal of Finance* 60(3), 1129–1165.
- Hennessy, C. A. and T. M. Whited (2007). How costly is external financing? evidence from a structural estimation. *The Journal of Finance* 62(4), 1705–1745.
- Hinzen, F. J., K. John, and F. Saleh (2019). Bitcoin’s fatal flaw: The limited adoption problem. *NYU Stern School of Business*.
- Hu, A. S., C. A. Parlour, and U. Rajan (2019). Cryptocurrencies: Stylized facts on a new investible instrument. *Financial Management* 48(4), 1049–1068.
- Huberman, G., J. D. Leshno, and C. C. Moallemi (2019). An economic analysis of the Bitcoin payment system.
- Hugonnier, J., S. Malamud, and E. Morellec (2015). Capital supply uncertainty, cash holdings, and investment. *The Review of Financial Studies* 28(2), 391–445.

- John, K., T. J. Rivera, and F. Saleh (2020). Economic implications of scaling blockchains: Why the consensus protocol matters. Working paper, New York University, McGill University, and Wake Forest University.
- John, K., T. J. Rivera, and F. Saleh (2021). Equilibrium staking levels in a proof-of-stake blockchain. *Available at SSRN 3965599*.
- Jones, C. I. and C. Tonetti (2020). Nonrivalry and the economics of data. *American Economic Review* 110(9), 2819–58.
- Jorgenson, D. W. (1963). Capital theory and investment behavior. *The American Economic Review* 53(2), 247–259.
- J.P. Morgan Global Research (2021, February). Digital transformation and the rise of fintech: blockchain, bitcoin, and digital finance 2021.
- Kacperczyk, M. and P. Schnabl (2013). How Safe Are Money Market Funds? *The Quarterly Journal of Economics* 128(3), 1073–1122.
- Kim, T. W. and A. Zetlin-Jones (2019). The ethics of contentious hard forks in blockchain networks with fixed features. *Frontiers in Blockchain* 2, 9.
- Klimenko, N., S. Pfeil, J.-C. Rochet, and G. D. Nicolo (2016). Aggregate bank capital and credit dynamics. Swiss Finance Institute Research Paper Series 16-42.
- Kondor, P. (2009). Risk in dynamic arbitrage: The price effects of convergence trading. *The Journal of Finance* 64(2), 631–655.
- Kozhan, R. and G. Viswanath-Natraj (2021). Decentralized stablecoins and collateral risk. *WBS Finance Group Research Paper Forthcoming*.
- La Spada, G. (2018). Competition, reach for yield, and money market funds. *Journal of Financial Economics* 129(1), 87–110.
- Laffont, J.-J. and J. Tirole (1994). Access pricing and competition. *European Economic Review* 38(9), 1673 – 1710.
- Lee, I., S. Lochhead, J. Ritter, and Q. Zhao (1996). The costs of raising capital. *Journal of Financial Research* 19(1), 59–74.

- Lehar, A. and C. A. Parlour (2020). Miner collusion and the bitcoin protocol. Working paper, University of Calgary and University of California Berkeley.
- Lehar, A. and C. A. Parlour (2021). Decentralized exchanges. working paper, University of Calgary and University of California, Berkeley.
- Li, J. and W. Mann (2020). Digital tokens and platform building. *Working Paper*.
- Li, L., Y. Li, M. Macchiavelli, and X. Zhou (2021). Liquidity restrictions, runs, and central bank interventions: Evidence from money market funds. *Review of Financial Studies forthcoming*.
- Liu, Y., J. Sheng, and W. Wang (2020). Do cryptocurrencies have fundamental values? *Working paper*.
- Liu, Y. and A. Tsyvinski (2020). Risks and Returns of Cryptocurrency. *The Review of Financial Studies* 34(6), 2689–2727.
- Liu, Y., A. Tsyvinski, and X. Wu (2019). Common risk factors in cryptocurrency. Working Paper 25882, National Bureau of Economic Research.
- Ljungqvist, L. and T. J. Sargent (2004). *Recursive Macroeconomic Theory, 2nd Edition*, Volume 1 of *MIT Press Books*. The MIT Press.
- Lucas, R. E. and J. P. Nicolini (2015). On the stability of money demand. *Journal of Monetary Economics* 73, 48 – 65.
- Lyons, R. K. and G. Viswanath-Natraj (2020, May). What keeps stablecoins stable? Working Paper 27136, National Bureau of Economic Research.
- Makarov, I. and A. Schoar (2020). Trading and arbitrage in cryptocurrency markets. *Journal of Financial Economics* 135(2), 293–319.
- Massad, T. (2021, May). Can a cryptocurrency break the buck? Bloomberg.
- Mayer, S. (2020). Token-based platforms and speculators. *Available at SSRN 3471977*.
- Moreira, A. and A. Savov (2017). The macroeconomics of shadow banking. *The Journal of Finance* 72(6), 2381–2432.
- Morris, S. and H. S. Shin (1998). Unique equilibrium in a model of self-fulfilling currency attacks. *The American Economic Review* 88(3), 587–597.

- Nagel, S. (2016). The Liquidity Premium of Near-Money Assets. *The Quarterly Journal of Economics* 131(4), 1927–1971.
- Nikolov, B., L. Schmid, and R. Steri (2019). Dynamic corporate liquidity. *Journal of Financial Economics* 132(1), 76–102.
- Nikolov, B. and T. M. Whited (2014). Agency conflicts and cash: Estimates from a dynamic model. *The Journal of Finance* 69(5), 1883–1921.
- Ordoñez, G. (2013). The asymmetric effects of financial frictions. *Journal of Political Economy* 121(5), 844–895.
- Pagnotta, E. and A. Buraschi (2018). An equilibrium valuation of Bitcoin and decentralized network assets. Working paper, Imperial College.
- Pagnotta, E. S. (2021). Decentralizing Money: Bitcoin Prices and Blockchain Security. *The Review of Financial Studies*. hhaa149.
- Parlato, C. (2016). Fragility in money market funds: Sponsor support and regulation. *Journal of Financial Economics* 121(3), 595–623.
- Parlour, C. A., U. Rajan, and J. Walden (2020). Payment system externalities and the role of central bank digital currency. *Journal of Finance* forthcoming.
- Parlour, C. A., U. Rajan, and H. Zhu (2020). When fintech competes for payment flows. Working paper, Massachusetts Institute of Technology, University of California (Berkeley), and University of Michigan.
- Penati, A. and G. Pennacchi (1989). Optimal portfolio choice and the collapse of a fixed-exchange rate regime. *Journal of International Economics* 27(1), 1–24.
- Pennacchi, G. (2010). A structural model of contingent bank capital. Working Papers (Old Series) 1004, Federal Reserve Bank of Cleveland.
- Pennacchi, G. (2012). Narrow banking. *Annual Review of Financial Economics* 4(1), 141–159.
- Pennacchi, G. and A. Tchisty (2018). Contingent Convertibles with Stock Price Triggers: The Case of Perpetuities. *The Review of Financial Studies* 32(6), 2302–2340.

- Pennacchi, G. and A. Tchisty (2019). On equilibrium when contingent capital has a market trigger: A correction to sundaresan and wang journal of finance (2015). *The Journal of Finance* 74(3), 1559–1576.
- Philippon, T. (2015). Has the us finance industry become less efficient? on the theory and measurement of financial intermediation. *The American Economic Review* 105(4), 1408–1438.
- Piazzesi, M. and M. Schneider (2016). Payments, credit and asset prices. Working paper, Stanford University.
- Poterba, J. M. and J. J. Rotemberg (1986). Money in the utility function: An empirical implementation. Working Paper 1796, National Bureau of Economic Research.
- Prat, J. and B. Walter (2021). An equilibrium model of the market for bitcoin mining. *Journal of Political Economy* 129(8).
- Pratt, J. W. (1964). Risk aversion in the small and in the large. *Econometrica* 32(1/2), 122–136.
- Raskin, M. and D. Yermack (2016). Digital currencies, decentralized ledgers, and the future of central banking. Working Paper 22238, National Bureau of Economic Research.
- Riddick, L. A. and T. M. Whited (2009). The corporate propensity to save. *The Journal of Finance* 64(4), 1729–1766.
- Rochet, J.-C. and J. Tirole (2003). Platform competition in two-sided markets. *Journal of the European Economic Association* 1(4), 990–1029.
- Rochet, J.-C. and J. Tirole (2006). Two-sided markets: A progress report. *The RAND Journal of Economics* 37(3), 645–667.
- Routledge, B. and A. Zetlin-Jones (2021). Currency stability using blockchain technology. *Journal of Economic Dynamics and Control*, 104155.
- Rysman, M. (2009). The economics of two-sided markets. *The Journal of Economic Perspectives* 23(3), 125–143.
- Saengchote, K. (2021). Where do defi stablecoins go? a closer look at what defi composability really means. *A closer look at what DeFi composability really means. (July 26, 2021)*.

- Saleh, F. (2020). Blockchain without Waste: Proof-of-Stake. *The Review of Financial Studies* 34(3), 1156–1190.
- Schilling, L. and H. Uhlig (2019). Some simple bitcoin economics. *Journal of Monetary Economics* 106, 16–26. SPECIAL CONFERENCE ISSUE: “Money Creation and Currency Competition” October 19-20, 2018 Sponsored by the Study Center Gerzensee and Swiss National Bank.
- Schmidt, L., A. Timmermann, and R. Wermers (2016). Runs on money market mutual funds. *American Economic Review* 106(9), 2625–57.
- Shafir, E., P. Diamond, and A. Tversky (1997). Money Illusion. *The Quarterly Journal of Economics* 112(2), 341–374.
- Shams, A. (2020). The structure of cryptocurrency returns. Charles A. Dice Center Working Paper 2020-11, The Ohio State University Fisher College of Business.
- Sockin, M. and W. Xiong (2018). A model of cryptocurrencies. Working paper, Princeton University and University of Texas at Austin.
- Stulz, R. M. (2019). Fintech, bigtech, and the future of banks. *Journal of Applied Corporate Finance* 31(4), 86–97.
- Tinn, K. (2017). Smart contracts and external financing. working paper, McGill University.
- Tobin, J. (1956). The interest-elasticity of transactions demand for cash. *The Review of Economics and Statistics* 38(3), 241–247.
- Tobin, J. (1963). Commercial banks as creators of “money”. Cowles Foundation Discussion Papers 159, Cowles Foundation for Research in Economics, Yale University.
- U.S. Department of the Treasury (2021, November). President’s working group on financial markets releases report and recommendations on stablecoins. Press Release.
- Veldkamp, L. and C. Chung (2019). Data and the aggregate economy. Working paper.
- Veldkamp, L. L. (2005). Slow boom, sudden crash. *Journal of Economic Theory* 124(2), 230 – 257. Learning and Bounded Rationality.
- Walsh, C. E. (2003). *Monetary Theory and Policy, 2nd Edition* (2 ed.). The MIT Press.

A Proofs

A.1 Proof of Propositions 1 and 2

The proof of Propositions 1 and 2 is split in three parts. Part I derives the HJB equation and its boundary conditions. Part II establishes the concavity of the value function. Part III shows that there is no liquidation.

Part I — HJB equation and dividend payouts

Recall that the platform chooses dividends $\{dDiv_t\}$, transaction volume $\{N_t\}$ (or equivalently transaction fees $\{f_t\}$), and token price volatility $\{\sigma_t^P\}$ (which implicitly pins down token price and the choice of token supply via the market clearing condition $N_t = S_t P_t$) to maximize the future expected discounted value of dividends. By the dynamic programming principle, the platform solves (18) subject to $dDiv_t \geq 0$ and the law of motion (17). As such, platform value $V(C) = V(C_t)$ satisfies the following HJB equation (in differential form):

$$\rho V(C)dt = \max_{N \in [0, \bar{N}], \sigma^P, dDiv \geq 0} \{dDiv + \mathbb{E}[dV(C)]\}. \quad (\text{A.1})$$

In what follows, we assume that (A.1) admits a unique and twice differentiable solution $V(C)$.

Using Ito's Lemma and expanding the right-hand-side, we obtain

$$\rho V(C)dt = \max_{\{N \in [0, \bar{N}], \sigma^P, dDiv \geq 0\}} \left\{ (1 - V'(C))dDiv + V'(C) \left(rC + N^\xi A^{1-\xi} - \eta N |\sigma_t^P| \right) dt \right. \quad (\text{A.2})$$

$$\left. + \frac{1}{2} V''(C) N^2 (\sigma - \sigma^P)^2 dt \right\}. \quad (\text{A.3})$$

It follows that dividend payouts are optimal if and only if $V'(C) \geq 1$. As in Bolton et al. (2011), the optimal dividend policy therefore follows a barrier strategy, so that (in optimum) dividend payouts $dDiv$ cause C_t to reflect at \bar{C} , i.e., $dDiv_t = \max\{C_t - \bar{C}, 0\}$. And, the threshold \bar{C} satisfies smooth pasting and super contact conditions (for details, see, e.g., Dumas (1991)), i.e.,

$$V'(\bar{C}) - 1 = V''(\bar{C}) = 0.$$

Given this dividend policy, the HJB equation (A.2) simplifies to (23) whenever $C_t \leq \bar{C}$, as stated in Proposition 2. In addition, the optimal dividend policy also implies $C_t \leq \bar{C}$ for all $t \geq 0$.

Part II — Value function concavity

We prove the concavity of value function in Proposition 1. Recall the HJB equation (23), that is,

$$\rho V(C) = \max_{\{N \in [0, \bar{N}], \sigma^P\}} \left\{ V'(C) \left(rC + N^\xi A^{1-\xi} - \eta N |\sigma^P| \right) + \frac{1}{2} V''(C) N^2 (\sigma - \sigma^P)^2 \right\}.$$

Using the envelope theorem, we differentiate both sides of the HJB equation (evaluated under the optimal controls N and σ^P) with respect to C to obtain

$$\rho V'(C) = rV'(C) + V''(C) \left(rC + N^\xi A^{1-\xi} - \eta N |\sigma_t^P| \right) + \frac{1}{2} V'''(C) N^2 (\sigma - \sigma^P)^2.$$

We can solve for

$$V'''(C) = \frac{2}{N^2 (\sigma - \sigma^P)^2} \left[(\rho - r) V'(C) - V''(C) \left(rC + N^\xi A^{1-\xi} - \eta N |\sigma^P| \right) \right]$$

Using the smooth pasting condition, $V'(\bar{C}) = 1$, and the super-contact condition, $V''(\bar{C}) = 0$, we obtain $V'''(\bar{C}) > 0$. As $V''(\bar{C}) = 0$, it follows that $V''(C) < 0$ in a left-neighbourhood of \bar{C} , in that there exists $\varepsilon > 0$ so that $V''(C) < 0$ for $C \in (\bar{C} - \varepsilon, \bar{C})$.

We show now that $V''(C) < 0$ for all $C \in [0, \bar{C})$. Suppose to the contrary that there exists $\hat{C} < \bar{C}$ with $V''(\hat{C}) \geq 0$ and set without loss of generality

$$\hat{C} = \sup\{C \in (0, \bar{C} - \varepsilon) : V''(C) \geq 0\}. \quad (\text{A.4})$$

As $V''(C) < 0$ on the interval $(\bar{C} - \varepsilon, \bar{C})$ and the value function is twice continuously differentiable, it follows that $V''(\hat{C}) = 0$ and therefore the optimization in the HJB equation (23) implies $\sigma^P(\hat{C}) < \sigma$. In addition, $V'(\hat{C}) \geq 1$, so that $V'''(\hat{C}) > 0$. Thus, there exists $C' > \hat{C}$ with $V''(C') \geq 0$, a contradiction. Therefore, the value function is strictly concave on $[0, \bar{C})$.

Part III — There is no liquidation

Consider that C_t approaches zero, i.e., $C_t \rightarrow 0$. If the volatility of dC_t , $\sigma_C(C_t) = N_t(\sigma - \sigma^P(C_t))$ does not tend to zero as C_t approaches zero, C_t drops below zero and the platform is liquidated with probability one in which case the platform owners' value becomes zero. To prevent liquidation as C_t approaches zero, it must be that i) the volatility of dC_t , $\sigma_C(C_t) = N_t(\sigma - \sigma_t^P)$, tends to zero and ii) the drift of dC_t , $\mu_C(C_t) = rC_t + N_t^\xi A^{1-\xi} - N_t \eta |\sigma_t^P|$, remains positive positive. Formally,

$$\lim_{C \rightarrow 0^+} \mu_C(C) > 0 = \lim_{C \rightarrow 0^+} \sigma_C(C), \quad (\text{A.5})$$

must hold.

Thus, if the platform prevents liquidation, then — by the law of motion (17) — it must be $\lim_{C \rightarrow 0^+} \sigma^P(C) = \sigma$. As $V(C)$ is concave with $V'(\bar{C}) = 1$, it follows that $V'(C) > 0$ for all $C \in [0, \bar{C}]$. As such, when $\sigma^P(C) \rightarrow \sigma$, then

$$V(C) \rightarrow \frac{1}{\rho} V'(C) \mu_C(C).$$

Therefore, when $\lim_{C \rightarrow 0^+} \sigma^P(C) \rightarrow 0$, the equivalence

$$\lim_{C \rightarrow 0^+} V(C) > 0 \iff \lim_{C \rightarrow 0^+} \mu_C(C) > 0$$

holds.

Next, using the HJB equation (23), we obtain

$$\begin{aligned} V(C) &\geq \frac{V'(C)}{\rho} \left(rC + \max_{\{N \in [0, \bar{N}]\}} \{N^\xi A^{1-\xi} - \eta N \sigma\} \right) \\ &\geq \frac{1}{\rho} \left(\max_{\{N \in [0, \bar{N}]\}} \{N^\xi A^{1-\xi} - \eta N \sigma\} \right) > 0. \end{aligned}$$

The first inequality uses that setting $\sigma^P = \sigma$ is always possible (but not necessarily optimal) and the second inequality uses $C \geq 0$ and $V'(C) \geq 1$. As such, the platform obtains strictly positive value from continuation, implying that liquidation is not optimal and the platform optimally prevents liquidation. Thus, liquidation never occurs, and (A.5) holds.

A.2 Proof of Proposition 3

The proof of Proposition 3 is split in three parts. Part I characterizes the optimal controls $N(C)$ and $\sigma^P(C)$. Part II shows that platform risk-aversion $\gamma(C)$ decreases with C . Part III demonstrates that there exists \tilde{C} so that for $C < \tilde{C}$ ($C \geq \tilde{C}$), $\sigma^P(C) > 0$ ($\sigma^P(C) = 0$).

Part I — Optimal control variables

We characterize the optimization in (23) and solve for the optimal control variables $N = N(C)$ and $\sigma^P = \sigma^P(C)$ in Proposition 3. To start with, we define

$$\underline{N} = \arg \max_{N \leq \bar{N}} \{N^\xi A^{1-\xi} - \eta N \sigma\}, \quad (\text{A.6})$$

which yields

$$\underline{N} = \min \left\{ \left(\frac{\xi A^{1-\xi}}{\eta \sigma} \right)^{\frac{1}{1-\xi}}, \bar{N} \right\}.$$

Now, we first optimize the HJB equation (23) over σ^P or equivalently over $N\sigma^P$.

If interior (i.e., $\sigma^P > 0$), the choice of σ^P satisfies the first order optimality condition

$$\frac{\partial V(C)}{\partial \sigma^P} = 0 \iff -\eta V'(C) - V''(C)(N\sigma - N\sigma^P) = 0.$$

We can rearrange the above first order condition to derive

$$N\sigma^P = \frac{-\eta V'(C) - N\sigma V''(C)}{-V''(C)}. \quad (\text{A.7})$$

It is clear from the maximization in the HJB equation (23) that setting $\sigma^P < 0$ is never optimal. As such, to obtain the optimal choice of σ^P we truncate the expression in (A.7) from below by zero and obtain

$$N\sigma^P = \max \left\{ 0, \frac{-\eta V'(C) - N\sigma V''(C)}{-V''(C)} \right\} = \max \left\{ 0, -\frac{\eta V'(C)}{-V''(C)} + N\sigma \right\}. \quad (\text{A.8})$$

Note that by (12), users' aggregate token holdings are always positive (i.e., $N_t > 0$ at all times $t \geq 0$) so that $\sigma^P > 0 \iff N\sigma^P > 0$ and $\sigma^P = 0 \iff N\sigma^P = 0$. We distinguish between two different cases: 1) $\sigma^P = 0$ and 2) $\sigma^P > 0$.

1. First, consider $\sigma^P > 0$. Then, we can insert the relation (A.7) (or (A.8) noting that $N\sigma^P > 0$) into (23) to get

$$\rho V(C) = \max_{N \in [0, \bar{N}]} \left\{ V'(C) \left[rC + N^\xi A^{1-\xi} - \eta N\sigma - \frac{\eta^2 V'(C)}{V''(C)} \right] + \frac{1}{V''(C)} \left[\frac{(\eta V'(C))^2}{2} \right] \right\}.$$

Thus, by (A.6), $N = \underline{N} > 0$ is the optimal choice of N , so that by means of (A.8):

$$\sigma^P = \max \left\{ 0, -\frac{\eta V'(C)}{-V''(C)\underline{N}} + \sigma \right\} = \max \left\{ 0, \sigma - \frac{\eta}{\gamma(C)\underline{N}} \right\}, \quad (\text{A.9})$$

where the last equality uses the definition $\gamma(C) = -\frac{V''(C)}{V'(C)}$.

2. Second, consider $\sigma^P = 0$. Inserting $\sigma^P = 0$ into (23), the HJB equation becomes

$$\rho V(C) = \max_{N \in [0, \bar{N}]} \left\{ V'(C)[rC + N^\xi A^{1-\xi}] + V''(C) \left[\frac{N^2 \sigma^2}{2} \right] \right\}. \quad (\text{A.10})$$

If interior (i.e., $N(C) < \bar{N}$), the optimal choice of $N = N(C)$ must solve the first order condition

$$V'(C)\xi N^{\xi-1} A^{1-\xi} + V''(C)N\sigma^2 = 0 \iff V'(C)\xi N^{\xi-2} A^{1-\xi} + V''(C)\sigma^2 = 0.$$

Thus, optimal $N = N(C)$ reads

$$N(C) = \min \left\{ \left(\frac{A^{1-\xi} \xi V'(C)}{-V''(C)\sigma^2} \right)^{\frac{1}{2-\xi}}, \bar{N} \right\}, \quad (\text{A.11})$$

where we truncate above by \bar{N} .

Overall, note that $\sigma^P(C)$ (partially) decreases with $\gamma(C)$, the platform's risk-aversion, in that $\frac{\partial \sigma^P(C)}{\partial \gamma(C)} \leq 0$. When $\sigma^P(C) > 0$, this follows from (A.9), and, when $\sigma^P = 0$, this trivially holds.

Part II — Effective risk-aversion

We prove $\gamma'(C) < 0$, i.e., $\frac{d(-V''(C)/V'(C))}{dC} < 0$, in Proposition 3. To do so, we consider the following two cases, 1) $\sigma^P = 0$ and 2) $\sigma^P = 0$:

1. Consider $\sigma^P > 0$ so that $N = \underline{N}$. Then, the HJB equation (23) can be simplified to

$$\rho \frac{V(C)}{V'(C)} = rC + \underline{N}^\xi A^{1-\xi} - \eta \underline{N} \sigma - \frac{\eta^2}{2} \frac{V'(C)}{V''(C)}. \quad (\text{A.12})$$

Differentiating the equation above with respect to C , we obtain

$$\rho \left(1 - \frac{V''(C)V(C)}{V'(C)^2} \right) = r - \frac{\eta^2}{2} \frac{d(V'(C)/V''(C))}{dC},$$

which can be rewritten as

$$\frac{d(V'(C)/V''(C))}{dC} = \frac{2}{\eta^2} \left[(r - \rho) + \rho \left(\frac{V''(C)V(C)}{V'(C)^2} \right) \right].$$

Note that because $\rho > r$ and $V''(C) < 0$, it follows that implies $\frac{d(V'(C)/V''(C))}{dC} < 0$, i.e., $\frac{d(-V''(C)/V'(C))}{dC} = \gamma'(C) < 0$.

2. Consider $\sigma^P = 0$, so the HJB (23) simplifies to

$$\rho V(C) = \max_{N \in [0, \bar{N}]} \left\{ V'(C)[rC + N^\xi A^{1-\xi}] + V''(C) \left[\frac{N^2 \sigma^2}{2} \right] \right\}, \quad (\text{A.13})$$

In this case, we further consider two cases, a) $N = N(C) < \bar{N}$ and b) $N = N(C) = \bar{N}$:

- a) $N(C) < \bar{N}$ and $N = \left(\frac{A^{1-\xi} \xi V'(C)}{-V''(C) \sigma^2} \right)^{\frac{1}{2-\xi}}$. In this case, the HJB can be simplified to

$$\rho \frac{V(C)}{V'(C)} = rC + \frac{1}{2} \left(\frac{\xi A^{1-\xi}}{\sigma^\xi} \right)^{\frac{2}{2-\xi}} \left(\frac{2-\xi}{\xi} \right) \left(\frac{V'(C)}{-V''(C)} \right)^{\frac{\xi}{2-\xi}}. \quad (\text{A.14})$$

Differentiating the equation above with respect to C , we obtain

$$\rho \left(1 - \frac{V''(C)V(C)}{V'(C)^2} \right) = r - \frac{1}{2} \left(\frac{\xi A^{1-\xi}}{\sigma^\xi} \right)^{\frac{2}{2-\xi}} \left(\frac{V'(C)}{-V''(C)} \right)^{\frac{2\xi-2}{2-\xi}} \frac{d(-V'(C)/V''(C))}{dC}, \quad (\text{A.15})$$

implying $\frac{d(V'(C)/V''(C))}{dC} < 0$ (because $V''(C) < 0$ and $\rho > r$), that is, $\frac{d(-V''(C)/V'(C))}{dC} = \gamma'(C) < 0$.

- b) $N(C) = \bar{N}$. In this case, the HJB can be simplified to

$$\rho \frac{V(C)}{V'(C)} = rC + \bar{N}^\xi A^{1-\xi} + \frac{\bar{N}^2 \sigma^2}{2} \frac{V''(C)}{V'(C)}. \quad (\text{A.16})$$

Differentiating the equation above with respect to C , we obtain

$$\rho \left(1 - \frac{V''(C)V(C)}{V'(C)^2} \right) = r - \frac{\bar{N}^2 \sigma^2}{2} \frac{d(-V''(C)/V'(C))}{dC}, \quad (\text{A.17})$$

which implies $\frac{d(-V''(C)/V'(C))}{dC} = \gamma'(C) < 0$ (because $V''(C) < 0$ and $\rho > r$).

Part III — Existence of threshold \tilde{C}

In Part I, we have shown that $\sigma^P(C)$ increases with $\gamma(C)$ and, in Part II, we have shown that $\gamma(C)$ decreases with C with $\gamma(\bar{C}) = 0$. Therefore, $\sigma^P(C)$ decreases with C . As $\gamma(\bar{C}) = 0$, it must be that $\sigma^P(C) = 0$ in a left-neighbourhood of \bar{C} . Because there is no liquidation, it holds that $\lim_{C \rightarrow 0^+} \sigma^P(C) = \sigma$ and thus — by continuity — $\sigma^P(C) > 0$ in a right-neighbourhood of $C = 0$. As $\sigma^P(C)$ is continuous and decreases with C on $[0, \bar{C}]$, there exists unique $\tilde{C} \in (0, \bar{C})$ so that $\sigma^P(C) > 0$ for $C < \tilde{C}$ and $\sigma^P(C) = 0$ for $C \geq \tilde{C}$ (while $C \in [0, \bar{C}]$). The threshold \tilde{C} solves

$$\sigma - \frac{\eta}{\gamma(\tilde{C})\underline{N}} = 0,$$

which implicitly defines \tilde{C} (see (A.9)). This concludes the argument.

A.3 Proof of Corollary 1

First, consider that $C < \tilde{C}$, so $\sigma^P(C) > 0$ and $N(C) = \underline{N}$. Using (13), we obtain

$$f(C) = \left(\frac{A}{\underline{N}} \right)^{1-\xi} - r + \mu^P(C) - \eta |\sigma^P(C)|. \quad (\text{A.18})$$

Second, consider that $C \geq \tilde{C}$ and $N(C) < \bar{N}$. Then, $\sigma^P(C) = \mu^P(C) = 0$ and

$$N(C) = \left(\frac{\xi A^{1-\xi}}{\gamma(C)\sigma^2} \right)^{\frac{1}{2-\xi}}.$$

Using (13) and simplifying, we obtain

$$f(C) = \left(\frac{A\gamma(C)\sigma^2}{\xi} \right)^{\frac{1-\xi}{2-\xi}} - r.$$

Third, consider $C \geq \tilde{C}$ and $N(C) = \bar{N}$ so that $\mu^P(C) = \sigma^P(C) = 0$. Using (13), we obtain

$$f(C) = \left(\frac{A}{\bar{N}} \right)^{1-\xi} - r.$$

Finally, note that because $\gamma(C)$ decreases with C , $N(C)$ increases with C for $C \geq \tilde{C}$ with $N(\bar{C}) = \bar{N}$. Therefore, there exists $\tilde{C}' \geq \tilde{C}$ so that $N(C) = \bar{N}$ if $C \in [\tilde{C}', \bar{C}]$.

A.4 Proof of Corollary 2 and Proposition 4

The relevant arguments are already presented in the main text. In a Markov equilibrium with state variable C , token price $P(C)$ and $\sigma^P(C)$ are functions of C only. Ito's Lemma implies

$$\sigma^P(C) = \frac{P'(C)}{P(C)}N(C)(\sigma - \sigma^P(C)),$$

as desired. We normalize $P(\bar{C}) = 1$. For $C \geq \tilde{C}$, it holds that $\sigma^P(C) = 0$ and thus $P'(C) = P''(C) = 0$, so $\mu^P(C) = 0$. For $C < \tilde{C}$, it holds that $\sigma^P(C) > 0$ and so $P'(C) > 0$.

A.5 Proof of Proposition 5

Follows from the arguments presented in the main text.

A.6 Proof of Corollary 3

Follows from the arguments presented in the main text.

A.7 Proof of Proposition 6

To start with, recall the law of motion of the state variables C_t (see (45)),

$$dC_t = \left(rC_t + A_t n_t^\xi - \eta A_t n_t |\sigma_t^P| \right) dt + A_t n_t (\sigma - \sigma_t^P) dZ_t - dDiv_t, \quad (\text{A.19})$$

and A_t ,

$$\frac{dA_t}{A_t} = \kappa n_t^\xi dt.$$

Define $n_t = N_t/A_t$. Using Ito's Lemma, we can calculate

$$dc_t = \left(rc_t + n_t^\xi - \eta n_t |\sigma_t^P| - \kappa n_t^\xi c_t \right) dt + n_t (\sigma - \sigma_t^P) dZ_t - \frac{dDiv_t}{A_t}, \quad (\text{A.20})$$

with drift $\mu_c(c_t) \equiv rc_t + n_t^\xi - \eta n_t |\sigma_t^P| - \kappa n_t^\xi c_t$ and volatility $\sigma_c(c_t) = n_t (\sigma - \sigma_t^P)$.

By the dynamic programming principle, the platform's value function $V(C, A)$ solves the following HJB equation (in differential form):

$$\rho V(C, A) dt = \max_{\sigma^P, N \in [0, \bar{N}], dDiv \geq 0} \{ dDiv + \mathbb{E}[dV(C, A)] \}.$$

We can use Ito's Lemma to expand the right-hand-side of the HJB equation:

$$\begin{aligned} \rho V(C, A) dt = \max_{\sigma^P, N \in [0, \bar{N}], dDiv \geq 0} & \left\{ dDiv(1 - V_C(C, A)) + V_C(C, A) \left(rC + An^\xi - \eta An |\sigma^P| \right) dt \right. \\ & \left. + V_A(C, A) A \kappa n^\xi dt + \frac{V_{CC}(C, A) N^2 (\sigma - \sigma^P)^2}{2} dt \right\}, \quad (\text{A.21}) \end{aligned}$$

where a subscript denotes the partial derivative (e.g., $V_C(C, A) = \frac{\partial V(C, A)}{\partial C}$). As such, dividend payouts $dDiv > 0$ are optimal if and only if $V_C(C, A) \leq 1$; otherwise, $dDiv = 0$. Using the conjecture $V(C, A) = Av(c)$, we obtain

$$V_C(C, A) = v'(c), \quad V_A(C, A) = v(c) - v'(c)c, \quad \text{and} \quad V_{CC}(C, A) = \frac{v''(c)}{A}. \quad (\text{A.22})$$

As is standard (see, e.g., [Bolton et al. \(2011\)](#)), optimal dividend payouts cause c_t to reflect at \bar{c} , where the payout threshold \bar{c} satisfies $v'(\bar{c}) - 1 = v''(\bar{c}) = 0$. That is, $dDiv = A \max\{c - \bar{c}, 0\}$, and $c_t \leq \bar{c}$ at all times $t \geq 0$.

When there are no dividend payouts, the HJB equation [\(A.21\)](#) therefore becomes (using [\(A.22\)](#), dividing both sides by dt and A , and simplifying):

$$\rho v(c) = \max_{n \in [0, \bar{n}], \sigma^P} \left\{ [v(c) - v'(c)c] \kappa n^\xi + v'(c) (rc + n^\xi - \eta n |\sigma^P|) + \frac{1}{2} v''(c) n^2 (\sigma - \sigma^P)^2 \right\}, \quad (\text{A.23})$$

which is [\(47\)](#).

As c approaches zero, the platform can either liquidate (yielding $v(0) = 0$) or prevent liquidation by i) setting $\sigma^P(c) \rightarrow \sigma$ and ii) ensuring that the drift of dc , $\mu_c(c)$, remains positive. Formally, to prevent liquidation as $c \rightarrow 0$,

$$\lim_{c \rightarrow 0^+} \mu_c(c) > 0 = \lim_{c \rightarrow 0^+} \sigma_c(c) \quad (\text{A.24})$$

must hold. Setting $\sigma^P(c) \rightarrow \sigma$ as $c \rightarrow 0$ yields

$$\lim_{c \rightarrow 0^+} \rho v(c) = \max_{n \in [0, \bar{n}]} \lim_{c \rightarrow 0^+} \left(v(c) \kappa n^\xi + v'(c) (n^\xi - \eta n \sigma) \right) > 0.$$

Note that because $\kappa \bar{n}^\xi < \rho$ and $v'(c) \geq 1$, $\lim_{c \rightarrow 0^+} v(c) > 0$ implies $\lim_{c \rightarrow 0^+} \mu_c(c) > 0$, as (under the optimal controls)

$$\lim_{c \rightarrow 0^+} (\rho - \kappa n(c)^\xi) v(c) = \lim_{c \rightarrow 0^+} v'(c) \max_{n \in [0, \bar{n}]} \mu_c(c).$$

As $v'(c) \geq 1$ for all $c \leq \bar{c}$ and so

$$\lim_{c \rightarrow 0^+} \max_{n \in [0, \bar{n}]} v'(c) \mu_c(c) \geq \max_{n \in [0, \bar{n}]} (n^\xi - \eta n \sigma) > 0, \quad (\text{A.25})$$

it follows that $\lim_{c \rightarrow 0^+} v(c) > 0$, and the platform is better off averting liquidation. In optimum, liquidation never occurs and [\(A.24\)](#) holds, implying $\lim_{c \rightarrow 0^+} \sigma^P(c) = 0$.

A.8 Proof of Proposition 7

The optimal control variables, $n = n(c)$ and $\sigma^P = \sigma^P(c)$, are determined by the optimization in the HJB equation (47), that is,

$$\rho v(c) = \max_{n \in [0, \bar{n}], \sigma^P} \left\{ [v(c) - v'(c)c] \kappa n^\xi + v'(c) \left(rc + n^\xi - \eta n |\sigma^P| \right) + \frac{1}{2} v''(c) n^2 (\sigma - \sigma^P)^2 \right\}. \quad (\text{A.26})$$

We consider the following two cases, 1) $\sigma^P > 0$ and 2) $\sigma^P = 0$.

1. If $\sigma^P > 0$, then the first order condition

$$\frac{\partial v(c)}{\partial \sigma^P} = 0 \iff -v'(c)\eta n(c) - v''(c)n(c)^2(\sigma - \sigma^P(c)) = 0$$

must hold. We can solve for

$$\sigma^P(c) = \sigma - \frac{\eta v'(c)}{v''(c)n(c)} = \sigma - \frac{\eta}{\Gamma(c)n(c)} \in (0, \sigma),$$

where

$$\Gamma(c) = -\frac{v''(c)}{v'(c)}.$$

Inserting the optimal choice of $\sigma^P(c)$ back into (47), we obtain

$$\rho v(c) = \max_{n \in [0, \bar{n}], \sigma^P} \left\{ [v(c) - v'(c)c] \kappa n^\xi + v'(c) \left(rc + n^\xi - \eta \sigma n + \frac{\eta}{\Gamma(c)} \right) + \frac{1}{2} v''(c) \left(\frac{\eta}{\Gamma(c)} \right)^2 \right\}.$$

If interior (i.e., $n(c) < \bar{n}$), the optimal choice of $n = n(c)$ solves the first order condition

$$\kappa \xi [v(c) - v'(c)c] n(c)^{\xi-1} + v'(c) (\xi n(c)^{\xi-1} - \eta \sigma) = 0.$$

We define

$$q(c) = v(c) - v'(c)c$$

and solve for

$$n(c)^{\xi-1} = \frac{v'(c)\eta\sigma}{\kappa\xi q(c) + \xi v'(c)} \iff n(c) = \left(\frac{\xi(v'(c) + \kappa q(c))}{\eta\sigma v'(c)} \right)^{\frac{1}{1-\xi}}.$$

Thus,

$$n(c) = \left[\frac{\xi}{\eta\sigma} \left(1 + \frac{\kappa q(c)}{v'(c)} \right) \right]^{\frac{1}{1-\xi}} \wedge \bar{n},$$

as desired.

2. Consider $\sigma^P(c) = 0$. If interior (i.e., $n(c) \in (0, \bar{n})$), optimal $n = n(c)$ must solve the first

order condition

$$\xi[\kappa q(c) + v'(c)]n(c)^{\xi-1} + v''(c)n(c)\sigma^2 = 0.$$

Dividing both sides through $n(c) > 0$, we obtain

$$\xi[\kappa q(c) + v'(c)]n(c)^{\xi-2} + v''(c)\sigma^2 = 0 \iff n(c)^{\xi-2} = \frac{-v''(c)\sigma^2}{\xi(\kappa q(c) + v'(c))}$$

We can solve for

$$n(c) = \left(\frac{\xi(\kappa q(c) + v'(c))}{-v''(c)\sigma^2} \right)^{\frac{1}{2-\xi}}.$$

Thus,

$$n(c) = \left[\frac{\xi}{\Gamma(c)\sigma^2} \left(1 + \frac{\kappa q(c)}{v'(c)} \right) \right]^{\frac{1}{2-\xi}} \wedge \bar{n},$$

which was to show.

Finally, note that analogous to the baseline, there exist three regions and two thresholds \tilde{c} and \tilde{c}' such that i) $\sigma^P(c) > 0$ if and only if $c < \tilde{c}$ (otherwise, $\sigma^P(c) = 0$) and ii) $n(c) = \bar{n}$ if and only if $c \geq \tilde{c}'$ (otherwise, $n(c) < \bar{n}$).

B Derivations

B.1 Calculating the Expected Recovery Time

Note that there exists $\tilde{C} \in (0, \bar{C})$ such that $\sigma^P(C) = 0$. Given $C_t = C$ at time t , we define

$$\tau(C_t) = \mathbb{E}[\tau^* - t | C_t = C] \quad \text{with} \quad \tau^* = \inf\{s \geq t : C_s \geq \tilde{C}\},$$

which is the expected time until net liquidity reaches \tilde{C} and token price volatility vanishes.

We can rewrite $\tau(C_t)$ as

$$\tau(C_t) = \mathbb{E}_t \left[\int_t^{\tau^*} 1 dt \right]. \tag{B.27}$$

By definition, it holds that when $C_t = C \geq \tilde{C}$, then $\tau^* = t$ and

$$\tau(C_t) = \tau(C) = 0.$$

By the integral expression (B.27) and the dynamic programming principle, it follows that For $C \leq \tau(C)$, the function $\tau(C)$ solves the ODE

$$0 = 1 + \tau'(C)\mu_C(C) + \frac{\sigma_C(C)^2 \tau''(C)}{2}, \tag{B.28}$$

where

$$\begin{aligned}\mu_C(C) &= rC + N(C)^\xi A^{1-\xi} - \eta N(C)|\sigma^P(C)| \\ \sigma_C(C) &= N(C)(\sigma - \sigma^P(C))\end{aligned}$$

are drift and volatility of net liquidity C respectively. The ODE (B.28) is solved subject to the boundary condition

$$\tau(\tilde{C}) = 0 \tag{B.29}$$

at $C = \tilde{C}$. At $C = C_L$ (possibly $C_L = 0$), the lower boundary of the state space, the boundary condition

$$\lim_{C \rightarrow C_L} [1 + \tau'(C)\mu_C(C)] = 0$$

applies.

B.2 Model with Additional Reserve Risk and Returns

Setup. We modify the dynamics of dM_t in (8) by considering that reserve shocks (partially) scale with the level of M_t , in that

$$dM_t = rM_t dt + (P_t + dP_t)dS_t + N_t f_t dt + N_t \sigma dZ_t - dDiv_t + M_t(\hat{\mu} dt + \hat{\sigma} dZ_t). \tag{B.30}$$

Using (13), (16), and $M_t = C_t + N_t$ (i.e., $C_t = M_t - S_t P_t = M_t - N_t$), we obtain the dynamics of excess reserves:

$$dC_t = \left(rC_t + N_t^\xi A^{1-\xi} - N_t \eta |\sigma_t^P| \right) dt + N_t (\sigma - \sigma_t^P) dZ_t + (C_t + N_t) (\hat{\mu} dt + \hat{\sigma} dZ_t) - dDiv_t, \tag{B.31}$$

This model specification nests the baseline. The baseline is obtained for $\hat{\mu} = \hat{\sigma} = 0$, in which case (B.30) becomes (8) and (B.31) becomes (17). We solve for a Markov in which all quantities and the platform's value function $V(C)$ are expressed in terms of excess reserves C . Unless necessary, we omit time subscripts.

HJB Equation. As in the baseline, dividend payouts occur once C reaches the payout boundary \bar{C} . The location of the payout boundary is determined by smooth pasting and super contact conditions, that is, $V'(\bar{C}) - 1 = V''(\bar{C}) = 0$. In the interior of the state space when $C \in (0, \bar{C})$, the

HJB equation for the value function becomes

$$\rho V(C) = \max_{\{N \in [0, \bar{N}], \sigma^P\}} \left\{ V'(C) \left(rC + \hat{\mu}(C + N) + N^\xi A^{1-\xi} - \eta N |\sigma^P| \right) + \frac{1}{2} V''(C) [N(\sigma - \sigma^P) + (C + N)\hat{\sigma}]^2 \right\}, \quad (\text{B.32})$$

subject to $V'(\bar{C}) - 1 = V''(\bar{C}) = 0$.

Optimal Controls. We solve now for the optimal controls, $N(C)$ and $\sigma^P(C)$, determined via the optimization in (B.32). For this purpose, define $\gamma(C) = -\frac{V''(C)}{V'(C)}$ as the platform's effective risk-aversion, just as in the main text and baseline. If $\sigma^P(C) > 0$, then $\sigma^P(C)$ satisfies the first order condition, $\frac{\partial V(C)}{\partial \sigma^P} = 0$. The first order condition with respect to σ^P reads

$$-\eta N V'(C) - V''(C) [N(\sigma - \sigma^P) + \hat{\sigma}(C + N)] N = 0.$$

Thus,

$$N(\sigma - \sigma^P) + \hat{\sigma}(C + N) = \frac{\eta}{\gamma(C)} \iff \sigma^P(C) = \sigma + \frac{\hat{\sigma}(C + N)}{N} - \frac{\eta \gamma(C)}{N}, \quad (\text{B.33})$$

where $\sigma_C(C) = N(\sigma - \sigma^P) + \hat{\sigma}(C + N)$ is the volatility of excess reserves. When above expression for $\sigma^P(C)$ in (B.33) is negative, then $\sigma^P(C) = 0$.

We distinguish now between two cases:

1. First, consider $\sigma^P > 0$. Inserting the expression for σ^P from (B.33) into the HJB equation (B.32) and simplifying, we calculate

$$\rho V(C) = \max_{N \in [0, \bar{N}]} \left\{ V'(C) \left(rC + \hat{\mu}(C + N) + N^\xi A^{1-\xi} - \eta [(\sigma + \hat{\sigma})N + \hat{\sigma}C - \eta \gamma(C)] \right) + \frac{1}{V''(C)} \left[\frac{(\eta V'(C))^2}{2} \right] \right\}. \quad (\text{B.34})$$

If $N = N(C)$ is interior (i.e., $N(C) \in (0, \bar{N})$), the first order condition $\frac{\partial V(C)}{\partial N} = 0$ holds. Using (B.34), the first order condition with respect to N reads then

$$\hat{\mu} + \xi N^{\xi-1} A^{1-\xi} - \eta(\sigma + \hat{\sigma}) = 0,$$

so that

$$N = \underline{N} \equiv A \left(\frac{\xi}{\eta(\sigma + \hat{\sigma}) - \hat{\mu}} \right)^{\frac{1}{1-\xi}} \wedge \bar{N}. \quad (\text{B.35})$$

Re-inserting the expression for N (i.e., $N = \underline{N}$) into the expression (B.33) for σ^P yields

$$\sigma^P(C) = \sigma + \hat{\sigma} - \frac{\eta\gamma(C) - \hat{\sigma}C}{\underline{N}}.$$

2. Second, consider that $\sigma^P = 0$. Inserting $\sigma^P = 0$ into (B.32), we can calculate the first order condition with respect to N , $\frac{\partial V(C)}{\partial N} = 0$:

$$V'(C)\left(\hat{\mu} + \xi N^{\xi-1} A^{1-\xi}\right) + V''(C)[N\sigma + \hat{\sigma}(C + N)](\sigma + \hat{\sigma}) = 0. \quad (\text{B.36})$$

In general, this equation (B.36) cannot be solved for N in closed-form. Let $N^*(C)$ the solution to (B.36). Then,

$$N(C) = N^*(C) \wedge \bar{N},$$

where we account for the exogenous upper boundary \bar{N} on N .

Final Solution Steps. Next, we characterize the boundary behavior of $V(C)$ as C approaches zero. Recall that $\sigma_C(C) = N(\sigma - \sigma^P) + \hat{\sigma}(C + N)$ is the volatility of excess reserves. Similar to the baseline, as C approaches zero, $\sigma_C(C) \rightarrow 0$ which implies $\sigma^P(C) \rightarrow \sigma + \hat{\sigma}$. Recall that we have shown that $N(C) = \underline{N} \iff \sigma^P(C) > 0$. Therefore, we can use the simplified HJB equation (B.34) to derive

$$\lim_{C \rightarrow 0} V(C) = \lim_{C \rightarrow 0} \frac{V'(C)}{\rho} \left(A^{1-\xi} \underline{N}^\xi + \hat{\mu} \underline{N} - \eta \underline{N} (\sigma + \hat{\sigma}) \right).$$

To solve the model it is useful to solve an expression for $V'''(C)$. To do so, differentiate both sides of the HJB under the envelope theorem with respect to C to obtain:

$$(\rho - r - \hat{\mu})V'(C) = V''(C)\mu_C(C) + V''(C)\sigma_C(C)\hat{\sigma} + \frac{V'''(C)\sigma_C(C)^2}{2}.$$

For the value function to be concave and for a non-degenerate solution to exist, it must be that $V'''(\bar{C}) > 0$, which requires

$$r + \hat{\mu} < \rho.$$

That is, shareholders' discount rate ρ must exceed the rate of return on excess reserves, $r + \hat{\mu}$. Otherwise, holding excess reserves would not be costly and shareholders would indefinitely delay dividend payouts. For the formal proof of value function concavity in the baseline (i.e., $\hat{\mu} = \hat{\sigma} = 0$), see Appendix A.1. The arguments of this proof can easily be adjusted to extend the proof of value function concavity when $\hat{\mu} > 0$ or $\hat{\sigma} > 0$.

B.3 Solution when reserve shocks scale with M_t

Recall that the model of Appendix B.2 nests the baseline model. Also note that upon setting $\sigma = 0$, $\hat{\mu} = 0$, and $\hat{\sigma} > 0$, we obtain that Brownian shocks to reserves M_t are $M_t \hat{\sigma} dZ_t$ in (B.30) and scale with the level of reserves M_t . We present the numerical solution of this alternative

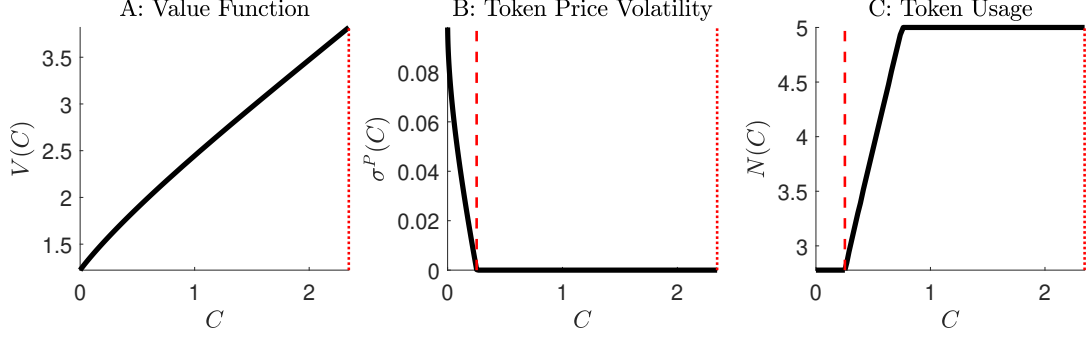


Figure B.1: **Model Solution when reserve shocks scale with M_t .** We use our baseline parameters from Figure 2 except that we set $\sigma = 0$ and $\hat{\sigma} = 0.1$. We also set $\hat{\mu} = 0$.

model specification in Figure B.1. We use our baseline parameters, except that we set $\hat{\sigma} = 0.1$, $\sigma = 0$, and $\hat{\mu} = 0$. The findings are qualitatively the same as in the baseline. The value function is increasing and concave in C (left panel A). The middle panel B shows that the token price is stable, if C is sufficiently large (i.e., $C \geq \tilde{C}$), and there is token price volatility for lower values of C and, in particular, as C approaches zero. Token price volatility decreases with excess reserves and becomes zero at some threshold $C = \tilde{C}$ (vertical dashed red line). And, the right panel C illustrates that token usage increases with C , just as in the baseline. As such, we conclude that the specific specification of the Brownian shocks to reserves in (8) does not drive our results.

B.4 Calculating User Welfare

B.4.1 Baseline

To start with, recall that any users' utility flow is

$$dR_{it} \equiv N_t^\alpha A^{1-\xi} \frac{u_{it}^\beta}{\beta} dt + u_{it} \left(\frac{dP_t}{P_t} - r dt - f_t dt - \eta |\sigma_t^P| dt \right)$$

As such,

$$\mathbb{E}[dR_{it}] = N_t^\alpha A^{1-\xi} \frac{u_{it}^\beta}{\beta} dt + u_{it} \left(\mu_t^P dt - r dt - f_t dt - \eta |\sigma_t^P| dt \right).$$

Inserting $u_{it} = N_t$ and (13) and using $\xi = \alpha + \beta$ yields

$$\begin{aligned} \mathbb{E}[dR_{it}] &= \frac{N_t^\xi A^{1-\xi}}{\beta} dt + N_t \left(\mu_t^P dt - r dt - (N_t^{\xi-1} A^{1-\xi} + \mu_t^P - r - \eta |\sigma_t^P|) dt - \eta |\sigma_t^P| dt \right) \\ &= \frac{N_t^\xi A^{1-\xi}}{\beta} dt - N_t^\xi A^{1-\xi} dt = \frac{(1-\beta) A^{1-\xi}}{\beta} N_t^\xi dt. \end{aligned} \quad (\text{B.37})$$

As a next step, define the user welfare from time t onward, i.e.,

$$W_t := \mathbb{E} \left[\int_t^\infty e^{-r(s-t)} dR_{is} \right]. \quad (\text{B.38})$$

As C is the payoff-relevant state variable, we can express user welfare as function of C , in that $W_t = W(C_t)$. The dynamic programming principle implies that user welfare solves on $[0, \bar{C}]$ the ODE

$$rW(C_t)dt = \mathbb{E}[dR_{it}] + \mathbb{E}[dW(C_t)].$$

We can rewrite the ODE as

$$rW(C) = \frac{(1-\beta)A^{1-\xi}}{\beta}N(C)^\xi + W'(C)\mu_C(C) + \frac{W''(C)\sigma_C(C)^2}{2}, \quad (\text{B.39})$$

whereby

$$\begin{aligned} \mu_C(C) &= rC + N(C)^\xi A^{1-\xi} - \eta N(C)|\sigma^P(C) + \hat{\mu}(C + N(C))| \\ \sigma_C(C) &= N(C)(\sigma - \sigma^P(C)) + \hat{\sigma}(C + N(C)) \end{aligned}$$

are drift and volatility of net liquidity C respectively. For the baseline, we set $\hat{\mu} = \hat{\sigma} = 0$. For the model extension in Appendix B.2, $\hat{\mu}$ and $\hat{\sigma}$ are potentially positive.

The ODE (B.39) is solved subject to the boundary conditions

$$W'(\bar{C}) = 0$$

and

$$\lim_{C \rightarrow 0^+} W(C) = \frac{1}{r} \lim_{C \rightarrow 0^+} \left(\frac{(1-\beta)A^{1-\xi}}{\beta}N(C)^\xi + W'(C)\mu_C(C) \right).$$

B.4.2 Model extension with Big Data as a Productive Asset

In the model extension with big data as a productive asset, user welfare is a function $W(C, A)$, that is, $W_t = W(C_t, A_t)$. We conjecture and verify that $W(C, A)$ scales with A , i.e., $W(C, A) = Aw(c)$ with $c = C/A$. First, we recall (B.37), that is,

$$\mathbb{E}[dR_{it}] = \frac{(1-\beta)A^{1-\xi}}{\beta}N_t^\xi dt = \frac{(1-\beta)A}{\beta}n_t^\xi dt,$$

and note that $n_t = N_t/A_t$ is a function of $c_t = C_t/A_t$ only, i.e., $n_t = n(c_t)$. Second, the dynamic programming principle implies that user welfare solves the ODE

$$rW(C_t, A_t)dt = \mathbb{E}[dR_{it}] + \mathbb{E}[dW(C_t, A_t)]. \quad (\text{B.40})$$

Using the conjecture $W(C, A) = Aw(c)$, we obtain

$$W_C(C, A) = w'(c), \quad W_A(C, A) = w(c) - w'(c)c, \quad \text{and} \quad W_{CC}(C, A) = \frac{w''(c)}{A}. \quad (\text{B.41})$$

Expanding the right hand side of (B.40), using (B.41) and $W(C, A) = Aw(c)$, simplifying and dividing both sides of (B.40) by dt , one derives

$$(r - \kappa n(c)^\xi)w(c) = w'(c)\mu_c(c) + \frac{w''(c)\sigma_c(c)^2}{2}, \quad (\text{B.42})$$

with drift $\mu_c(c) \equiv rc + n(c)^\xi - \eta n(c)|\sigma^P(c)| - \kappa n(c)^\xi c$ and volatility $\sigma_c(c) = n(c)(\sigma - \sigma^P(c))$. The ODE (B.42) is solved subject to the boundary conditions $w'(\bar{c}) = 0$ and

$$\lim_{c \rightarrow 0^+} (r - \kappa n(c)^\xi)w(c) = \lim_{c \rightarrow 0^+} w'(c)\mu_c(c).$$

B.5 Details on the Model with User Collateral

In this section, we provide the solution details under the model specification with user collateral requirements. To start with, take users' problem (38) (facing collateral requirements m_t):

$$\max_{u_{i,t}} \left\{ \frac{1}{\beta} N_t^\alpha u_{i,t}^\beta A^{(1-\alpha-\beta)} dt + u_{i,t} (\mu_t^P - \eta |\sigma_t^P| - f_t) dt + u_{i,t} m_t (\tilde{\mu} - \delta - r) dt \right\}.$$

All users act the same so that $u_{i,t} = N_t$. Analogous to the baseline, we then calculate optimal platform transaction volume (after solving users' optimization and invoking $u_{i,t} = N_t$):

$$N_t = \frac{A}{(r + f_t - \mu_t^P + \eta |\sigma_t^P| + m_t(\tilde{\mu} - \delta - r))^{\frac{1}{1-\xi}}},$$

when $N_t < \bar{N}$. We can solve the above for f_t , yielding (39), i.e.,

$$f_t = \left(\frac{A}{N_t} \right)^{1-\xi} - m_t(r + \delta - \tilde{\mu}) + \mu_t^P - \eta |\sigma_t^P|.$$

As a next step in the solution, we calculate

$$\begin{aligned} \int_{1-\frac{1}{m_t}}^1 (1 - m_t(1 - \theta_a)) d\theta_a &= [\theta - m_t\theta + 0.5m_t\theta_a^2]_{1-\frac{1}{m_t}}^1 \\ &= 1 - 0.5m_t - \left(1 - \frac{1}{m_t} - m_t + 1 + 0.5m_t \left[1 + \frac{1}{m_t^2} - \frac{2}{m_t} \right] \right) \\ &= \frac{1}{2m_t}, \end{aligned}$$

so

$$\begin{aligned} &2(\delta dt - \sigma dZ_t) \times \mathbb{P}(\{m_t(1 - \theta_a) < 1\}) \mathbb{E}[1 - m_t(1 - \theta_a) | m_t(1 - \theta_a) < 1] \\ &= 2(\delta dt - \sigma dZ_t) \times \left(\int_{1-\frac{1}{m_t}}^1 (1 - m_t(1 - \theta_a)) d\theta_a \right) = \frac{1}{m_t}(\delta dt - \sigma dZ_t), \end{aligned} \quad (\text{B.43})$$

which was to show.

Under this alternative specification, platform reserves follow

$$dM_t = rM_t dt + (P_t + dP_t)dS_t + N_t f_t dt - \frac{\delta N_t}{m_t} dt + \frac{N_t \sigma}{m_t} dZ_t - dDiv_t.$$

Inserting (39), we obtain

$$dM_t - (P_t + dP_t)dS_t = rM_t dt + N_t^\xi A^{1-\xi} dt - \frac{\delta N_t}{m_t} dt - m_t(r + \delta - \tilde{\mu})N_t dt \quad (\text{B.44})$$

$$+ N_t (\mu_t^P - \eta|\sigma_t^P|) dt - \frac{N_t \sigma}{m_t} dZ_t - dDiv_t. \quad (\text{B.45})$$

By Ito's Lemma, $d(S_t P_t) = dS_t P_t + S_t dP_t + dS_t dP_t$. As a result, we can calculate that C_t follows

$$dC_t = \mu_C(C_t)dt + \sigma_C(C_t)dZ_t - dDiv_t,$$

with

$$\mu_C(C) = rC - r(m-1)N(C) + m(\tilde{\mu} - \delta)N(C) + N(C)^\xi A^{1-\xi} - N(C)\eta|\sigma^P(C)| - \frac{N(C)\delta}{m}$$

$$\sigma_C(C) = N(C) \left(\frac{\sigma}{m} - \sigma^P(C) \right)$$

and $\sigma_t^P = \sigma^P(C_t)$ and $N_t = N(C_t)$.

As in the baseline, dividend payouts occur at the upper reflecting boundary \bar{C} , satisfying $V'(\bar{C}) - 1 = V''(\bar{C}) = 0$. Then, the dynamic programming principle, the HJB equation for $C \in (0, \bar{C})$ can be written as

$$\rho V(C) = \max_{N \in [0, \bar{N}], m, \sigma^P} V'(C)\mu_C(C) + \frac{\sigma_C(C)^2 V''(C)}{2}.$$

To solve for the optimal controls, we distinguish between the cases 1) $\sigma^P(C) > 0$ and 2) $\sigma^P(C) = 0$:

1. Suppose that $\sigma^P(C) > 0$. Then, the first order condition with respect to σ^P yields

$$\frac{\partial V(C)}{\partial \sigma^P} = 0 \iff -\eta V'(C) - V''(C) \left(\frac{N\sigma}{m} - N\sigma^P \right) = 0$$

so that

$$N\sigma^P = \frac{-\eta V'(C) - V''(C) \frac{N\sigma}{m}}{-V''(C)}.$$

Overall,

$$N\sigma^P = \max \left\{ 0, \frac{-\eta V'(C) - V''(C) \frac{N\sigma}{m}}{-V''(C)} \right\} = \max \left\{ 0, -\frac{\eta V'(C)}{-V''(C)} + \frac{N\sigma}{m} \right\}.$$

We can insert this expression for σ^P into (23) to get

$$\rho V(C) = \max_{N \in [0, \bar{N}], m} \left\{ V'(C) \left[rC + N^\xi A^{1-\xi} - \frac{\eta N \sigma}{m} - r(m-1)N + m(\tilde{\mu} - \delta)N - \frac{N\delta}{m} - \frac{\eta^2 V'(C)}{V''(C)} \right] + \frac{1}{V''(C)} \left[\frac{(\eta V'(C))^2}{2} \right] \right\}.$$

The choice of m is independent of N . One can calculate that optimal m solves the first-order condition

$$\tilde{\mu} - \delta - r + \frac{\delta}{m^2} + \frac{\eta\sigma}{m^2} = 0,$$

so that

$$\frac{1}{m^2} = \frac{r + \delta - \tilde{\mu}}{\delta + \eta\sigma} \iff m = \bar{m} \equiv \sqrt{\frac{\delta + \eta\sigma}{r + \delta - \tilde{\mu}}}.$$

Next, we can take the first-order condition with respect to N to obtain

$$\xi N^{\xi-1} A^{1-\xi} - \frac{\eta\sigma}{m} - r(m-1) + m(\tilde{\mu} - \delta) - \frac{\delta}{m} = 0.$$

Thus,

$$N(C) = \underline{N} = A \left(\frac{\xi}{\frac{\eta\sigma}{m} + r(\bar{m}-1) - \bar{m}(\tilde{\mu} - \delta) + \frac{\delta}{m}} \right)^{\frac{1}{1-\xi}} \wedge \bar{N} \quad (\text{B.46})$$

2. Suppose that $\sigma^P = 0$. Then, taking the derivative with respect to N yields

$$\frac{\partial V(C)}{\partial N} = \frac{1}{\rho} \left(V'(C) \left[\xi N^{\xi-1} A^{1-\xi} - r(m-1) + m(\tilde{\mu} - \delta) - \frac{\delta}{m} \right] + N \left(\frac{\sigma}{m} \right)^2 V''(C) \right).$$

Taking the first-order condition with respect to m yields

$$\frac{\partial V(C)}{\partial m} = 0 \iff V'(C)N \left[\tilde{\mu} - \delta - r + \frac{\delta}{m^2} \right] - N^2 V''(C) \frac{\sigma^2}{m^3} = 0. \quad (\text{B.47})$$

Thus,

$$N = N(C) = \frac{-V'(C)}{V''(C)} \left(\frac{r + \delta - \delta/m^2 - \tilde{\mu}}{\sigma^2/m^3} \right) = \frac{-V'(C)}{V''(C)} \left(\frac{(r + \delta - \tilde{\mu})m^3 - \delta m}{\sigma^2} \right)$$

Finally, we discuss the value function at the payout boundary \bar{C} where $V'(\bar{C}) - 1 = V''(\bar{C}) = 0$. At $C = \bar{C}$, we have — as in the baseline — $\gamma(\bar{C}) = V''(\bar{C}) = 0$. As such,

$$\sigma^P(\bar{C}) = 0$$

and

$$N(\bar{C}) = \bar{N}.$$

Using (B.47), we obtain

$$m(\bar{C}) = \sqrt{\frac{\delta}{r + \delta - \tilde{\mu}}}$$

as the margin requirement at $C = \bar{C}$. Analogous to the baseline, there exist three regions and two thresholds \tilde{C} and \tilde{C}' such that i) $\sigma^P(C) > 0$ if and only if $C < \tilde{C}$ (otherwise, $\sigma^P(C) = 0$) and ii) $N(C) = \bar{N}$ if and only if $C \geq \tilde{C}'$ (otherwise, $N(C) < \bar{N}$). The platform optimally prevents liquidation as C approaches zero, leading to the boundary condition

$$\lim_{C \rightarrow 0^+} \sigma^P(C) = 0 \iff \lim_{C \rightarrow 0^+} \sigma^P(C) = \frac{\sigma}{\bar{m}}.$$

This boundary condition can be manipulated to obtain a condition analogous to (??). Using that

$$\lim_{C \rightarrow 0^+} N(C) = \underline{N}, \quad \lim_{C \rightarrow 0^+} m(C) = \bar{m} \quad \text{and} \quad \lim_{C \rightarrow 0^+} \sigma_C(C) = 0,$$

we obtain

$$\lim_{C \rightarrow 0^+} \frac{V(C)}{V'(C)} = \frac{1}{\rho} \left\{ -r(\bar{m} - 1)\underline{N} + m(\tilde{\mu} - \delta)\underline{N} + \underline{N}^\xi A^{1-\xi} - \underline{N}\eta \frac{\sigma}{\bar{m}} - \frac{N\delta}{\bar{m}} \right\}.$$

B.6 Negative Lower Bound in the State Space

In this Section, we provide the model solution without the assumption of over-collateralization, $C_t \geq 0$. Instead, the lower bound on C_t , denoted C_L , can potentially be negative. For simplicity, we do not consider a run under $C_t < 0$. We characterize a no-run equilibrium in the following. To start with, note that regardless of the value of the lower bound C_L , the law of motion (17) applies for C_t , and transaction volume N_t is characterized in (12). In a Markov equilibrium, all quantities can be expressed as functions of C only, so we omit time subscripts unless necessary. As is standard, dividend payouts are made at an endogenous payout boundary \bar{C} , with $V'(\bar{C}) - 1 = V''(\bar{C}) = 0$. On (C_L, \bar{C}) , the platform's value function $V(C)$ solves the HJB equation (23). The optimal controls $\sigma^P(C)$ and $N(C)$ are determined according to the optimization in the HJB equation (23).

The platform operates under $C \geq C_L$ and $M \geq 0$ (i.e., the value of reserves must remain positive). We analyze the case of $C_L < 0$. To begin with, note that

$$M = C + SP \geq 0 \iff C \geq -SP = -N,$$

where token market clearing implies $SP = N$ (see (7)). Due to $N \leq \bar{N}$ and $M \geq 0$, it follows that $C \geq -\bar{N}$. That is, $C_L \geq -\bar{N}$. Another observation is that for $C < 0$, the optimization constraint $N(C) \geq -C \iff M \geq 0$ applies to the optimization in the HJB equation (23) to ensure reserves M remain positive. We numerically verify that this constraint never binds under our baseline parameters.

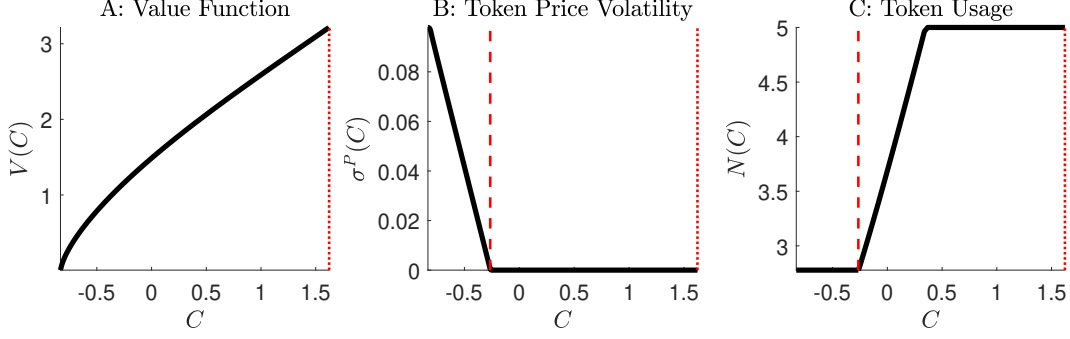


Figure B.2: **Solution with A Negative Lower Bound on C** . This figure plots the platform value function (Panel A), token price volatility (Panel B), and token demand and usage (Panel C) as functions of excess reserves C . The parameterization follows Figure 2, and the lower bound is $C_L = -0.823$.

To ensure $C_t \geq C_L$ at all times $t \geq 0$ and so to prevent C from dropping below C_L , it is necessary that i) the drift of dC remains positive and ii) the volatility of dC vanishes, as C approaches C_L . According to (17), the second requirement ii) is equivalent to

$$\lim_{C \rightarrow C_L} \sigma^P(C) = \sigma.$$

And, recall that by maximization in the HJB equation (23), optimal transaction volume becomes $N(C) = \underline{N}$ whenever $\sigma^P(C) > 0$ and the constraint $N(C) \geq -C$ does not bind, where \underline{N} is characterized in closed-form in (26) (for details, see Part I of the proof of Proposition 3). As a result, $\lim_{C \rightarrow C_L} N(C) = \max\{\underline{N}, -C_L\}$. Inserting $C = C_L$, $\sigma^P(C) = \sigma$, and $N(C) = \max\{\underline{N}, -C_L\}$ into (17), we obtain the following drift of dC , denoted $\mu_C(C)$, as C approaches C_L :

$$\lim_{C \rightarrow C_L} \mu_C(C) = \max\{\underline{N}, -C_L\}^\xi A^{1-\xi} - \eta \max\{\underline{N}, -C_L\} \sigma + rC_L.$$

Equating above expression to zero, we obtain that the drift of dC remains zero as C approaches C_L as long as

$$C_L \geq \frac{1}{r} \left(\eta \max\{\underline{N}, -C_L\} \sigma - (\max\{\underline{N}, -C_L\})^\xi A^{1-\xi} \right) =: \hat{C}_L(C_L). \quad (\text{B.48})$$

Combining this relation with $C_L \geq -\bar{N}$, we obtain the lowest possible C_L , which we call C_L^{\min} :

$$C_L^{\min} = \max \left\{ \hat{C}_L(\hat{C}_L), -\bar{N} \right\}.$$

We solve the model for the lowest possible C_L , that is, $C_L = C_L^{\min}$.⁶⁰ Because drift and volatility of excess reserves vanish as C approaches $C_L = C_L^{\min}$, the boundary condition $\lim_{C \rightarrow C_L} V(C) = 0$ applies.

⁶⁰Note that a decrease of C_L relaxes the platform's optimization constraint $C \geq C_L$ and therefore is beneficial for the platform.

Figure B.2 presents the model solution with lower bound $C_L = C_L^{min}$ under our baseline parameters. Under our baseline parameters, $C_L^{min} = -0.823$, $\underline{N} = 2.778 > -C_L$ and $C_L > -\bar{N} = -5$. We verify that the constraint $N(C) \geq -C$ never binds under our baseline parameters. A novel finding is that depending on the circumstances, the same stablecoin may be under- or over-collateralized, in that C takes in equilibrium both positive and negative values. The other findings are qualitatively the same as in the baseline. The value function is increasing and concave in C (left panel A). The middle panel B shows that the token price is stable, if C is sufficiently large (i.e., $C \geq \tilde{C}$), and there is token price volatility for lower values of C and, in particular, as C approaches the lower bound C_L and tokens become under-collateralized. Token price volatility decreases with excess reserves and becomes zero at some threshold $C = \tilde{C}$ (vertical dashed red line). And, the right panel C illustrates that token usage increases with C , just as in the baseline. As such, we conclude that the focus on over-collateralization, $C \geq 0$ (i.e., $C_L = 0$), does not drive our results.